WT-33
Copy ___5__ A

OPERATION

GREENHOUSE

SCIENTIFIC DIRECTOR'S REPORT

ANNEX 8.3 SPECIAL RADAR, RADIO, AND PHOTOGRAPHIC

STUDIES OF WEAPONS EFFECTS

PARTS I, II, III, AND IV

NUCLEAR

EXPLOSIONS

1951

DTIC QUALITY INSPECTED 5

Declassified by DNA, Chief, ISTS

Date:

Classification (Cancelled) (Changed to ___2-6-5)
By Authority of ___
Date ___ 2 AUG 1952

1950721 016

DISCLAIMER NOTICE

THIS DOCUMENT IS BEST QUALITY AVAILABLE. THE COPY FURNISHED TO DTIC CONTAINED A SIGNIFICANT NUMBER OF PAGES WHICH DO NOT REPRODUCE LEGIBLY.

This document consists of 416 plus 4 pages
(counting preliminary pages)

No. 5 of 150 copies, Series A

DTIC
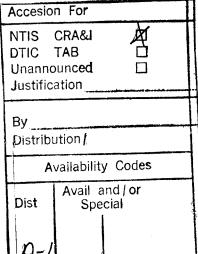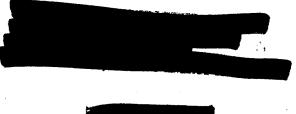S ELECTE
JUL 2 4 1995
G

Scientific Director's Report
of Atomic Weapon Tests
at Eniwetok, 1951

Annex 8.3

Special Radar, Radio, and Photographic Studies
of Weapons Effects

Parts I, II, III, and IV

Accesion For		
NTIS CRA&I	☒	
DTIC TAB	☐	
Unannounced	☐	
Justification		
By		
Distribution /		
Availability Codes		
Dist	Avail and / or Special	
A-1		

i

Distribution

|	Copy			Copy
DEPARTMENT OF DEFENSE			**AIR FORCE**	
Armed Forces Special Weapons Project (Sandia)	1–3		Deputy Chief of Staff for Development (AFDRD)	47
Armed Forces Special Weapons Project (Washington)	4–15		Director of Operations (Operations Analysis Division)	48
			Director of Plans (AFOPD-P1)	49
ARMY			Director of Requirements	50–51
			Director of Research and Development	52–53
Army Field Forces	16		Eglin Air Force Base, Air Proving Ground	54–55
Assistant Chief of Staff, G-3	17			
Assistant Chief of Staff, G-4	18–19		Ent Air Force Base, Air Defense Command	56–57
Chief Signal Officer	20–23			
Chief of Ordnance	24–25		Kirtland Air Force Base, Special Weapons Command	58–60
NAVY			Langley Air Force Base, Tactical Air Command	61–62
Bureau of Ordnance	26		Maxwell Air Force Base, Air University	63–64
Bureau of Ships	27–28			
Chief of Naval Operations	29		Offutt Air Force Base, Strategic Air Command	65–67
Chief of Naval Research	30			
Commandant, Marine Corps	31		1009th Special Weapons Squadron	68
Naval Electronics Laboratory	32–33		Rand Corporation	69–70
Naval Radiological Defense Laboratory	34–35		Scott Air Force Base, Air Training Command	71–72
			⬛ ⬛ Development Center	73–75
AIR FORCE			⬛ Command	76–77
Air Force Cambridge Research Center	36		**ATOMIC ENERGY COMMISSION**	
Air Research and Development Command	37–40		Atomic Energy Commission, Washington	78–80
Air Targets Division, Directorate of Intelligence (Phys. Vul. Branch)	41–42		Los Alamos Scientific Laboratory, Report Library	81–85
Assistant for Atomic Energy	43–44		Sandia Corporation	86–87
Assistant for Development Programming	45		Technical Information Service, Oak Ridge (surplus)	88–149
Assistant for Materiel Program Control	46		Weapon Test Reports Group, TIS	150
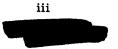
SPECIAL RADAR, RADIO, AND PHOTOGRAPHIC STUDIES OF WEAPON EFFECTS

PARTS I, II, III, AND IV

Approved by: ROBERT E. JARMON
Colonel, USAF
Director, Program 8

Approved by: ALVIN C. GRAVES
Scientific Director

CRPL = Central Radio Propagation Laboratories, National Bureau of Stds.

Wright Air Development Center
Headquarters, Joint Task Force Three
Los Alamos Scientific Laboratory

CONTENTS

PART I—RADAR-SCOPE PHOTOGRAPHY

CONTENTS (Continued)

PART II–EFFECTS OF ATOMIC DETONATION ON RADIO PROPAGATION

SECTION 1. IONOSPHERIC INVESTIGATION

CONTENTS (Continued)

CONTENTS (Continued)

PART III—PHOTOGRAPHIC ASSESSMENT OF BOMB DAMAGE

PART IV—FILM FOGGING STUDIES

CONTENTS (Continued)

ILLUSTRATIONS

PART I—RADAR-SCOPE PHOTOGRAPHY

ILLUSTRATIONS (Continued)

PART II—EFFECTS OF ATOMIC DETONATION
ON RADIO PROPAGATION

CHAPTER 1 INTRODUCTION

SECTION 1. IONOSPHERIC INVESTIGATION

CHAPTER 3 TEST RESULTS

ILLUSTRATIONS (Continued)

ILLUSTRATIONS (Continued)

ILLUSTRATIONS (Continued)

ILLUSTRATIONS (Continued)

ILLUSTRATIONS (Continued)

ILLUSTRATIONS (Continued)

ILLUSTRATIONS (Continued)

ILLUSTRATIONS (Continued)

ILLUSTRATIONS (Continued)

PART IV—FILM FOGGING STUDIES

CHAPTER 3 RESULTS

ILLUSTRATIONS (Continued)

TABLES

PART IV—FILM FOGGING STUDIES

CHAPTER 3 RESULTS

Part I
RADAR-SCOPE PHOTOGRAPHY

by

W. R. BOARIO

and

C. W. ABBITT
Major, USAF

Aircraft Radiation Laboratory
Wright Air Development Center
Wright-Patterson Air Force Base
Dayton, Ohio

October 1951

Preface

The purpose of this report is to present a preliminary analysis of radar-scope photography data which were obtained on Project 8.3A, Operation Greenhouse. It has been recognized that, in the tactical and strategic use of atomic bombs, a method of indirect analysis of bomb damage is desirable in order to permit effective analysis and tactical planning. Since radar returns had previously been observed on airborne radar systems from atomic explosions, it was felt desirable to investigate this phenomenon further in order to determine whether it could be used for this purpose.

The Aircraft Radiation Laboratory at Wright-Patterson Air Force Base was presented with this problem and was requested to investigate this possibility and to derive a solution. In order to accomplish this investigation in the time interval available, it was necessary to use the maximum amount of available equipment and to minimize the design and fabrication of supplementary equipment in order to obtain a reasonable amount of data. As a result, the quantity and accuracy of the information obtained were compromised. However, results which indicated significant trends were obtained and are presented in this report.

We wish to acknowledge the assistance and work performed by all personnel directly associated with Project 8.3A. We also wish to acknowledge the support furnished by Task Groups 3.1 and 3.4 of Joint Task Force Three, without whose able assistance this project might not have been performed.

Abstract

Radar echoes have been observed during previous atomic detonations but with little additional data. Measurements on echo intensity and characteristics were obtained and recorded by use of an X-band radar system. To accomplish the desired results, the video signals from the AN/APQ-24 radar receivers, one located in each of two B-50D aircraft, were displayed on a calibrated oscillograph and photographed with a low-speed conventional 35-mm movie camera at 32 frames/sec and a modified General Radio 651 AE oscillograph camera operating at 27 ft/sec. The radar signals were displayed on a DuMont 294-A oscillograph with a 5XP11 cathode-ray tube operating at a 12-kv acceleration voltage to obtain sufficient light intensity for recording. The photographic recordings thus obtained were used for further analysis to determine the value of the data.

Preliminary analysis of three records obtained shows that, under the conditions that existed, radar returns were easily obtained.

The source of the radar returns appears to be located on, or very near, the earth's surface approximately 4 sec after detonation of high-yield bombs, and close coincidence exists between the origin of the return and the leading edge of the shock wave. At time periods of less than 4 sec, returns were obtained, and their positions were compared with direct measurement data on shock-wave position. Correlation was again found to exist between the origin of the radar returns and shock-wave position. Evidence was obtained which indicated that, within the first 2 sec after detonation, the radar returns from the explosion were visible over the land area of the shot island.

Data on the amplitude of the return as a function of time did not indicate any significant trend, but this point cannot be considered conclusive owing to the short period devoted to analysis.

It is recommended that further data be obtained on this problem during future overland tests.

Chapter 1

Introduction

1.1 PURPOSE

The purpose of this project was to investigate the possibility of determining ground zero and the approximate yield of an atomic explosion by illuminating with airborne radar, at the time of detonation, the area in which the explosion occurs and by analyzing the returning radar signals.

1.2 JUSTIFICATION

When operational requirements do not permit visual methods of bombing and observation to be employed, some method of indirect bomb-damage assessment must be devised. It is known that clouds, which completely obscure the ground from an observer above them, usually have only a minor effect on radar signals. Then if it were possible to obtain sufficient information from the radar upon detonation of the bomb to approximate the resulting damage, regardless of weather conditions, a more intelligent plan could be employed in the immediate future for the efficient tactical and strategic use of such bombs.

1.3 SCOPE

By obtaining standard radar plan-position-indicator (PPI) photographs and photographs of a laboratory cathode-ray oscillograph using the common A-type presentation (signal amplitude vs time) during three atomic detonations from two aircraft at different locations, it was felt that sufficient data could be secured to determine the feasibility of this approach to the bomb-damage-assessment problem.

This report consists in a general description of the equipment installed in the aircraft for this purpose (Chap. 2), the procedure used in calibrating this equipment (Chap. 3), the techniques used during flights (Chap. 4), and a presentation of the data recorded during these tests with a general discussion of the results (Chap. 5).

Several photographs are given in Chap. 5 showing the general trend of the radar echoes resulting from the explosions as a function of time. Graphs which point to the close coincidence of the shock wave with these echoes are also included in Chap. 5.

If the reader is interested in more accurate data on the propagation of these echoes than can be obtained directly from these graphs, he is referred to the appendixes, where all such data are tabulated.

Chapter 2

Description of Apparatus

2.1 LIST OF EQUIPMENT

The installation in each of the two B-50D manned aircraft consisted of one of each of the following major components:

1. Radar set AN/APQ-24
2. Cathode-ray oscillograph
3. High-speed oscilloscope camera
4. Bomb-spotting aircraft camera, Type A-4
5. Radar-scope recording camera, Type O-15
6. Selector control unit
7. Miscellaneous equipment for furnishing

additional power to special installation, equipment for furnishing timing information, and various other minor components.

2.2 DESCRIPTION OF COMPONENTS

A general description of each of the components used is given here. For a more thorough description of these components the reader is referred to the Bibliography, where references of a more technical nature are listed.

2.2.1 Radar Set AN/APQ-24

Radar set AN/APQ-24 is an airborne radar navigational and bombing system operating in the X-band of the frequency spectrum. It consists of radar set AN/APS-23 and ground position indicator AN/APA-44. The peak power is 55 kw, and during the complete test the pulse width was fixed at $\frac{3}{8}$ μsec with a repetition rate of approximately 800 pulses/sec. The intermediate-frequency band width is rated at 8 Mc/sec.

The radar antenna radiates r-f energy in a horizontally polarized beam $1\frac{1}{2}°$ wide in the horizontal plane and approximately 55° wide in the vertical plane. The vertical plane of the radiated beam is shaped in accordance with the cosecant-squared law to provide a received signal of relatively constant strength irrespective of the target distance from the aircraft. The antenna may be made to rotate over the complete 360° continuously, or sector scan may be used. In the latter case the operator is able to keep the desired target near the center of the indicator, and the antenna scans about this target in a sector which may be adjusted between 40 and 180°. The operator may choose an antenna speed of approximately 6 or 22 rpm.

The AN/APQ-24 employs the PPI type of presentation. Azimuth bearing and ground-range distance of the targets with respect to the aircraft are displayed on the indicator. The true azimuth bearing of a particular echo or target is indicated by the angular displacement of the observed echo from true north at the top of the indicator screen. The ground position indicator provides a pair of cross hairs in the form of the intersection of a range circle and a radial azimuth mark, which may be placed at will on any target within 20 miles north or south and 20 miles east or west of the aircraft. The azimuth mark is displayed on the screen at an angle from north equal to the true heading of the aircraft. When proper wind information has been set into the APA-44, the cross hairs automatically remain on, or track, the selected target regardless of the motion of the aircraft. The antenna then automatically sector-scans about the azimuth cross hair. The apex of the sector is displaced to the edge of the indicator. The apex of the sector represents the location of the aircraft and follows the aircraft movement with respect to the selected target. Range is automatically controlled so that this target

always appears near the center of the screen. For a more complete description of the standard AN/APQ-24 the reader is referred to the first and second publications listed in the Bibliography at the end of this report.

One minor modification was necessary in adapting this radar set to meet the requirements of this project. It was found that the video amplifier following the second detector in the receiver (receiver-transmitter RT-124/APS-23) was limiting the received video signal when of relatively high amplitude. While this condition was satisfactory upon the presentation of the signals on a PPI, it was not satisfactory when the presentation was the A-type. It was necessary, therefore, to add an additional second detector, a cathode follower, and a special video output so that the additional special cathode-ray oscillograph could display signals varying over a much larger dynamic range than those contained in the output to the standard PPI. The band width of this special video circuit was found to be from 3½ to 4 Mc/sec. In addition a trigger pulse which occurred simultaneously with the transmitter pulse was obtained from the AN/APS-23 to synchronize the A-scope with the radar set. Antenna rotational data for the operation of camera timing lights were also obtained from the AN/APS-23, and range data were obtained from the AN/APA-44, for presentation with the video signal on the cathode-ray oscillograph.

2.2.2 Cathode-ray Oscillograph

The special video output from the radar set mentioned above was applied to the vertical deflection plates of a standard DuMont Type 294-A oscillograph. This oscillograph is a general-purpose laboratory item especially adaptable to the investigation of short pulses because of its wide band width and the high accelerating potentials available. The accelerating potential used was 12 kv, which, when applied to the 5XP11 cathode-ray tube, produced a high-intensity short persistent wave-form suitable for high-speed photography.

The screen of the oscillograph was made visible to the two cameras by use of a semi-transparent mirror. Ninety per cent of the light was permitted to pass through the mirror to the high-speed oscilloscope recording camera, while the remaining 10 per cent was re-flected to the low-speed camera which was pointed perpendicular to the viewing axis of the oscillograph.

2.2.3 High-speed Oscilloscope Recording Camera

This camera was used to record instantaneous variations in the returning radar signal appearing on the oscillograph described above. It was a General Radio Type 651-AE oscillograph recorder modified for a film capacity of 1,000 ft of 35-mm film. The film was driven continuously past the lens aperture (projected image) at approximately 25 ft/sec so that a complete record of the cathode-ray spot was obtained.

Two timing lights were incorporated in the camera body for the purpose of supplying data to the film on the position of the radar antenna and the time elapsed after time zero.

2.2.4 Bomb-spotting Aircraft Camera, Type A-4 (Low-speed Camera)

This camera was used to obtain motion-picture recordings of the returning radar signals appearing on the oscillograph. The camera was operated at a speed which integrated in the order of 16 pulses and their corresponding echoes into each camera frame, in contrast to the high-speed camera in which each frame represented only one pulse and its corresponding echoes. Thirty-five-millimeter film was used, the capacity of the camera being 100 ft.

Two timing lights were incorporated into this camera for supplying information identical with that described in the high-speed camera.

2.2.5 Radar-scope Recording Camera, Type O-15

The radar-scope image-recording camera was used to photograph the luminous images traced on the PPI of the radar set AN/APQ-24. When the radar antenna is scanned about a sector, this camera will take photographs of the indicator for the duration of each clockwise scan, each second clockwise scan, each fourth clockwise scan, or each twelfth clockwise scan. In an effort to obtain as much radar information as possible, the aircraft installations were modified so that the O-15 cameras would take photographs on each clockwise scan and each

counterclockwise scan. On the average, a complete picture of the PPI was obtained each 0.65 sec.

A clock and a frame counter were photographed on each frame in addition to the radar image.

2.2.6 Selector Control Unit

To permit proper display and recordings of the radar data, it was necessary to integrate within a selector control unit various circuitry to permit the accomplishment of the desired end results. Besides acting as a junction box it consisted of the following circuitry and associated components.

2.2.6.1 Sweep-trigger Delay Circuit

To permit efficient use of the sweep trace on the DuMont 294-A oscillograph, it was considered desirable to delay the sweep trigger to permit displaying only the portion of the radar returns of interest. Since spot-size limitation limits the time period which may be viewed on the 5XP11 cathode-ray tube, a sweep length of 48,000 ft was found to be the maximum usable time period for the $\frac{3}{8}$-μsec pulse radiated by the radar which could be displayed without reducing the resolving power to a point where it would be considered detrimental to the data to be recorded. The delay circuit receives a trigger pulse of $\frac{3}{8}$ μsec duration, synchronized with the radar transmitter pulse, and delays this pulse with respect to the transmitter pulse by means of a phanastron delay circuit. The amount of delay is variable between 2,500 and 20,000 yd. This is controlled by a potentiometer and a calibrated dial which may be set from the exterior of the selector control unit. The calibration may be checked and rezeroed by means of a TS-102 precision range calibrator. The delayed trigger pulse is then used to trigger the horizontal sweep circuit of the cathode-ray oscillograph. By utilizing the delay circuit, the oscillograph may be made to present any radar returns occurring after the limits of the delay circuit but within the time period displayed on the oscillograph.

2.2.6.2 Cross-hair Separator

The function of the cross-hair separator is to remove and to pass on to the video amplifier the 0.2-μsec pulse which constitutes the computer range marker from the 1,000-μsec pedestal which forms the radial line giving azimuth position from the APA-44. The position of the A-scope trace on the face of the cathode-ray tube is governed by the average value of the displayed signal component. The high amplitude and duration of the 1,000-μsec pedestal would therefore cause a large sudden displacement of the A-scope trace at the instant it was displayed, thus possibly causing the data to deteriorate at the critical moment when the antenna swept over point zero. Owing to the great differences in time-interval duration of these two signals, it was possible to use a differentiator circuit to virtually eliminate the 1,000-μsec signal. To accomplish this the cross-hair signals were obtained from the AN/APA-44, amplified, differentiated by use of a Utah blocking-oscillator transformer, clipped by a crystal diode, and then fed to the video amplifier and mixer.

2.2.6.3 Video Amplifier and Mixer

The video amplifier and mixer was used to amplify the signal from the receiver of the radar set and to correct the frequency response of the over-all auxiliary video system. In addition, the range marker from the cross-hair separator was mixed with the conventional video signal as a negative signal to permit easy identification. The range marker is normally used by the radar operator to track a target and, once properly set, remains at this ground position, thus enabling this range to be recorded on the A-scope at all times. This aided considerably in the final evaluation.

2.2.6.4 Azimuth Data Circuit

This circuit consisted simply of a relay which was interconnected to the APS-23 antenna control circuit. The relay controlled a 300-v potential which was applied to the small gas glow tube in the cameras in such a manner that the light was on during a counterclockwise scan of the antenna. This, in turn, marked the film to permit correlation at a later date between the PPI photographs, the low-speed camera, the high-speed camera, and the antenna position.

2.2.6.5 Timing Circuits

To permit time correlation between the various cameras and time zero, 100- and 2,000-

cycle signals were obtained from the timing decoder in the aircraft. The 2,000-cycle signal, which came on at time zero − 5 sec, was used to turn on all timing lights at time zero. This was accomplished by taking the 3- to 6-v signal supplied by the decoder, amplifying it, and then using it to control the grid of a vacuum tube in whose plate a sensitive relay, which controlled the 300-v potential to the remainder of the timing circuit, was incorporated. At time zero the 2,000-cycle signal was cut off, thereby actuating the relay and applying the 300 v to the timing circuits mentioned above. The 100-cycle signal of approximately 3 to 6 v was also amplified, clipped, and further amplified so that short pulses of approximately 3 msec duration at a rate of 100 pulses/sec were applied to the gas glow tubes in the cameras. These signals, in turn, appeared as dots, or markers, along the edge of the film on the high- and low-speed cameras.

2.2.6.6 Power Circuits

Power circuits consisted of the necessary wiring and distribution required to supply the oscilloscope and cameras with the power required for their operation and of switching circuits for their control. A master off-on switch was incorporated in this unit for all auxiliary equipment. A relay actuated by a current from the decoder at time zero − 5 sec turned on the low- and high-speed cameras. In addition, an override switch was provided to enable the operator to start the cameras manually in case the signal from the decoder failed. The d-c power required to operate the vacuum tubes was supplied by a modified RA-88A regulated power supply and was connected to the selector control unit by an exterior cable. Filament power for the vacuum tubes was supplied by a filament transformer incorporated in the selector control unit.

Chapter 3

Preoperational Procedure

3.1 GENERAL DISCUSSION

The preoperational procedure consisted in two basic steps: (1) calibration of the radar receiver and (2) calibration of the A-scope trace.

3.1.1 Calibration of the Radar Receiver

Before Dog Shot the receivers from both aircraft were calibrated by means of signal generator TS-35A/AP. This test equipment consists of an X-band signal generator, a frequency meter, and a power-output meter. By means of this test equipment, an X-band signal at the frequency of the radar transmitter was introduced into the radar receiver, and the amount of deflection produced on the A-scope trace was measured and tabulated. This consisted in injecting a signal into a calibrated wave selector placed near the antenna, whose loss had been previously determined. By knowing the loss of the cable interconnecting the wave selector and the TS-35A, it was possible to obtain signal-in vs A-scope deflection amplitude characteristics to an accuracy of ±1½ db.

In order to be capable of resetting the receiver gain to a predetermined level, a means had to be devised which would permit the operator to set the gain with reasonable accuracy in the short time available. The receiver-gain setting which was chosen was one which would permit the radar system to have average land painting over normal terrain, or approximately where the receiver background noise was perceptible on the PPI display. It was decided that the most satisfactory means under existing conditions would be to monitor the receiver-output average noise value. A meter was placed in the cathode circuit of the video cathode-follower stage for this purpose. Since the second-detector output was directly coupled to the cathode follower, d-c level problems were eliminated, and the current flow through the cathode follower was used as an indication of the average noise level. It had been previously determined that the average current through this tube would change only a small percentage owing to the small amount of land radar return obtained in the vicinity of Eniwetok Atoll. Tests were run on this method of determining the receiver gain, and over a period of several days it was found that the receiver gain could be duplicated within 1½ db for the over-all radar and A-scope system. This included reading errors encountered by using various persons to set up the TS-35A and reading the A-scope deflection. However, since maintenance, which involved the replacement of vacuum tubes and other component parts, had to be performed constantly on the equipment, the system was calibrated before each shot as near the time of shot as possible to ensure reasonably accurate receiver calibration curves. Calibration precautions were taken to permit the receiver and test equipment to be turned on before each shot for a time period comparable to that which the equipment would be on during the flight to permit the greatest degree of stability to be obtained.

During this procedure the vertical amplifier gain of the DuMont 294-A oscilloscope was set so that the receiver noise caused a deflection of 0.15 to 0.20 in. on the A-trace. Owing to the receiver characteristics, this permitted a deflection of approximately 1.5 to 1.9 in. for a signal of 35 to 40 db above receiver noise.

Receiver sensitivity measurements on minimum detectable signal for aircraft 340 were as follows: Dog Shot, 100 db below 1 mw; Easy Shot, 99 db below 1 mw; and George Shot, 99 db below 1 mw. Similar measurements on the radar in aircraft 290 were as follows: Dog Shot, 99 db below 1 mw; Easy Shot, 99 db below 1 mw; and George Shot, 98 db below 1 mw.

Before the first mission the sector scan width, controlled by the APA-44, was reduced to approximately 45°. The narrow sector was preferred in order to obtain as many "looks" at the given target area as possible. Ideally it would have been more desirable to have the antenna pointing across the target area in order to obtain continuous range data only. However, existing equipment did not provide any satisfactory means of obtaining this feature, and, to avoid the possibility of the antenna being off the target area by an unknown amount at time of detonation and immediately following, it was decided to obtain sequential data by permitting the antenna to scan at the highest rate permissible. It was found that the sector width chosen exhibited erratic behavior just prior to Dog Shot. Therefore on Easy and George Shots the sector width was increased to 50°.

3.1.2 Calibration of the A-scope Trace

Before each shot the delay circuit for the A-scope trace and A-scope trace length and sweep speed were checked and calibrated. Similar to the receiver sensitivity check, this was accomplished as near the time of shot as possible.

Calibration of the range delay circuit consisted in using a range calibrator TS-102/AP to trigger the radar set and in using the precision marker generator of the TS-102/AP to calibrate the delay against these markers. In order to obtain maximum accuracy the delay was zeroed specifically to the delay required during a particular shot. Previous laboratory measurements had indicated that, by using this technique, an accuracy of ±100 ft would be maintained if the equipment were permitted to stabilize. However, tests also indicated that, even without this time allowed for stabilization, an accuracy of ±200 ft was realized. Throughout all the tests at Operation Greenhouse, during both calibration and actual flights, ut-

most care was observed to ensure maximum accuracy.

During Dog Shot, in order to obtain most efficient use of the A-trace, a delay of 18,000 ft was used on aircraft 340, and a delay of 24,000 ft was used on aircraft 290. During Easy Shot the A-scopes in both aircraft were triggered directly by the transmitter pulse in order to obtain a recording of the A-trace showing the time interval between the first ground return and the aircraft. During George Shot a sweep delay of 27,000 ft was used on aircraft 340 and a delay of 30,000 ft on No. 290. As has been mentioned previously, a maximum A-trace length of 48,000 ft had been determined to be the maximum usable length with the DuMont 294 A-scope. This sweep length was used during all tests participated in.

The A-trace sweep was also calibrated by means of the TS-102A precision range calibrator. To accomplish this, the radar was again triggered by the TS-102, and the range markers were inserted on the A-trace by use of the cross-hair input jack of the selector control unit. The markers were then phased so that the leading edge of a marker coincided with the beginning of the A-trace. The sweep speed and length were then adjusted so that they were the equivalent of 48,000 ft in length. The lineal length on the face of the cathode-ray tube was also adjusted to a predetermined reference value which consisted of engraved markings on a plexiglas screen in contact with the face of the cathode-ray tube. To provide a future scale-factor reference, the markers from the TS-102 were then adjusted to 1-in. deflection amplitude on the cathode-ray tube, and a length of film was run through both the high- and low-speed cameras to obtain a calibration record giving both deflection factor and sweep calibration of the A-scope.

Previous tests indicated that the stability of the two oscilloscopes used in the aircraft, when turned on for a sufficient period, was such that a sweep calibration drift of less than 1 per cent of the sweep length was encountered. This error was the maximum that could be expected at any point on the sweep and would be proportional to the distance from the beginning of the sweep to the point in question. That is, for a point 20,000 ft from the beginning of the A-trace, a sweep error of less than 200 ft would be possible. All tests indicated that errors due

to this cause usually were such that distances measured were greater by the above tolerance.

Before take-off on each mission the O-15 cameras and the low-speed cameras were loaded with 100-ft rolls of Kodak Linagraph Pan film, and the magazines of the high-speed cameras, which had been previously loaded with 1,000-ft Kodak Linagraph Pan film, were attached to the camera, and threading of the film was accomplished.

Chapter 4

Operational Procedure

4.1 GENERAL DISCUSSION

During the three shots participated in by Project 8.3A, the placing of the aircraft was at the discretion of Project 8.1 since the basic purpose of the aircraft was to obtain blast-effect data. In order to ensure proper positioning of the aircraft, it was necessary for the radar operator to use the APQ-24 system as a navigational device up to within 30 sec of shot time. During the 30 sec before shot time it was the duty of the radar operator to readjust the APQ-24 system so that the receiver gain was at the predetermined level, adjust the antenna to scan the area which had been predesignated, and adjust the antenna tilt to obtain optimum radar illumination of this area. In addition, if time permitted, the operator was to place accurately the cross hairs from the APA-44 on the shot tower and to permit them to track this point. This was done in order to obtain an exact record of its distance from the aircraft.

An operator to control the special equipment, in the meantime, would have turned on the A-scope and associated equipment at the predetermined time and, shortly before detonation, would check the A-scope intensity, focus, A-trace positioning, and lineal length. Shortly before detonation time the switch which controlled the camera drive motor was placed in the automatic position, and time hack over the communication system of the aircraft was monitored. At time zero − 5 sec the camera started automatically and continued until the film was exhausted. Film running time was approximately 35 sec for the high-speed camera and 45 sec for the low-speed camera. If, at time zero − 5 sec, the light indicating the start of the cameras did not operate, it was the duty

of the operator to throw the camera control switch to the override position and start the cameras manually. During all three tests the automatic camera starting functioned properly, and manual operation was not required.

4.2 AIRCRAFT POSITIONING

4.2.1 Aircraft 340 and 290, Dog Shot
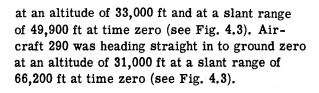
During Dog Shot, aircraft 340 was heading straight toward the shot tower at the time of detonation. Operational plans called for this aircraft to be at an altitude of 29,000 ft and at a slant range of 51,520 ft at the time of detonation (see Fig. 4.1). The flight plan for aircraft 290 required this aircraft to fly at an altitude of 29,000 ft on a course displaced 29,000 ft from the tower at a slant range of 43,100 ft from ground zero at the time of detonation (see Fig. 4.1).

4.2.2 Aircraft 340 and 290, Easy Shot

On Easy Shot the operational plan for aircraft 340 called for a flight path parallel to a line through the tower but displaced 19,000 ft and at an altitude of 19,000 ft. Slant range from ground zero at time zero was to be 27,970 ft (see Fig. 4.2). Aircraft 290 was to fly on a path directly over ground zero at an altitude of 25,000 ft and to have just passed over the target by 7,940 ft at the time of detonation (see Fig. 4.2).

4.2.3 Aircraft 340 and 290, George Shot

On George Shot, plans called for aircraft 340 to be flying on a path parallel to a line drawn through ground zero and displaced 33,000 ft and

at an altitude of 33,000 ft and at a slant range of 49,900 ft at time zero (see Fig. 4.3). Aircraft 290 was heading straight in to ground zero at an altitude of 31,000 ft at a slant range of 66,200 ft at time zero (see Fig. 4.3).

4.3 FILM PROCESSING

Upon return of the planes to the base after each mission, film was removed from all cameras and magazines and processed as follows:

High-speed recording camera	11 min, D-19
Low-speed recording camera, Type A-4	9 min, D-19
Radar-scope camera, Type O-15	12 min, D-76

Negatives thus processed were found to be of sufficient density to permit further analysis.

Chapter 5

Experimental Data and Discussion

5.1 GENERAL DISCUSSION

During the first mission all equipment operated satisfactorily, and recorded data were obtained. However, on one aircraft the operator was unable to center the sector scan on ground zero in the 30-sec time interval available, but the plane was sufficiently close to obtain satisfactory results.

On Easy Shot the receivers were not set to the predetermined levels at the time of detonation, thus necessitating recalibration upon return of the aircraft in order to obtain the desired results. All equipment, however, operated as planned, and recorded data were found to be satisfactory.

On George Shot the radar set failed to function in one aircraft owing to the failure of air pressure from the air pump. In the second aircraft the high-speed camera jammed shortly after starting, and the O-15 camera failed shortly before time zero. However, the low-speed camera functioned properly, and satisfactory data were obtained for analysis.

Initial examination of the processed film revealed that radar returns had been received as a result of the effects of the detonation during all tests.

Photographic data obtained by the operational procedure previously described consisted of 35-mm negatives of the PPI display and, in the case of the low-speed camera, sequential frames of the A-scope. In the cases where a film speed of 32 frames/sec was used, each frame consisted of approximately 16 pulses integrated on the film. The resulting film from the high-speed camera consisted of a record of the radar returns from each individual transmitted pulse.

In the case of the A-scope film, in order to obtain range and amplitude data, the film was projected on the ground-glass screen of an Eastman Recordax viewer. Prior to making these measurements, the proper calibration film, which had been previously run through each camera, was projected on the Recordax screen, and the range and amplitude factors were marked on the screen so that direct readings could be made on the film under examination.

During the period in which this report was in preparation, time limitations permitted only a relatively close examination and analysis of the data obtained from the film of the low-speed camera. This work was confined to only three of the records obtained: aircraft 340 on Dog Shot and both aircraft 340 and 290 on Easy Shot. The film from the high-speed camera was used to determine only the general nature of the data. A more complete analysis remains to be accomplished at a later date.

During the process of reading the data it was necessary to correlate directly a particular frame of the A-trace with the corresponding scan of the PPI photographs. Fortunately in most cases sufficient reference points were found to permit this to be accomplished. By the use of the azimuth marker light, which was recorded on the edge of the film for both the high- and low-speed cameras, it was possible to determine which frame of the low-speed camera was exposed as the antenna illuminated ground zero during its scan period. By the use of the 100-cycle timing markers, which were recorded on the other edge of the film, it was possible to determine within 0.05 sec the time when the antenna was in this position. Once these frames had been determined for the

various successive sector scans, the range, amplitude, and time measurements of the radar return of interest were taken and tabulated. One of the difficulties found when attempting to obtain accurate range data from the A-scope recordings was the problem of finding the exact position of the leading edge of the returning echo. The returned echoes were found to contain many modulation components which caused large changes in amplitude between successive pulses. This also affected the position of the leading edges. Fortunately the A-scope recordings consisted of a number of integrated pulses which tended to reduce this problem but did not entirely eliminate it.

Once these integrated-pulse data were obtained, graphs of the various conditions were plotted to determine the general trend of the data. Graphs of the returns produced by the shock wave, giving slant range from the aircraft as a function of time, were plotted, and an average curve for each shot was drawn. In addition, when it was found that the computer cross hairs had been tracking properly on the general ground track of the aircraft, the aircraft distance as a function of time also was plotted to determine its velocity. With these data it was then possible to make an estimate of the radar-return position and effective velocity and, in general, to compare these data with those obtained from theoretical and measured shock-wave propagation data.

5.2 RESULTS, AIRCRAFT 340, DOG SHOT

Figure 5.1 shows a graph of the data obtained from the low-speed camera photographs taken in aircraft 340 on Dog Shot. The return due to the effects of the shock wave was visible for 36 scans of the antenna over a time period of 23 sec. At this point the distance of the return exceeded the range of the A-scope, and further range data were not recorded.

Curve A is a graph of time vs slant range from the radar return progressing away from the aircraft as measured on a line from the aircraft through ground zero. Curve B is that caused by the effects of the shock wave measured on the same line as Curve A but with the shock wave advancing at a decreasing slant range with respect to the aircraft. Curve C is a graph of the computer range mark tracking the

ground but displaced from the shot tower. This displacement was due to the fact that the operator did not have sufficient time to place the cross hairs directly on the tower before time zero. Curve D is the range to the shot tower as seen up until time zero by the radar. From Curves C and D a ground speed for this aircraft as it approached ground zero was determined to be 405 ± 4 ft/sec.

The antenna scan over point zero nearest time zero occurred at time zero + 0.21 sec. The photographic recording of this scan did not indicate any new returns from point zero. However, the return from the shot tower which is visible on earlier antenna scans is missing from this recording. The first radar return recorded on the radar PPI was seen at time zero + 0.85 sec (see Fig. 5.2). As will be noted on this photograph, a return is not visible on the far side of point zero. The A-trace below the PPI photograph in Fig. 5.2 is the A-trace photograph obtained as the radar set was looking across ground zero. The trace presented immediately below the A-trace is that of the 1,500-ft calibration markers which had been obtained during the scope calibration procedure. It will be noted that there are no radar echoes visible on the A-trace immediately beyond point zero. This suggests that there is considerable attenuation of the radar signal in this region during this time period.

On the second scan of the radar system over ground zero, which occurred at time zero + 1.45 sec, the conditions mentioned above still persisted, but the effect causing the radar return has moved closer to the aircraft and farther from point zero. This is visible in Fig. 5.3. Immediately below the PPI photograph are the A-trace and calibration markers corresponding to those presented in Fig. 5.2.

It was not until the antenna scanned over ground zero at time zero + 2.12 sec that radar returns were visible for the entire 360° around ground zero (see Fig. 5.4). It will be noted in this figure, on both the PPI photographs and the A-trace, that the radar return is moving away from point zero.

Figures 5.5 and 5.6, taken at times zero + 6.56 and zero + 10.27 sec, respectively, show the development of this return as it progresses outward from ground zero.

The data plotted in Fig. 5.1 were then used to obtain a graphical solution of the most probable

position of the radar return. Figure 5.7 is a graph of this solution. Referring to Fig. 5.7, it will be noted that the horizontal axis of this graph represents ground distance, and the vertical axis represents altitude. From the data obtained with the A-scope recordings it was found that the aircraft was at an average altitude of 29,400 ft. The positions of the aircraft at 2- and 4-sec intervals, beginning at time zero, are represented by the successive positions indicated on the upper right-hand corner of this graph. From each of these positions an arc was drawn whose radius was proportional to the slant range between the aircraft and radar returns as obtained from Fig. 5.1. The position of ground zero marked on the horizontal axis was obtained in a similar manner from the extrapolation of data from Fig. 5.1. From this ground-zero point the position of the shock wave at the indicated time intervals was drawn to the proper scale shown in broken lines on the graph. The various positions of the shock wave are based on a theoretical 90-kt yield. The positions of the shock wave for the fractional time periods (0.96, 2.00, 2.99, and 4.14 sec) were extracted from Table 3.1 of NOBL Summary Report of Blast Measurements (Operation Greenhouse). It will be noted that the shock-wave positions and the planes to which the radar returns were measured are approximately coincident on the ground surface. For all cases in which the distance to the shock wave is increasing with respect to the aircraft, the position of the measured return and that of the shock wave coincided, at or near the ground level, within approximately 400 ft during the time intervals recorded.

For those cases in which the return from the effects of the shock wave was moving toward the aircraft, considering the effect to be located on or near the ground surface, coincidence with the shock wave within 600 ft during the time intervals recorded was indicated. However, beyond approximately 8 sec elapsed time it is believed that the radar data deteriorated rapidly, probably owing to poor radar aspect angle, and hence should not be relied upon. The possibility that considerable refraction of the r-f energy occurs may account for the fact that the radar distance is slightly longer than the actual distance to the shock wave at ground level. As will be noted from the

A-scope photographs of the radar return, the general character of the return pulses indicated reflections due to either particle dispersion or a similar complex reflective surface. Such a surface could also result if refraction resulted in multipath propagation.

Since point zero was determined by extrapolation of radar data on the effective distance of the shot tower (see Fig. 5.1) and all shock-wave positions were then plotted relative to this point, it is evident that resultant errors will appear in the apparent positions of the shock wave.

Data from which the graphs in Figs. 5.1 and 5.7 were obtained may be found in tabular form in Appendixes A and B of this report.

5.3 RESULTS, AIRCRAFT 290, DOG SHOT

Data obtained from aircraft 290 during Dog Shot appeared, on a preliminary examination, to have the same trend as that obtained from aircraft 340. Time has not permitted a more complete reading and plotting of these data.

5.4 RESULTS, AIRCRAFT 290, EASY SHOT

The data from both aircraft during Easy Shot were read, tabulated, and plotted to obtain a further extension to the data from aircraft 340 on Dog Shot.

Aircraft 290 at time zero was flying at an altitude of approximately 25,300 ft, as determined by measurements made on the A-scope recordings and was found to be 9,630 ft ground range beyond point zero. During this period the PPI was displaying a relatively poor picture of the ground terrain owing to the poor aspect angle from which the target was illuminated and probably owing also to a high bias setting on the cathode-ray-tube indicator. However, examination of the photographs indicated that the range marker, although tracking the ground surface properly, had not been set on ground zero at the time of detonation. A graph of the range marker as shown on Fig. 5.8 was used to determine the ground speed of the aircraft, which was 393.4 ± 4 ft/sec. Examination of the PPI photographs and comparison with aeronautical maps of this area enabled an estimation to be made of the displacement error of the range marker. This was obtained by pro-

jecting the PPI image, obtained approximately 30 sec after detonation, on the map. The scale factor which gave the best possible coincidence of the outline of Engebi was found. A measurement was then made directly on the map to determine the ground-range displacement of the range marker. This was estimated to be 1,000 ±200 ft. A graph of the range marker, corrected for this amount and based on the preceding ground speed, is shown in Curve D of Fig. 5.8. Data as read from the A-scope of the effects of the shock wave as it moved away from the aircraft are plotted in Fig. 5.8, and the data in tabular form are given in Appendix C. These data and those presented from aircraft 340 on Dog Shot consisted of range-only data as the antenna crossed over ground zero.

Owing to the very high aspect angle at which the radar was viewing ground zero and normal water return below the aircraft, it was not possible to read accurately the range to the reflection from shock wave as it progressed toward the aircraft from ground zero. Although this return was visible on the A-trace, it could not be measured with sufficient accuracy to warrant plotting.

The first scan of the antenna over ground zero occurred at approximately 0.35 sec. Examination of the PPI photograph at this time interval did not indicate any visible return. This may have been due to a lack of return, improper bias setting on the PPI, or possibly an excessive delay set in the altitude delay circuit of the APS-23. Examination of the A-scope and the PPI pictures at this time did not indicate sufficient information to permit close correlation between A-trace photographs and those obtained on the PPI.

The first measurement of the shock wave which was visible on the A-scope was made at 1.13 sec after detonation. Figure 5.9 is a photograph of the PPI, the A-scope, and calibration markers taken at approximately this time. The return due to the effects of the shock wave appeared initially to propagate outwardly at a very rapid rate. This apparent high speed was probably due to the short scale factor of the PPI caused by the relative position of the aircraft with the point being tracked. A photograph of the PPI taken as the antenna swept across point zero at approximately 11 sec is shown in Fig. 5.10 with the accompanying A-scope and calibration-marker photographs.

The return was visible and readable on the A-trace up to 17.8 sec, at which time the return was at a range greater than that recordable on the A-scope.

During this shot the A-scope in aircraft 290 was operating without any trigger delay so that both the transmitter pulse and the pulse caused by the first return from below the aircraft were visible. In both Figs. 5.9 and 5.10 the high-amplitude pulse appearing in the center of the A-trace is the first ground return from directly below the aircraft. The small pulse appearing just to the right of this pulse in Fig. 5.9 was the first radar return detected from this aircraft. An effort was made to determine whether the effects which caused the radar return were at any time at a range shorter than that of the first ground (or water) return directly below the aircraft. Examination of the A-scope, both in a Recordax and by rapid playback in a Moviola, indicated that the return was visible at a slant range less than that to ground zero and was propagated such that this distance decreased with time. However, owing to the large amount of water return recorded, the return was very indistinct, and no evidence has been found that it propagated to a point at which the range was shorter than the altitude of the aircraft.

The data obtained as a result of Fig. 5.8 were used to plot Fig. 5.11 in a manner similar to that used to plot Fig. 5.7 obtained from aircraft 340 on Dog Shot. Data for this graph are given in tabular form in Appendix D.

As in Dog Shot, it was found by the use of Fig. 5.11 that, when comparing the data available on the theoretical position of the shock wave for a 50-kt yield, correlation between the shock-wave position on the surface and that measured by the radar in the aircraft coincided to within 400 to 600 ft. In most cases coincidences are within 400 ft, but two points, measured at 1 and 8 sec, indicate that the shock wave preceded the radar return by 600 ft. The generally random nature of these range discrepancies indicates measuring-technique errors. However, similar discrepancies may have been due to the radar signal propagating through a region which caused considerable refraction. This possibility could not be determined owing to the incompleteness of the data and the complex nature of the radar return as recorded on the A-trace. However, all available data after

4 sec indicate that the return comes from the surface or a region near the earth's surface. The shock-wave position at time intervals of 1.09 and 2.06 sec are from actual measurements.

5.5 RESULTS, AIRCRAFT 340, EASY SHOT

During Easy Shot, for aircraft 340, which was flying nearly tangent to the blast at time zero, both PPI and A-scope recordings were obtained. Examination of the PPI photographs showed that the computer cross hairs, both range marker and azimuth marker, had not been placed directly on ground zero, thereby introducing an error in the range-marker data which were to be used for determining the rate of closure with respect to ground zero. It was, however, possible to get an estimate of the function of the aircraft's rate of closure with respect to ground zero.

The tower from which Easy Shot was detonated and its local surroundings were recorded on the A-scope up until time zero. By plotting the range on this tower it was possible to locate ground zero with reasonable accuracy and to extrapolate the movement of the aircraft relative to ground zero. These points were plotted in Fig. 5.12, and a slant range of approximately 27,800 ft was determined at a time slightly less than time zero. The first return was seen at 0.47 sec after detonation as the antenna swept over ground zero. However, this return was indistinct as recorded on the A-scope, and accurate range measurements could not be made (see Fig. 5.13). The first accurate range measurements were made when the antenna swept over ground zero at time zero + 0.97 sec (see Fig. 5.14). Distances were then recorded as the shock wave propagated both away from and toward the aircraft with respect to ground zero. Measurements at a time interval beyond time zero + 10 sec on the return between the aircraft and ground zero could not be made with satisfactory accuracy since the return was hidden owing to the return from the water surface below the aircraft. The return

from beyond point zero was seen up until 18 sec, at which time it exceeded the range-measuring capabilities of the A-scope. Figures 5.15 and 5.16 are photographs of the PPI, A-trace, and calibration markers of the return as it was recorded 3.60 and 6.20 sec after time zero.

Data on Fig. 5.12 were used to plot Fig. 5.17 in an effort to determine the position of the radar return. A study of this figure shows that the correlation between the radar return and the ground position of the shock wave is similar to that obtained from Fig. 5.7 (aircraft 340, Dog Shot) and Fig. 5.11 (aircraft 290, Easy Shot).

Of interest is the PPI photograph which was obtained during Easy Shot from aircraft 340 in Fig. 5.14. Measurements of the distance of the leading edge of the radar return indicated that it extended over the land area of Engebi. This was substantiated by projecting the photograph of the PPI on a map of the area and adjusting the scale factor to obtain best possible coincidence of the island. Figure 5.18 is a composite photograph showing the PPI superimposed on this map. Although perfect coincidence could not be obtained owing to distortion existing in the PPI, it was obtained to a sufficient degree to indicate that the return was over the land area. The exact cause of the return could not be determined, but the A-scope photographs indicate a complex return probably due to either multiple-path propagation, refraction, or particle dispersion.

5.6 RADAR-RETURN AMPLITUDE MEASUREMENTS

Measurements of the amplitude of the returning echoes were tabulated and studied, but direct correlation with yield has not been possible to date. Although partial examination of amplitude data as a function of time failed to reveal positive trends, characteristics common to all three recordings appeared to exist during the first few seconds after detonation.

Chapter 6

Summary

During Operation Greenhouse it was conclusively proved that, under the conditions which existed at the Eniwetok Atoll during the time period in which Operation Greenhouse was conducted, detonations of relatively high-yield atomic explosions were easily detected and displayed on the PPI of an X-band radar system. It was determined that the observed radar returns were probably near the earth's surface after a time period of 3 to 4 sec. Earlier returns may not have been located at the earth's surface since radar A-scope photographs indicated that the general characteristics of the returns were caused by either particle dispersion or by complex refraction and reflection of the energy radiated by the radar system.

Data obtained in all three cases revealed that the position of the phenomenon causing the radar return was within the instrumental measuring accuracy of the predicted position of the leading edge of the shock wave.

The return, when examined at a longer time interval after detonation, indicated that an appreciable amount of it may have been coming from the surface of the water. This was noticed on the water area over which the shock wave had previously traversed.

Under the conditions which existed during these tests it was found to be possible, by extrapolating the available data, to locate ground zero to an accuracy of approximately 500 ft. If similar data can be obtained over land areas regardless of climatic conditions, it appears feasible to expect that the above-mentioned tolerance can be reduced by properly designed equipment.

The possibility of determining yield within a reasonable degree of accuracy by this method will also depend on the ability to obtain satisfactory radar echoes from a detonation over a land area.

In the case of aircraft 340 during Easy Shot it was established with reasonable certainty that a radar return was obtained over the land area of the island of Engebi.

The exact cause and conditions required to obtain a radar return were not established during the period in which this report was under preparation.

It is recommended that similar tests be conducted over land areas with equipment designed on the basis of data obtained during Greenhouse. It is also recommended that further latitude be given to the positioning of aircraft and possibly ground equipment in order to obtain the desired data.

Appendix A

Tabular Data, Fig. 5.1

DATA FROM LOW-SPEED CAMERA, A-SCOPE RECORDINGS, FROM AIRCRAFT 340, DOG SHOT

Time* (sec)	SR(A)† (ft)	SR(B)‡ (ft)	SR(C)§ (ft)	SR(D)¶ (ft)	Time* (sec)	SR(A)† (ft)	SR(B)‡ (ft)	SR(C)§ (ft)	SR(D)¶ (ft)
−3.65			53,800	54,450	+10.27	63,300	38,650	49,000	
−2.97			53,500	54,300	+10.99	63,500	38,300	48,700	
−2.38			53,125	54,050	+11.55	63,950	37,650	48,550	
−1.70			52,900	53,800	+12.23	64,550	37,100	48,400	
−1.10			52,750	53,700	+12.84	65,200	36,350	48,150	
−0.42			51,650	53,225	+13.51	65,550	35,700	47,950	
+0.21					+14.08	66,000	34,900	47,700	
+0.85		51,075	51,950		+14.79	66,300	34,400	47,500	
+1.45		49,925	51,700		+15.36	68,800	34,375	47,300	
+2.12	57,400	48,700	51,525		+16.07	67,200	34,050	47,000	
+2.73	58,100	48,100	51,300		+16.64	67,650	33,650	46,825	
+3.40	58,300	47,100	51,150		+17.31	67,975	32,900	46,650	
+4.00	58,825	46,200	50,900		+17.91	68,500	32,775	46,425	
+4.67	59,100	45,200	50,725		+18.58	69,000	32,100	46,150	
+5.28	59,425	44,600	50,700		+19.18	69,350	32,150	46,050	
+5.95	60,400	43,700	50,400		+19.85	69,650	32,100	45,800	
+6.56	60,550	42,950	50,250		+20.46	59,850		45,700	
+7.27	60,850	42,150	49,900		+21.13	70,200		45,475	
+7.84	61,700	41,500	49,800		+21.69	70,400		45,200	
+8.52	61,900	40,800	49,600		+22.44	70,850		44,900	
+9.09	62,350	40,200	49,500		+23.00	71,400		44,650	
+9.70	62,650	39,300	49,250		+23.71			44,550	

*All times are measured with reference to time zero.

†SR(A) refers to slant range as shown graphically by Curve A, Fig. 5.1. This is the distance from the aircraft to the most distant radar return caused by the shock wave at the instant the radar antenna swept over ground zero.

‡SR(B) refers to slant range as shown graphically by Curve B, Fig. 5.1. This is the distance from the aircraft to the nearest radar return caused by the shock wave at the same instant.

§SR(C) refers to slant range as shown graphically by Curve C, Fig. 5.1. This is the distance from the aircraft to the point on the ground which the radar was tracking.

¶SR(D) refers to the slant range as shown on Curve D, Fig. 5.1. This is the slant range from the aircraft to the shot tower.

Appendix B

Tabular Data, Fig. 5.7

DATA FOR OBTAINING 1-SEC-
INTERVAL READINGS*

Time (sec)	SR(A) (ft)	SR(B) (ft)
0	53,225	53,225
1	56,100	50,725
2	57,350	49,025
3	58,075	47,550
4	58,800	46,200
5	59,475	44,925
6	60,180	43,650
7	60,875	42,475
8	61,625	41,350
9	62,325	40,275
10	63,075	39,250
11	63,800	38,250
12	64,525	37,175
13	65,175	36,175
14	65,850	35,250
15	66,525	34,425
16	67,175	33,675
17	67,850	
18	68,550	
19	69,825	

*Data are extracted from Curves A and B of Fig. 5.1 and are shown plotted in Fig. 5.7. The symbols are explained in Appendix A.

Appendix C

Tabular Data, Fig. 5.8

DATA FROM LOW-SPEED CAMERA FROM AIRCRAFT 290, EASY SHOT

Time* (sec)	SR(A)† (ft)	SR(C)‡ (ft)	Time* (sec)	SR(A)† (ft)	SR(C)‡ (ft)
0.00	27,070	26,730	9.48	36,925	28,150
1.13	28,950	26,900	10.04	37,800	28,250
1.70	29,500	26,900	10.86	38,675	28,350
2.49	29,800	26,900	11.46	39,500	28,450
3.11	30,300	27,000	12.24	40,500	28,550
3.83	31,050	27,100	12.92	41,250	28,775
4.45	31,800	27,250	13.64	42,250	28,900
5.25	32,500	27,350	14.30	43,050	29,050
5.89	32,950	27,550	15.01	44,000	29,225
6.65	33,750	27,650	15.71	45,075	29,325
7.25	34,450	27,750	16.45	46,000	29,475
8.03	35,250	27,900	17.07	46,800	29,575
8.59	36,125	28,025			

*All times are measured with reference to time zero.

†SR(A) refers to slant range (ft) shown graphically by Curve A, Fig. 5.8. It is the distance from the aircraft to the most distant radar return produced by the shock wave at the instant the antenna swept over ground zero.

‡SR(C) refers to slant range (ft) shown graphically by Curve C, Fig. 5.8. It is the distance from the aircraft to the point on the ground which the radar is tracking.

A third curve (Curve D) will be noted on Fig. 5.8. This is a curve drawn through three theoretical points which represent the slant range from the aircraft to point zero. These points were calculated on the basis of the range marker's being 1,000 ft displaced from ground zero and on a ground speed of 393.4 ft/sec.

These points were plotted using the following values:

Time (sec)	SR to Ground Zero (ft)
0	27,070
2	27,358
4	27,669

Appendix D

Tabular Data, Fig. 5.11

DATA FOR OBTAINING 1-SEC-
INTERVAL READINGS*

Time (sec)	SR(A) (ft)
0	27,070
1	28,825
2	29,600
3	30,275
4	31,300
5	32,225
6	33,175
7	34,225
8	35,325
9	36,475
10	37,625
11	38,875
12	40,125
13	41,400
14	42,675
15	44,000
16	45,375
17	46,775

*Data are extracted from Curve A of Fig. 5.8 and are shown plotted in Fig. 5.11. The symbols are explained in Appendix C.

Appendix E

Tabular Data, Fig. 5.12

DATA FROM LOW-SPEED CAMERA, A-SCOPE RECORDINGS, FROM
AIRCRAFT 340, EASY SHOT

Time* (Sec)	SR(A)† (ft)	SR(B)‡ (ft)	SR(D)§ (ft)	Time* (Sec)	SR(A)† (ft)	SR(B)‡ (ft)	SR(D)§ (ft)
–4.72			28,200	+7.05	35,900	21,600	
–4.21			28,200	+7.54	36,400	21,400	
–3.39			28,100	+8.38	37,450	21,300	
–2.88			28,100	+8.85	37,950	21,100	
–2.08			28,000	+9.70	38,700	21,000	
–1.60			27,950	+10.14	38,700		
–0.80			27,900	+11.07	40,000		
–0.32			27,800	+11.55	40,500		
+0.47				+12.42	41,400		
+0.97	29,950	25,850		+12.85	42,025		
+1.80	31,150	25,250		+13.73	42,750		
+2.30	31,375	24,700		+14.20	43,400		
+3.13	32,250	24,200		+15.06	44,000		
+3.60	32,900	23,700		+15.46	44,700		
+4.43	33,700	23,100		+16.41	45,500		
+4.90	34,100	22,850		+16.80	45,900		
+5.75	34,825	22,500		+17.71	46,800		
+6.20	35,150	22,100		+18.09	47,250		

*All times are measured with reference to time zero.

†SR(A) refers to slant range as shown by Curve A, Fig. 5.12, and is the distance from the aircraft to the most distant return produced by the shock wave at the instant the antenna swept over ground zero.

‡SR(B) refers to slant range as shown by Curve B, Fig. 5.12, and is the distance from the aircraft to the nearest radar return produced by the shock wave.

§SR(D) is the slant range shown plotted on Curve D, Fig. 5.12, and is the slant range from the aircraft to the shot tower.

Appendix F

Tabular Data, Fig. 5.16

DATA FOR OBTAINING 1-SEC-
INTERVAL READINGS*

Time (sec)	SR(A) (ft)	SR(B) (ft)
0	27,800	27,800
1	29,975	25,900
2	31,375	24,975
3	32,300	24,200
4	33,275	23,475
5	34,200	22,800
6	35,175	22,225
7	36,150	21,725
8	37,125	21,325
9	38,100	20,975
10	39,100	20,775
11	40,075	
12	41,075	
13	42,075	
14	43,075	
15	44,060	
16	45,050	

*Data are extracted from Curves A and B of
Fig. 5.12 and are shown plotted in Fig. 5.16.
The symbols are explained in Appendix E.

Bibliography

1. Handbook Maintenance Instructions for Radar Set AN/APS-23, No. CO-AN16-30 APS23-3, USAF official publication (Confidential).
2. Handbook Maintenance Instructions for Ground-position Indicator AN/APA-44, No. CO-AN16-30APA44-3, USAF official publication (Confidential).
3. Manual of Operation Instructions for the DuMont Type 294-A Cathode-ray Oscillograph, Allen B. DuMont Laboratories, Inc., Clifton, N. J.
4. Handbook of Instructions, Bomb-spotting Aircraft Camera, Type A-4, No. AN 10AA-4, USAF official publication.
5. Handbook Operation and Service Instructions, Type O-15 Recording Camera, No. AN 10-10EA-9, USAF official publication.
6. Handbook of Maintenance Instructions for Signal Generator TS-35A/AP, No. AN 16-35TS35-2, USAF official publication.
7. Handbook of Maintenance Instructions for Range Calibrator TS-102/AP, No. AN 16-35TS102-2, USAF official publication.
8. H. G. Booker and W. E. Gordon, A Theory of Radio Scattering in the Troposphere, Proc. Inst. Radio Engrs. and Waves and Electrons. Sect. I. Proc. I.R.E., 38: 401-412 (1950).
9. A. W. Friend, Theory and Practice of Tropospheric Sounding by Radar, Proc. Inst. Radio Engrs. and Waves and Electrons. Sect. I. Proc. I.R.E., 37: 116-138 (1949).
10. J. P. Day and L. G. Trolese, Propagation of Short Radio Waves over Desert Terrain, Proc. Inst. Radio Engrs. and Waves and Electrons. Sect. I. Proc. I.R.E., 38: 165-175 (1950).
11. M. Katzin, R. W. Bauchman, and W. Binnian, 3- and 9-Centimeter Propagation in Low Ocean Ducts, Proc. Inst. Radio Engrs. and Waves and Electrons. Sect. I. Proc. I.R.E., 35: 891-905 (1947).
12. C. L. Pekeris, Wave Theoretical Interpretation of Propagation of 10-Centimeter and 3-Centimeter Waves in Low-Level Ocean Ducts, Proc. Inst. Radio Engrs. and Waves and Electrons. Sect. I. Proc. I.R.E., 35: 453-462 (1947).
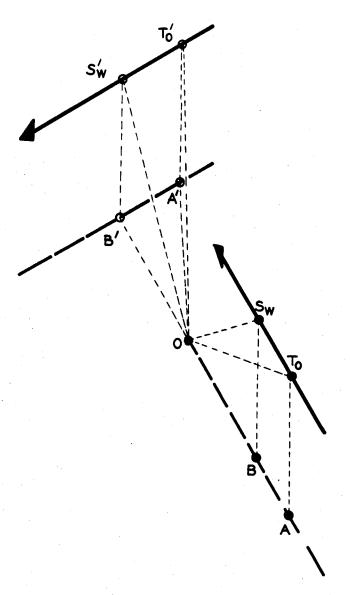
Fig. 4.1   Flight Plan for B-50D Aircraft 340 and 290, Dog Shot

——	Air paths of aircraft	OS_W	= 40,890 ft
- - -	Ground paths of aircraft	OT_0	= 51,520 ft
T_0	Position of aircraft 340 at time zero	OB	= 29,000 ft
S_W	Position of aircraft 340 when coincident with shock wave	BA	= 13,600 ft
		AT_0	= 29,000 ft
T_0'	Position of aircraft 290 at time zero	OS_W'	= 40,890 ft
S_W'	Position of aircraft 290 when coincident with shock wave	OT_0'	= 43,100 ft
		OB'	= 29,000 ft
O	Position of shot tower	$B'A'$	= 13,600 ft
		$A'T_0'$	= 29,000 ft
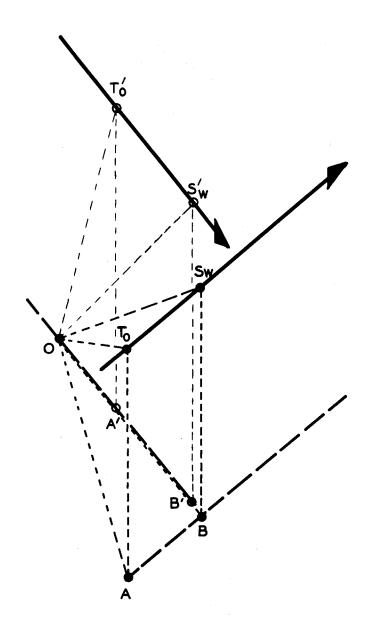
Fig. 4.2   Flight Plan for B-50D Aircraft 340 and 290, Easy Shot

——	Air paths of aircraft	OS_w	= 26,870 ft
- - -	Ground paths of aircraft	OT_0	= 27,970 ft
T_0	Position of aircraft 340 at time zero	OB	= 19,000 ft
S_w	Position of aircraft 340 when coincident with shock wave	BA	= 7,755 ft
		AT_0	= 19,000 ft
T_0'	Position of aircraft 290 at time zero	OS_w'	= 30,800 ft
S_w'	Position of aircraft 290 when coincident with shock wave	OT_0'	= 26,210 ft
		OB'	= 18,000 ft
O	Position of shot tower	$B'A'$	= 10,060 ft
		$A'T_0'$	= 25,000 ft
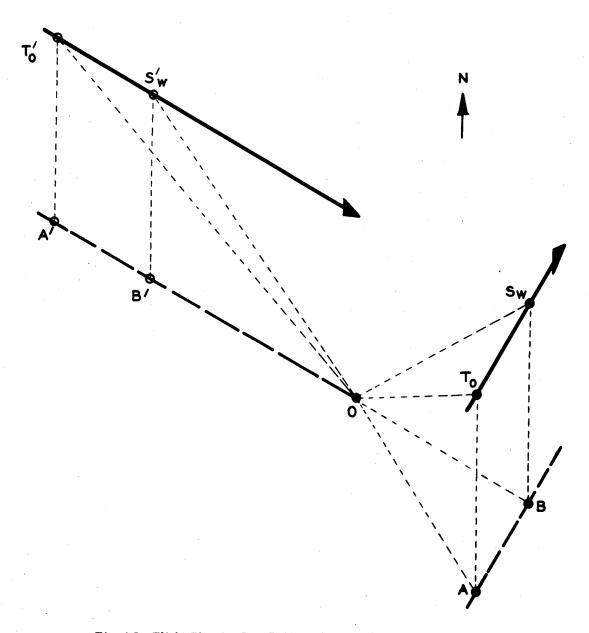
Fig. 4.3 Flight Plan for B-50D Aircraft 340 and 290, George Shot

——	Air paths of aircraft	OS_w	= 46,670 ft
---	Ground paths of aircraft	OT_0	= 49,900 ft
T_0	Position of aircraft 340 at time zero	OB	= 33,000 ft
S_w	Position of aircraft 340 when coincident with shock wave	BA	= 17,580 ft
		AT_0	= 33,000 ft
T_0'	Position of aircraft 290 at time zero	OS_w'	= 50,610 ft
S_w'	Position of aircraft 290 when coincident with shock wave	OT_0'	= 66,200 ft
		OB'	= 40,000 ft
O	Position of shot tower	$B'A'$	= 18,530 ft
		$A'T_0'$	= 31,000 ft
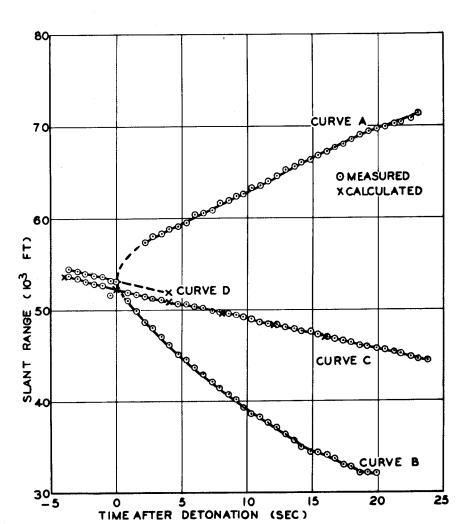
Fig. 5.1 Distance of Radar Returns as a Function of Time as Recorded in Aircraft 340 During Dog Shot. Distances are measured on a line from the aircraft through ground zero. Curve A is for radar returns beyond ground zero. Curve B is for radar returns between the aircraft and ground zero. Curve C is distance to AN/APA-44 range tracking marker. Curve D is the recorded effective distance to the shot tower.
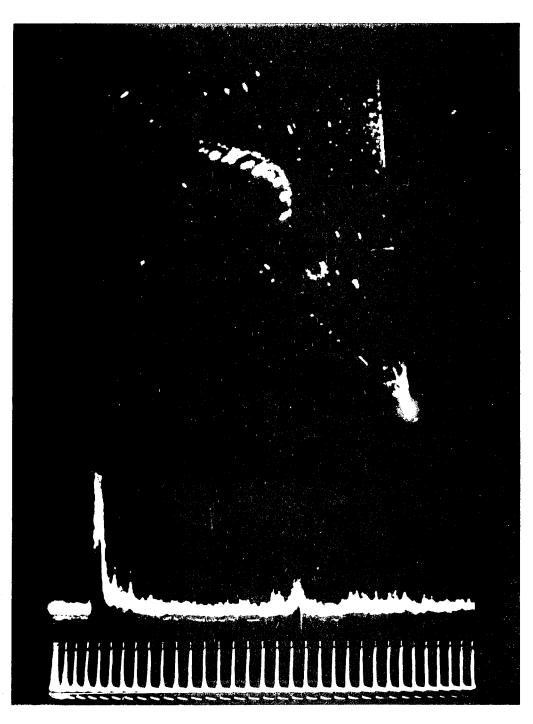
Fig. 5.2 Radar Displays Photographed in Aircraft 340, Dog Shot, at 0.85 Sec after Detonation. Top photograph is that of the PPI. Note semicircular-shaped radar return between aircraft and point zero. Center photograph is that of A-scope. Bottom, A-scope calibration marks (1,500 ft).
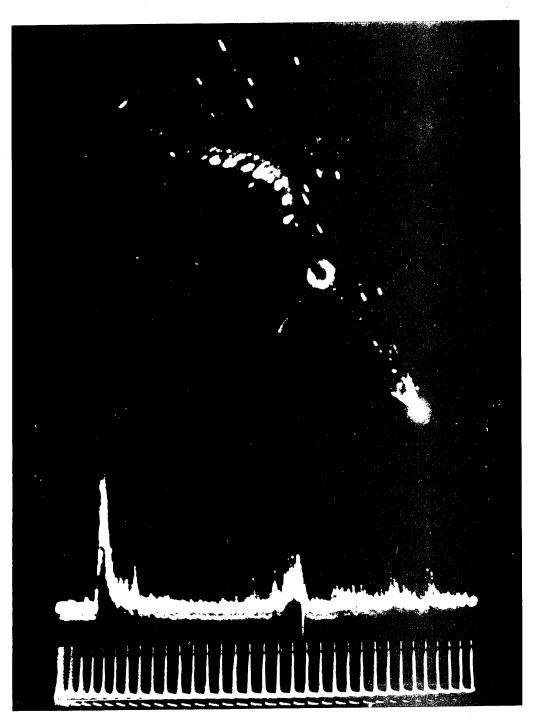
Fig. 5.3 Radar Displays Photographed in Aircraft 340, Dog Shot, at 1.45 Sec after Detonation. Top photograph is that of the PPI. Note radar return has increased beyond that visible in Fig. 5.2 and encircles point zero for approximately 270°. Center photograph is that of A-scope. Bottom, A-scope calibration marks (1,500 ft).
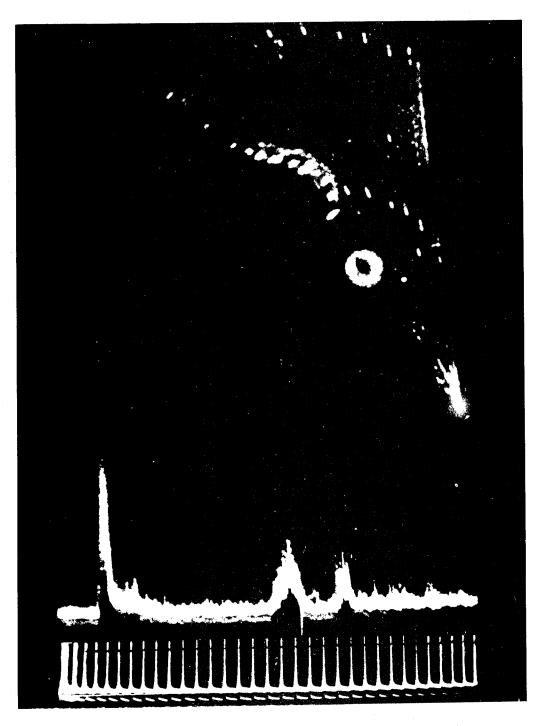
Fig. 5.4 Radar Displays Photographed in Aircraft 340, Dog Shot, at 2.12 Sec after Detonation. **Top** photograph is that of the PPI. Note radar return is now visible completely around point zero and is moving outward. Center photograph is that of A-scope. Bottom, A-scope calibration marks (1,500 ft).
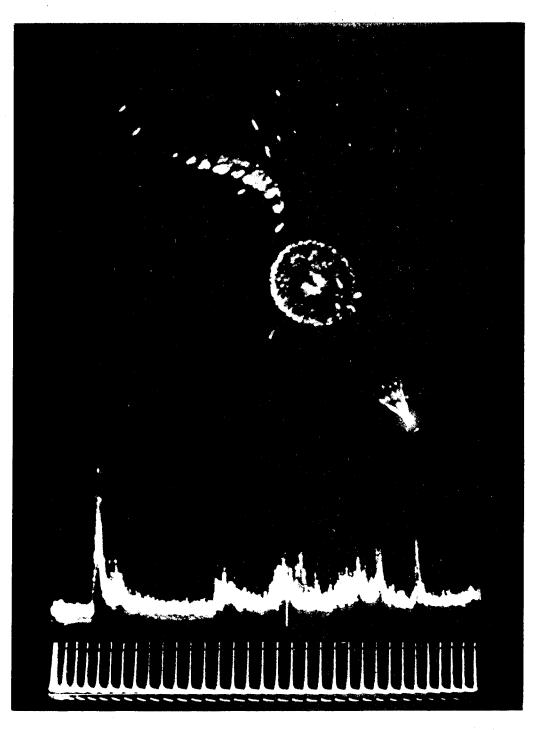
Fig. 5.5 **Radar Displays Photographed in Aircraft 340, Dog Shot, at 6.56 Sec after Detonation. Top** photograph is that of the PPI. Radar return now occurs further outward from point zero **and has ragged** edges. Center photograph is that of A-scope. Bottom, A-scope calibration marks (1,500 ft).
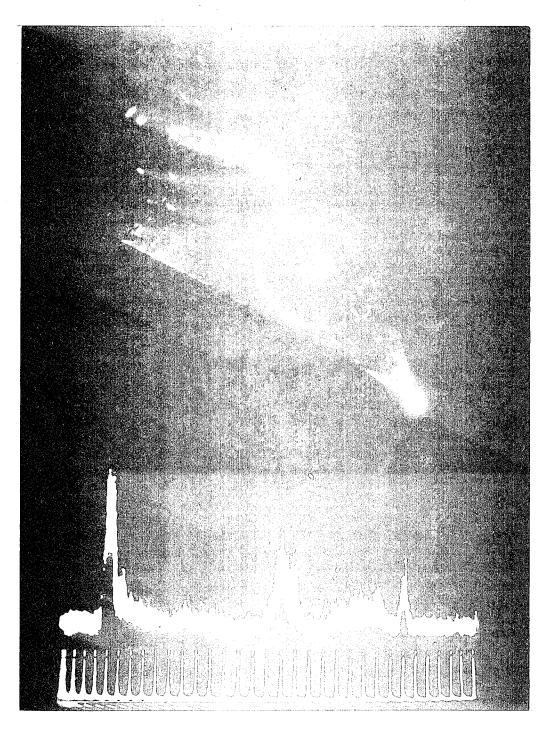
Fig. 5.6 Radar Displays Photographed in Aircraft 340, Dog Shot, at 10.27 Sec after Detonation. **Top photograph** is that of the PPI. Radar return has continued to move away from point zero and has decreased in intensity. Center photograph is that of A-scope. Bottom, A-scope calibration marks (1,500 ft).
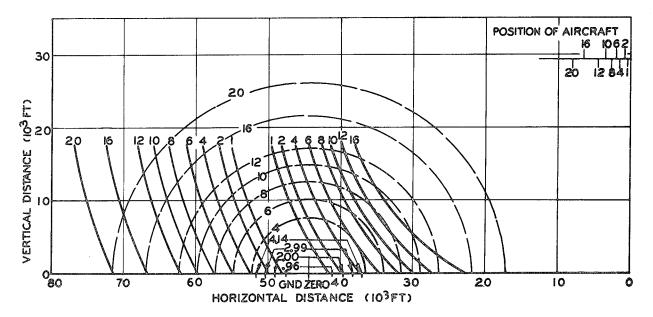
Fig. 5.7 Graphical Solution of Relation Between Radar Return Recorded in Aircraft 340 and Shock-wave Position During Dog Shot. All numbers within graph are in seconds relative to time zero. Bold lines indicate spherical plane to which the radar returns were measured. Broken lines indicate theoretical shock-wave positions in space for 90-kt yield. Shock-wave positions for 4.14, 2.99, 2.00, and 0.96 sec are ground positions only as extracted from Table 3.1 of NOBL Summary Report of Blast Measurements.
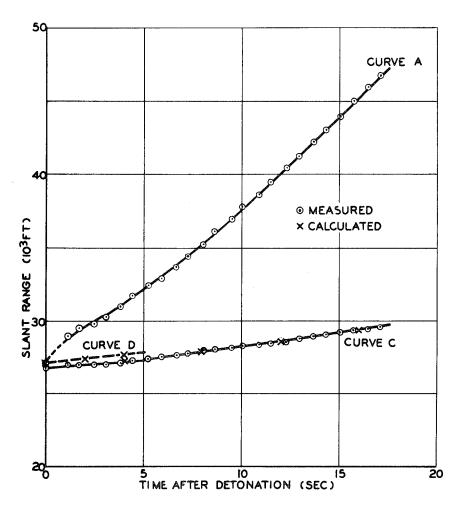
Fig. 5.8 Distance of Radar Returns as a Function of Time as Recorded in Aircraft 290 During Easy Shot. Distances are measured on a line from the aircraft through ground zero. Curve A is for radar returns beyond ground zero. Curve C is distance to AN/APA-44 range tracking marker. Curve D is distance to ground zero computed on the basis of Curve C and an estimate of the displacement between the range marker and ground zero as observed on the PPI recording.

41
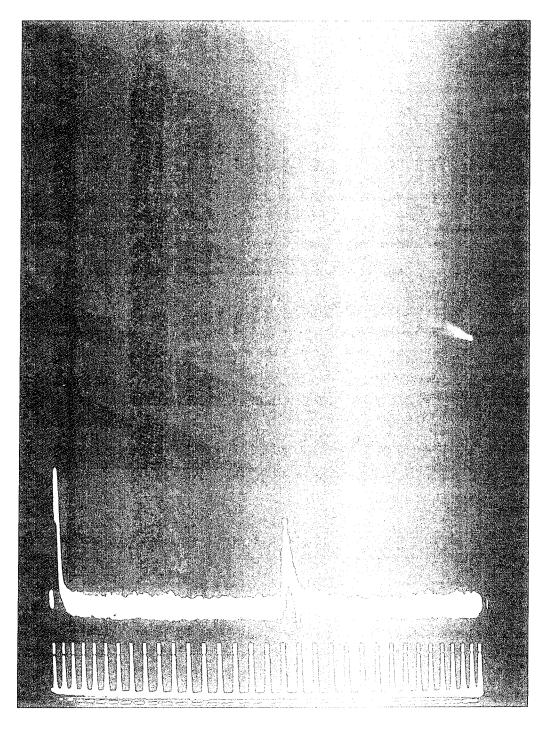
Fig. 5.9 Radar Displays Photographed in Aircraft 290, Easy Shot, at 1.13 Sec after Detonation. Top photograph is that of the PPI. Initial radar return is just visible, but indistinct, due to water return at the apex of the scanned sector. Center photograph is that of A-scope. Bottom, A-scope calibration marks (1,500 ft).
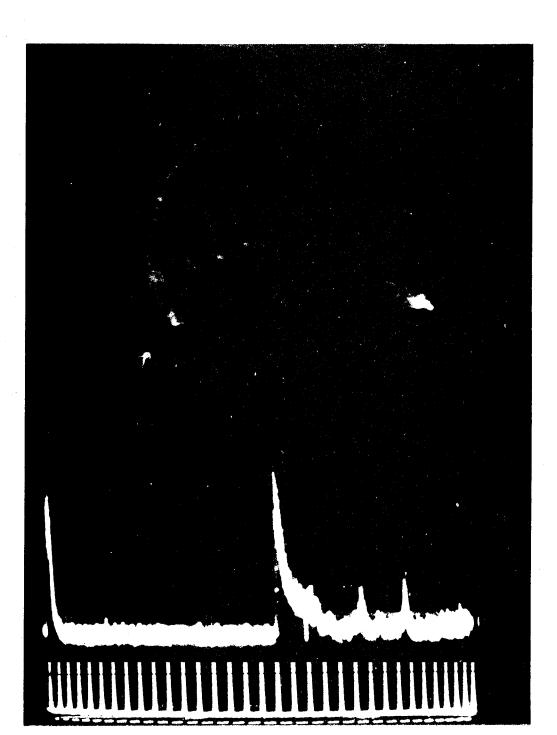
Fig. 5.10 Radar Displays Photographed in Aircraft 290, Easy Shot, at 10.86 Sec after Detonation. **Top photograph is that of the PPI.** Note radar return has moved outward from point zero and has crossed **over an adjacent island.** Center photograph is that of A-scope. Bottom, A-scope calibration marks (1,500 ft).
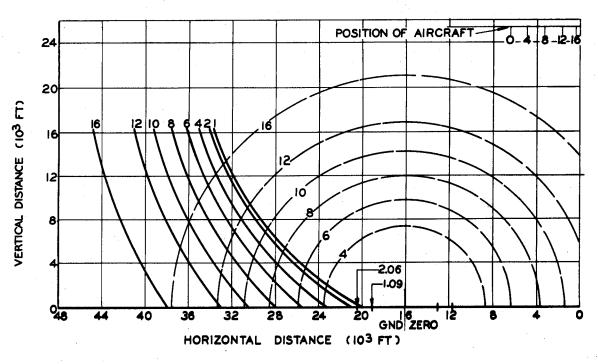
Fig. 5.11 Graphical Solution of Relation Between Radar Return Recorded in Aircraft 290 and Shock-wave Position During Easy Shot. All numbers within graph are times in seconds relative to time zero. Bold lines indicate spherical plane to which the radar returns were measured. Broken lines indicate theoretical shock-wave position in space for 50-kt yield. Shock-wave positions for 2.06 and 1.09 sec are ground positions only as extracted from Table 3.2 of NOBL Summary Report of Blast Measurements.
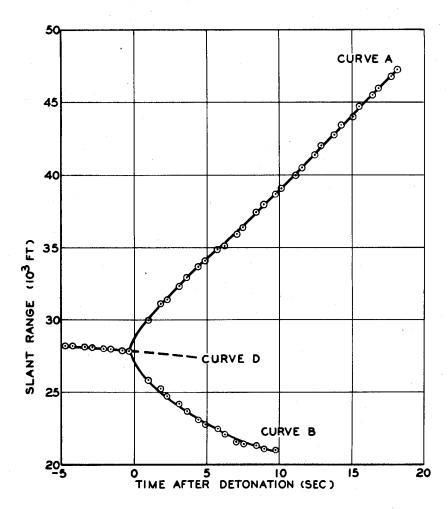
Fig. 5.12 Distance of Radar Returns as a Function of Time as Recorded in Aircraft 340 During Easy Shot. Distances are measured on a line from the aircraft through ground zero. Curve A is for radar returns beyond ground zero. Curve B is for returns between the aircraft and ground zero. Curve D is the recorded effective distance to the shot tower.
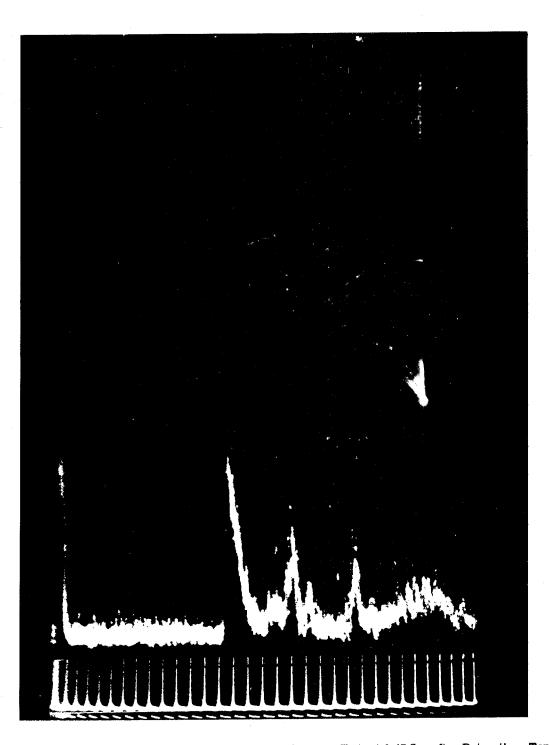
Fig. 5.13 Radar Displays Photographed in Aircraft 340, Easy Shot, at 0.47 Sec after Detonation. Top
photograph is that of the PPI. Semicircular-shaped radar return is detected between aircraft and point
zero, similar to Fig. 5.2. Center photograph is that of A-scope. Bottom, A-scope calibration marks
(1,500 ft).
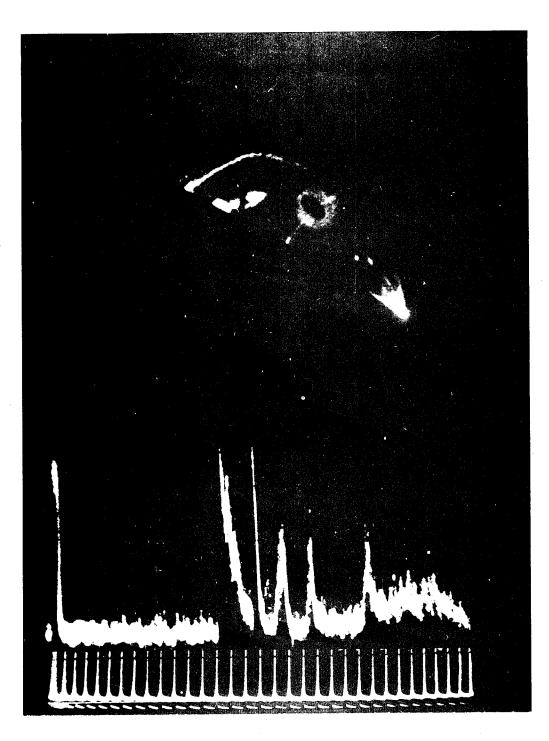
Fig. 5.14 Radar Displays Photographed in Aircraft 340, Easy Shot, at 0.97 Sec after Detonation. Top photograph is that of the PPI. Return is now visible for full 360° around point zero. Note elliptical shape of area surrounded by the radar return. Center photograph is that of A-scope. Bottom, A-scope calibration marks (1,500 ft).
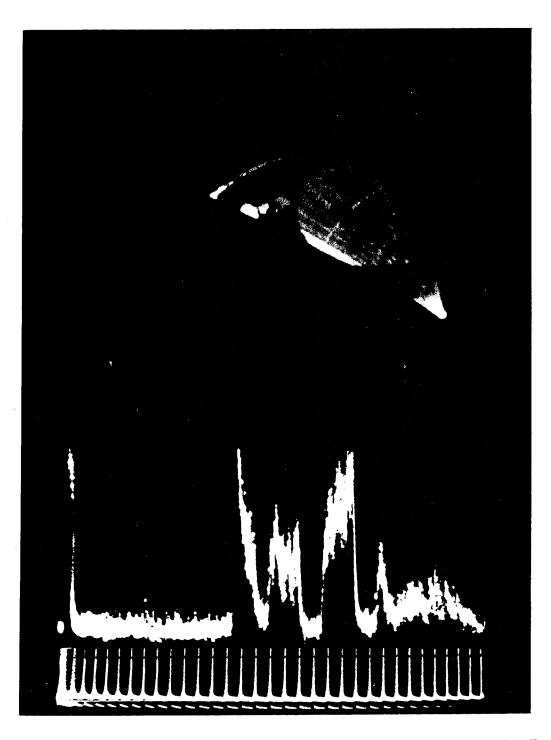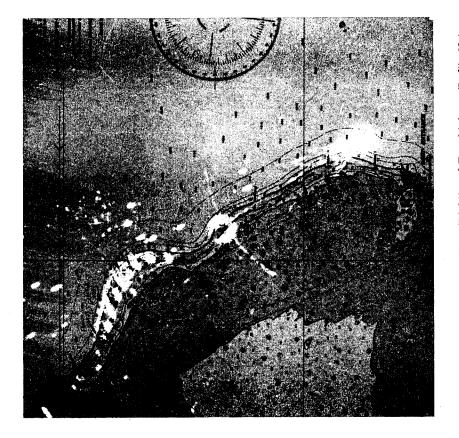
Fig. 5.15   Radar Displays Photographed in Aircraft 340, Easy Shot, at 3.60 Sec after Detonation. Top photograph is that of the PPI. Return has expanded further, and the leading edge is now beyond the land area of Engebi. Center photograph is that of A-scope. Bottom, A-scope calibration marks (1,500 ft).
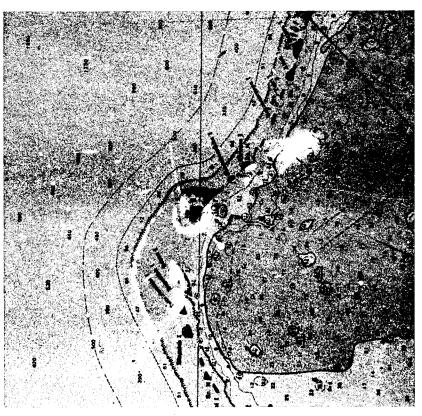
Fig. 5.18 Composite Photograph of Figs. 5.3 (Right) and 5.14 (Left) Superimposed upon Map of Runit Area (Right) and Engebi Area (Left). Note the presence of the radar return over the land areas. Scale factors of the radar display and map have been equalized to the greatest degree possible, but distortion in the radar PPI prevents perfect superimposition.

Part II

EFFECTS OF ATOMIC DETONATIONS ON RADIO PROPAGATION

by

LELAND H. STANFORD
Colonel, Signal Corps

Preface

The purpose of this report is to set forth the mission of Project 8.3B, to describe the methods employed, to analyze the result of each method for each test, and to arrive at conclusions as to results achieved by each method. The purpose of Project 8.3B is to determine what, if any, effect an atomic detonation has on radio propagation at all frequencies. It follows that there is also the job of recommending the procedure and equipment for confirmation of positive results achieved from this Project in Operation Greenhouse.

It is believed that the results achieved provide considerable material of positive value on the subject of the effect of atomic detonation on radio propagation.

Acknowledgments

It is desired to express appreciation to the following personnel for their contributions to the success of Project 8.3B:

Central Radio Propagation Laboratories, National Bureau of Standards (Newbern Smith, A. G. McNish, and H. G. Sellery) for making available an ionospheric recorder and for confirming the frequencies selected for overseas transmissions.

E. J. Wiewara for his efficient operation of the ionospheric recorder.

Coles Laboratory, Signal Corps Engineering Laboratories, for the provision of magnetic-recording equipment and other associated equipment for recording the transmissions and for analyzing their effects.

Navy Hydrographic Office (Warren C. Crump and G. Medina) for the prompt preparation of the azimuthal equidistant projections based on Eniwetok and for checking bearings of overseas transmissions and receptions.

W. J. Milsap, Frequency Section of Chief of Naval Operations, for selecting frequencies for overseas transmissions.

Army Security Agency, Arlington Hall, Va., for studying the overseas transmissions and recommending frequencies for their operation.

Captain W. G. Linaweaver, Communications Officer, CinCPac, and Captain Kinnert, Communications Officer, Marianas Command, for coordinating and supervising the radio transmissions from Truk and Yap; Capt R. D. Baskerville, Hq, AACS, Andrews Field, Col Charles B. Overacker and Col John Crawford 1808 AACS Wing, Tokyo, Maj Samuel B. Wadley, 1811 AACS Group, and personnel of the 1962 AACS Squadron, Okinawa, for their cooperation in supervising the transmissions from Okinawa.

Major Tom Sawyer, ASA, Hawaii; Capt Guy Iovine and Capt Richard J. Lloyd, 1960 AACS Squadron, Kwajalein; Captain Barnes, Task Unit 3.4.5, Majuro; and George Pickens, AFOAT-1 Program, Bikini, for receiving and recording the long-distance transmissions.

Other personnel subordinate to the foregoing and personnel of Headquarters, Joint Task Force Three, Task Groups 3.2, 3.3, and 3.4, for their contribution to the execution of the Project.

Abstract

The objective of Project 8.3B was to determine the effects of an atomic detonation on radio propagation at all frequencies. There are three sources of data for these investigations:

1. Ionospheric measurements at Eniwetok Atoll in the range of from 1 to 25 Mc before the detonation to more than 1 hr after.

2. Transmissions in periods H−5 to H+45 min from remote locations, such as Okinawa, Truk, and Yap, passing through the ionosphere on courses nearly over the Eniwetok Atoll and received and recorded at Kwajalein and Majuro, Honolulu, and Bikini, respectively.

3. Transmissions of surface waves in periods H−5 to H+5 min at short range on uhf, vhf, hf, and lf through the blast from a ship-to-shore station at Eniwetok.

The results of the Project did not reveal any apparent effect attributable to radiation, but the ionospheric recordings appeared to reveal a displacement of the ionosphere as the result of a shock wave which might have caused a disruption to radio transmission reflected in the vicinity of the blast site, over an area of undetermined size, if the points of reflection had been sufficiently near the blast site and if the periods of recording had been sufficiently prolonged to record the effect. It appears that the effect of the shock wave on the ionosphere is not the result of action on the layers themselves but on the earth's magnetic field. This is believed to be the first instance that man-made ionospheric disturbances have been recorded.

The results of the Project are such as to warrant a recommendation for a similar program in connection with subsequent atomic weapons tests, and it is indicated that the data obtained are far more valuable when the tests are conducted at times other than during the ionospheric changes which take place at dawn and dusk.

Chapter 1

Introduction

1.1 OBJECTIVE

The objective of Project 8.3B was to determine what, if any, effect there is on radio propagation as the result of an atomic detonation. As a corollary, it follows that, if there are effects of the detonation on radio propagation, it is within the scope of the Project to determine the nature and cause of these effects and to determine if they indicate or measure the strength of the blast. Likewise there should be an evaluation as to the extent that the observed effect would enable agents of a foreign power to determine the time and strength of a detonation. Furthermore, it is within the scope of the Project to evaluate the benefits of a future project of similar nature and to recommend the means and methods to be employed.

1.2 HISTORICAL BACKGROUND

Tests were conducted in Operation Crossroads to determine the effect of the detonation on radio propagation. The method consisted in photography of oscilloscope readings of local transmissions. The results were negative. It is understood that no steps were taken on Operation Sandstone to observe or to measure these effects. In both operations the use of an ionospheric recorder was contemplated, and the equipment was available. However, this equipment was not used in Operation Crossroads owing to the impracticability of erecting it aboard ship, and it was not used in Operation Sandstone owing to lack of clearance of the operating personnel.

In the preliminary planning the Directorate of Air Communications, Hq, USAF, established the requirement for a study of the effects of an atomic detonation on radio propagation in Operation Greenhouse. This Project was designated Project 4.4, and Lt Col C. J. Lester was assigned as Project Officer. Subsequently Project 4.4 was eliminated from the planned programs. When it was found that considerable planning had already gone into Project 4.4, it was reestablished as Project 8.3B, and Col Leland H. Stanford was assigned as Project Officer in addition to his duties as Assistant Chief of Staff, J-5 Division (Communications, Hq, JTF-3).

In December 1949 it was decided to include the following in the Project:

1. Transmissions over the blast site from remote CW transmitters to be received and recorded on magnetic tape at other remote sites, thus transmissions passing over the site at predetermined heights (see Fig. 1.1) could be obtained.

2. Transmissions from a remote site reflected in the ionosphere over the blast site and received at another remote site, thus providing a measure of the effect on the ionosphere itself over the blast site.

3. Transmissions of surface and line-of-sight waves through the blast, received at short range and recorded on magnetic tape.

In preliminary study, for the first step, Okinawa was selected to transmit to Kwajalein and Majuro; Truk, to transmit to Honolulu; and Yap, to transmit to Bikini. For the second step, Sasebo Naval Base was selected to transmit to Tutuila, Samoa, and for the third step, it was decided to send transmissions from an aircraft on radar frequency and from a naval vessel on radar and very high, high, and low

radio frequencies to the receiving station on Eniwetok.

Subsequently the Navy Hydrographic Office furnished the bearings of the transmitting and receiving antennas and furnished and prepared an azimuthal equidistant projection chart, with Eniwetok Atoll as a center and embracing 90° coverage from center. The Frequency Section of the Office of Chief of Naval Operations and the Army Security Agency made frequency studies to determine the most usable frequencies for the transmissions. As a result it was found that the circuit between Sasebo Naval Base and Tutuila would reflect at, and not over, Eniwetok, thus rendering it of negligible value for the purpose intended.

In checking transmission studies at the Central Radio Propagation Laboratories (CRPL), National Bureau of Standards (NBS), it was learned that an ionospheric recorder and personnel to operate it would be available upon request. Since this equipment would provide, in the range 1 to 25 Mc, the data which possibly would have been obtained from the Sasebo-Tutuila circuit had it been a practicable one to use, it was decided to obtain the ionospheric recorder on loan and to set it up at Eniwetok Atoll.

In connection with the inspection trip to Eniwetok in November 1950 and the outbound trip for station at Eniwetok in February 1951, preliminary arrangements were made with Hq, CinCPac; Hq, ASA, Hawaii; and Hq, AACS, for the transmissions and for certain of the receptions of the first-mentioned method. Upon arrival at Eniwetok, steps were taken to prepare the necessary instructions and to assemble the necessary equipment. Captain Fields delivered the recording equipment and instructions to ASA, Hawaii. Colonel Calkins delivered the recording equipment and instructions to TU 3.4.5 at Majuro, to AACS at Kwajalein, and to the AFOAT-1 personnel at Kwajalein for use at Bikini. Colonel Stanford visited Guam and conferred with Captain Kinnert, DCO, Marianas Command. Leaving Lieutenant Gavin and EM Hare at Guam, he proceeded to Truk and Yap with instructions to the operating personnel there. Colonel Stanford then traveled to Tokyo and conferred with the AACS and then to Okinawa, where instructions were given to the AACS Group personnel. Re-

turning to Guam, Colonel Stanford picked up Lieutenant Gavin and EM Hare and returned to Eniwetok.

During the tests the surface transmission reception was supervised by Lieutenant Gavin for Dog Shot and by Lieutenant Fisher for Easy and George Shots. There were no surface transmissions during Item Shot. The general supervision of the Project was by Colonel Stanford, except during Easy Shot, when general supervision was a responsibility of Colonel Calkins.

After the last test the high-fidelity single-channel recording equipment and all available records were sent to Hq, JTF-3, for analysis and for the preparation of this report.

1.3 BASIC THEORY

The generally accepted theory of radio propagation is the ionospheric theory which presupposes the existence of ionized strata surrounding the earth, generated by the electron stream from the sun striking the atmosphere. Another theory in regard to the existence of the layers considers them to be electrostatic fields within and outside the earth's external magnetic field and to have been induced by the cutting of the lines of force of the earth's magnetic field (Fig. 1.2).

The transmissions for Project 8.3B are shown graphically in Fig. 1.3. If the reflective layers of the ionosphere are of an ionized nature, it would be expected that they might be affected by radiation from the detonation traveling at the velocity of light or by blast action of the shock wave traveling at the speed of sound at the time that the shock-wave front impinged upon the layers themselves. On the other hand, if the reflective layers are the result of the action of the magnetic field, it is to be expected that they would be displaced by the shock wave striking the electromagnetic field which generated them.

The effects on the upper-air transmissions of the Project would probably have shown the practical value of the Project if transmissions and the associated reception and recording had lasted long enough to enable observations of the effect of the blast on the ionosphere at the point

of reflection of the transmissions. The distances to the points of reflection were so great that it would have been impossible to determine whether the practical effect was caused by action on the ionosphere itself or on the earth's magnetic field which might generate the ionosphere (Fig. 5.1). However, if the theory involving the earth's magnetic field is correct, it is to be expected that no effects would be observed until the shock wave reached the area of reflection on the F-layer or reached that portion of the magnetic field generating the F-layer.

In the case of the surface-wave transmissions there is no question as to the nature of the reflective layers, but the idea is that, if radar transmission produces a reflection from the blast cloud, then the recorded signal through the blast could show a diminution in strength that is the combination of energy lost by reflection and by absorption within the blast.

1.4 BASIC FACTS

Dog Shot was detonated on 7 April 1951, at 0634 (Marshall Islands time) on Runit Island, a distance of approximately 10 miles from Parry Island. It had a strength which, for the purposes of this report, will be considered to be approximately 2.

Easy Shot, having a relative strength of approximately unity, was detonated on 21 April 1951, at 0627 (Marshall Islands time) on the northwestern end of Engebi Island, a distance of about 20 miles from Parry Island.

George Shot, having a relative strength of about 5, was detonated on 9 May 1951, at 0930 (Marshall Islands time) on Eberiru Island, a distance of about 15 miles from Parry Island.

Item Shot, having a strength of approximately unity, was detonated on 25 May 1951, at 0617 (Marshall Islands time) on the approximate site of Easy Shot.

IONOSPHERIC INVESTIGATION

Chapter 2

Experimental Procedure

2.1 DESCRIPTION OF APPARATUS

The ionospheric recorder is a device engineered by CRPL and manufactured by Communications Measurements Laboratories, Inc., New York, N. Y. The model C-3 (No. 17) furnished on loan to JTF-3 consisted of a voltage-regulation device and a recorder unit. The recorder unit contained a transmitter which sent pulses at continuously varying frequencies in the band 1 to 25 Mc, a receiver to receive these pulses, a timing device, and two oscilloscopes for receiver presentation. After each pulse the transmitter was turned off, and the receiver was turned on to receive the echo as in a radar set. The output of the receiver was fed to duplicate oscilloscopes, each with a facility for mounting and controlling a camera to photograph the trace. One camera took still photographs on 35-mm film, and the other took motion pictures on 16-mm film. The sweep time covered a period of 7.5 sec, and the interval between sweeps could be set for continuous operation or for any intermediate time interval up to 1 hr. The presentation on the scopes painted its own grid with the abscissa representing frequency and the ordinate representing distance.

The motion-picture film can be viewed in a 16-mm projector. However, 1 min of continuous observations takes only ½ sec on the screen, and, particularly when the recorder is operated with an interval between sweeps, the projected image moves too fast to present a picture suitable for analysis. The 16-mm film was reprinted in a projection printer which made 4 frames of each original negative before progressing to the next one; this had the effect of slowing down by four times the rate at which action is depicted on the motion-picture film. This caused 1 min of observations to show on the screen during 2 sec. The 35-mm film was viewed for analysis by projection with a device furnished by CRPL.

The antenna system for the ionospheric recorder consists of two vertical half-rhombic or delta antennas suspended from a 65-ft pole with each antenna at right angles to the other. The base of the half-rhombic antennas is 130 ft. One antenna is for transmission and the other for reception with 90° polarization with respect to the transmissions. Initially the east-west antenna was used for transmission, but it was subsequently proved that results were improved when the north-south antenna was used for sending.

2.2 HISTORICAL BACKGROUND

CRPL made the ionospheric recorder available to Hq, JTF-3, and it was shipped by motor express to the San Francisco Naval Yard for

transshipment to Eniwetok aboard the USS Curtiss. However, the truck was delayed by storms, and the equipment reached San Francisco after the USS Curtiss had sailed. Hence, the equipment was transferred to Travis Air Force Base, and from there it was airlifted to Eniwetok. CRPL made E. J. Wiewara available to install and operate the equipment, and he was ordered to report to Hq, JTF-3, in Washington for briefing and initiation of his clearance papers. His clearance papers were prepared and submitted to J-2 Division, but owing to the late date they were not processed further. Wiewara was sent to Eniwetok aboard the USS Curtiss.

On arrival at Eniwetok, Wiewara and the Project Officer made a reconnaissance of sites for the ionospheric recorder. Eniwetok was not considered acceptable because of the interference that would be experienced from other radio transmitters and because of its distance from the shot islands. Japtan, from map considerations, was deemed a much better site because of the nearly total absence of nearby radio transmitting equipment and because of its proximity to the shot islands. However, Japtan was denied as an available site because Wiewara was not Q-cleared and would not be allowed on Japtan. As a compromise site, it was decided to install the ionospheric recorder on the south end of Parry Island. After the equipment was installed, it was found to have been sited near a storage area of active material. However, it was determined that this radiation would not adversely affect the film used in the recorder. The equipment was installed by Wiewara, assisted by Sgt M. C. Lundin, who was assigned to him as a Q-cleared assistant. Heavy labor was furnished by Holmes and Narver.

2.3 OPERATION

As soon as the equipment was installed, Wiewara began test operations and made ionospheric recordings for the benefit of CRPL. These recordings covered the following periods (local M time):

From	To
March 31 0449	April 02 1600
April 02 2000	04 2100
04 1445	04 1959

From	To
April 04 2130	April 05 2030
05 2102	06 2030
06 2100	07 2230
08 0801	09 0931
09 1024	10 2100
10 2147	11 1330
11 1345	11 2200
11 2239	12 2000
12 2002	12 2029
12 211	13 2029
13 2100	14 1449
17 1328	17 1430
17 1440	18 1928
18 2110	19 2100
19 2146	21 0330
21 0741	22 1100
22 1115	23 2100
23 2115	27 1610
27 1615	30 0800
30 0808	May 04 0845
May 04 0900	07 1535
07 0339	09 0800
09 1836	13 1545
13 1600	18 0745
18 0800	21 1004
14 1600	15 2045
15 2130	16 2015
16 2033	17 1313
21 1706	23 1527
23 2343	25 0500
25 0722	25 0804

These recordings were classified as restricted and were furnished to Wiewara for analysis and delivery to CRPL.

The recordings made on both 35- and 16-mm film during operational periods were as follows:

35 mm

Dog	April 08 0348—08 0740
Easy	21 0345—21 0727
George	09 0815—09 1032
	09 1036—09 1836
Item	May 25 0505—25 0718

16 mm

Dog	April 08 0406—08 0744
Easy	21 0330—21 0747
George	09 0922—09 1144
Item	May 25 0515—25 0830

2.4 ANALYSIS

During July Edward Wiewara, assisted by John Sullivan of CRPL, analyzed, frame by frame, the 35-mm films made at test times. The results were plotted on graph paper, and in the finished charts light lines showed data with respect to the E-layer, and heavy lines showed data with respect to the F-1 layer and the F-2 layer. The graph on the upper chart discloses the mean heights of the layers, the F-2 being higher than the F-1. The curves on the lower graphs disclose maximum and minimum frequency response to the ionospheric recorder of each layer. Since the lower limit of the F-1 is coincidental with the upper limit of the F-2, only three lines are used to show the frequencies of both F-layers. On the upper chart of each graph a dashed and broken line has been drawn to show the approximate height of the shock-wave front from H−0 to H+15 min.

After the graphs were made, significant frames of the ionospheric record were selected for reproduction. Only those frames revealing the preliminary state of the ionosphere or effects attributable to the detonation are included in this report. Each frame bears a time legend and covers a sweep time of 7.5 sec from left to right, there being 8 frames/min during periods of continuous recording. Synchronization with the TG 3.1 time signals is only approximate, being within 1 or 2 sec. Each picture of a frame has been given a legend descriptive of the data shown. The 16-mm motion-picture film was utilized to present the general behavior of the ionosphere as a preliminary to the detailed study and plotting of observations.

Chapter 3

Test Results

3.1 DOG SHOT

Figure 3.1 is a graph of the ionospheric recordings from D−64 to D+13 min, with recordings made each minute until D−1 min, when continuous recording began. Figure 3.2 covers continuously the period D+13 to D+35 min. Figure 3.3 shows the period from D+35 to D+66 min continuously until D+50 min, when readings at 1-min intervals were resumed. Figures 3.4 to 3.11, covering the periods as captioned, picture the data at corresponding times as plotted on the graphs described above.

From a review of the graph and an inspection of the pictures presented, it will be noted that there is considerable irregularity in the F-layer beginning at D−7.5 sec. Since this sweep began at D−7.5 sec and recorded the 2-Mc band at approximately H−5 sec, it is possible that the shot was fired at that time and that this effect on the F-layer could have been generated by the ionization due to radiation from the detonation, but in light of subsequent observations this possibility is doubtful. This condition in the F-2 layer persists until about D+5 min 45 sec, except for a reappearance of the F-layer during the period D+3 min 52.5 sec to D+4 min, which casts further doubt on the conjecture that it may have been caused by ionization.

Another effect is revealed at approximately D+8 min, wherein the frequency coverage of the E-layer is quickly expanded to as high as 9 Mc and gradually subsides to approximately 2 Mc during the next period of 1 min 15 sec. This effect on the E-layer takes place during the period that the altitude of the shock-wave front is between 160 and 185 km, having passed through the E-layer a few seconds short of D+5 min. There is little simultaneous effect noted in this instance on the F-layer. The effect as cited on the E-layer is possibly due to blast action of the shock wave encountering something existing between 160 and 185 km above the earth's surface, which is quite possibly that portion of the earth's magnetic field producing the E-layer. The effect on the E-layer which has previously been discussed recurs in about 9 min, and it is quite possible that, if the initial effect was due to a movement of the magnetic field, the effect occurring 9 min later may be ascribed to a subsiding oscillation of that field since the shock wave by this time has passed to an elevation approximately 100 km beyond that of the F-layer.

It will be noted from the graphs that there are certain periods marked "equipment failure." The first of these was due to the blast action, which shocked the vacuum tubes severely enough to cause a short between elements, which threw the circuit breaker. This was rectified by quickly replacing tubes and restoring the circuit breaker. The subsequent periods marked "equipment failure" are due to stoppage of the recorder to make minor adjustments. As revealed by the continuity of the graphs prior to and after the periods of failure, none of these failures or adjustments changed the continuity of subsequent readings.

3.2 EASY SHOT

Figure 3.12 shows the Easy Shot recordings made during the period E−57 to E+14 min. Figure 3.13 covers the period E+14 to E+36

min, and Fig. 3.14 shows the period E + 36 to E + 58 min. Figure 3.15 shows the conditions of the ionosphere existing at E −57 min. By a comparison of Fig. 3.15 with Fig. 3.16 taken at E −27 min, it will be noted that the ionosphere is in a state of transition and that the frequency response of the F-layer is decreasing, and, as revealed in Fig. 3.17, taken at E −1 min, the frequency response has still further diminished and the F-layer has lost altitude. Figure 3.18, taken in the period immediately preceding E-hour, reveals substantially the same conditions as shown in Fig. 3.17. This is also true of the record beginning at E −0 shown in Fig. 3.19. No unusual change in the ionosphere appears to be revealed in any portion of the sweep, which indicates that in the detonation of this weapon there was apparently no effect attributable to ionization. The conditions existing in Fig. 3.20, taken at E + 22.5 sec, remain practically constant. In Figs. 3.21 and 3.22, taken at E + 2 and E + 3 min, respectively, the frequency response of the E-layer expands over that shown in previous pictures of this series. From Fig. 3.23, taken at E + 4 min, and Fig. 3.24, taken at E + 9 min, it will be noted that the F-2 layer is steadily descending in altitude but progressively increasing in frequency response. Figure 3.25 reveals a phenomenon recorded on the graph at E + 9 min 45 sec, wherein there is a transient increase in the frequency response of the E-layer. This corresponds roughly to that noted on Dog Shot but is lesser in extent than previously observed, which is possibly attributable to the decreased strength of the weapon. Other phenomena of a similar nature but lesser in amplitude are to be noted on the graph at E + 16 and E + 20 min 20 sec. These again might be attributable to the disturbance of the magnetic field and an oscillatory return to normal. The first disturbance of the E-layer occurs when the shock-wave front is at an altitude of approximately 165 km and persists until the shock-wave front is at an altitude of approximately 250 km. This is between E + 9 min 20 sec and E + 12 min 20 sec. The oscillations appearing at E + 16 min and shortly after E + 20 min cannot be attributed to direct action of the shock-wave front since the shock wave will at this time have passed beyond the plotted minimum height of the F-2 layer. The results indicated in the ionospheric investigation of Easy Shot are lesser in extent than those ob-

served for Dog Shot, probably owing to the lesser strength of the weapon.

3.3 GEORGE SHOT

The ionospheric recordings taken during George Shot appear to be particularly significant partially because of the greatly increased power of the weapon and partially because of the fact that the hour of detonation was such that ionospheric conditions had more or less stabilized and disturbances in the ionosphere created by the weapon are not merged with transient conditions due to natural disturbances occurring in the early morning hours. Figure 3.26 is a graph of the recordings made each minute during the period G −60 to G −1 min and every 7.5 sec between G −1 and G + 14 min. Figure 3.27 shows recordings made every 7.5 sec in the period G + 14 to G + 36 min. Similarly Fig. 3.28 shows the continuous recordings made in the period G + 36 to G + 58 min. Figure 3.29 shows continuous recordings made during the period G + 58 to G + 62 min and each minute from G + 62 until G +90 min and from G +90 min every 6 min thereafter until G + 8.5 hr. Figure 3.30 taken at G −1 min and Fig. 3.31 taken at 7.5 sec before G-hour indicate the nature of the ionosphere immediately preceding the shot, and the similarity between these two figures indicates the stability of the ionosphere at this time.

Figures 3.32 and 3.33, taken at G-hour and at G + 22.5 sec, fail to reveal any disturbance occasioned by ionization. Figure 3.34 indicates an effect beginning in the E-layer which in Fig. 3.35 has progressed and begun to affect the the F-layers. This effect may be traced progressively through Figs. 3.36 and 3.37 with response from the F-layer disappearing and that of the E-layer reappearing in Fig. 3.38. In Fig. 3.39 the response from the F-layer has entirely disappeared, and the extent of the frequency response of the E-layer is expanded. In Fig. 3.40 the response of the F-layer reappears, and the frequency response of the E-layer diminishes slightly. In Fig. 3.41 the primary reflection of the F-layer goes up at about 10 Mc, whereas between 8 and 9 Mc there is no appearance of the primary reflection but a relatively strong appearance of the second reflection. The E-layer is losing its reflective

power. In Fig. 3.42 the strength of the first reflection of the F-layer is diminishing and that of the second reflection is increasing. The response of the E-layer is almost disappearing. In Figs. 3.43 and 3.44 the primary reflection of the F-layer has totally disappeared, whereas the secondary reflection has increased in strength and in frequency response, and that from the E-layer is almost wholly absent. In Fig. 3.45 the E-layer response has entirely disappeared. There is no reflection of the first image of the F-layer, and the second reflection, which was so prominent in previous recordings, is becoming less distinct. As a matter of fact it is almost gone in Fig. 3.46, which shows no trace of the E-layer and no primary reflection of the F-layer. In Figs. 3.47 and 3.48 there is no second reflection of the F-layer, but the primary image of the F-layer is beginning to reappear, as is also the E-layer at a much lower altitude than previously noted. The same conditions appear in Fig. 3.49, but in Fig. 3.50 all traces of the F-layer response, either primary or secondary, have disappeared. In Fig. 3.51 the secondary image of the F-layer response begins to reappear at 9 Mc, and there is a trace of the returning primary image at about 8 Mc. In Fig. 3.52 the frequency response of the primary image is increasing, and the secondary image has disappeared. These conditions continue through Figs. 3.53 and 3.54. In Figs. 3.55 and 3.56 the frequency response of the F-layer is increasing, as is also the case in Fig. 3.57. Not until G+2.5 hr, as shown in Fig. 3.58, does the normal condition in the ionosphere return, as may be seen by comparison with Fig. 3.31.

An inspection of the graph reveals that there is little apparent effect in this shot which may be attributed to radiation. It will be noted that at G-hour there is a fairly abrupt rise in the height of the F-2 layer and a considerable expansion of its frequency response. In view of the fact that this condition persists until about G+6.5 hr it is doubtful that it should be attributed to radiation. The shock-wave front reached the E-layer at about G+4 min, and at that time the E-layer disappeared to return again at G+7.5 min at a higher altitude in the higher frequency range until G+9.5 min, when its image again disappeared. As the shock-wave front reached an altitude of about 120 km at G+5.25 min, it further disrupted the re-

sponse of the F-1 layer, causing it to be totally lost until G+8.5 min, when it reappeared briefly, rising in altitude to merge with the F-2 layer at about G+9 min and not to reappear again until G+2.5 hr where it persisted until G+5 hr. When the shock-wave front reached an altitude of approximately 175 km at about G+7.75 hr, the image from the F-2 layer disappeared for a period of about 1 min, and then it returned for about 1 min and appeared to be increasing in altitude and frequency response. Thereupon the primary image of all the layers disappears at G+9 min, and the secondary image of the F-2 layer appears for about 3.5 min or until G+12.5 min. Up to this time the shock-wave front has not actually encountered the F-2 layer at all, but, when it does at G+13.5 min, the response of the F-2 layer is disrupted until G+16 min, when it reappears for 1 min and then disappears to return for about 20 sec just prior to G+18 min. It then again disappears, not to return until G+20.25 min. From then on during the course of the observations the behavior of the F-layer appears to be normal until about G+62 min, when its image disappears for approximately 1 min.

It is believed that many of the effects discussed can be attributed to the blast action of the shock wave of the detonation. However, in view of the fact that this is the first time that a man-made effect on the ionosphere has been recorded and there is no other information with which to correlate the phenomena recorded and discussed, it is difficult to make a positive finding from the results at hand.

A possible explanation of the existence of instances in which there is no reflection at all and other instances in which the primary reflection is missing but the secondary reflection is present is given by the reasoning shown graphically in Fig. 3.59. With reference to the figure, conceive an ionospheric recorder to be located at point A and transmitting to the ionospheric layer shown at F; the figure shows the channel by which primary and multiple reflections are received at point A in this instance. Now conceive that the ionosphere which had been at F is moved to the location of F'. The transmission from site A then progresses to the point A", where it is reflected back to the earth at point B and again into the ionosphere to point B', from whence it is reflected to

point A. These circumstances would cause the primary reflection to be missed at point A, but the secondary reflection would be received there. Now conceive that, in the period between the reflection at point A″ and the rereflection from the earth, the ionosphere has moved to position F″. In this instance the transmitted wave would proceed from point B to C′, where it would be reflected to the point C on the earth. Since neither point B nor C is in the proximity of site A, neither the primary nor the secondary reflection would be in evidence on the ionospheric-recorder screen located at site A. This explanation accounts for the total absence of an ionospheric record under the above conditions. In order to verify these assumptions and other assumptions and phenomena previously discussed, it would be necessary to have a repetition of the conditions giving rise to the effect noted.

Graphs showing ionospheric recordings at Guam and Maui on the days of George Shot are included as Figs. 3.60 and 3.61, respectively. On these graphs G-hour is shown by a broken and dotted line. It will be noted that Guam is 2 hr earlier on the same day and Maui is 2 hr later the day before. Each of these graphs reveals a stable condition with respect to the F-layer and a disturbed condition with respect to the E-layer. This indicates a probable natural stability of the F-layer at Eniwetok at the time and gives rise to confirmation of the fact that disturbances of the F-layer observed there were due to the detonation of the weapon.

3.4 ITEM SHOT

Figure 3.62 is a graph of the recordings of the ionosphere from I−62 to I+14 min, with the observations up to I−1 min being made with 1-min intervals and those thereafter being made continuous with a 7.5-sec sweep. Figure 3.63 covers the observations from I+14 to I+37 min, and Fig. 3.64 covers the continuous observations from I+37 to I+60 min. Figure 3.65 is a photograph of the ionospheric record at I−19 min, and Fig. 3.66 is a similar record at I−1 min. By a comparison of these two figures it will be noted that the image from F-layer is entirely absent in the time preceding the detonation of the weapon and that there is a transient effect at the time of the detonation as re-

vealed by the decrease in the number of repetitions of the reflections of the E-layer. Figures 3.67 and 3.68, taken just before and at I-hour, reveal little change in conditions at the instant of detonation. Figure 3.69 taken at I+1 min and Fig. 3.70 taken at I+5 min reveal that slight changes are taking place in that more reflections of the E-layer are appearing. This effect is further noted in Fig. 3.71 taken at I+10 min and Fig. 3.72 taken at I+30 min. In the last-mentioned figure there are a total of nine secondary reflections, whereas in Fig. 3.65, taken before the shot, there are only six secondary reflections.

It had originally been contemplated not to make ionospheric recordings of Item Shot because the yield of the weapons practically duplicated that of the Easy Shot and it was anticipated that the effect would probably be about the the same as that of Easy Shot. Furthermore it was desired to begin packing the ionospheric recorder for return shipment as early as possible in order to avoid transportation congestion and to obtain an early return of the equipment to CRPL. When it was announced that Item Shot would be fired a considerable time after sunrise, there was a quick change in plans on the part of the Project Officer, and arrangements were made to retain the equipment for recording the results of this test. The reasons for retention of the equipment were nullified when at the last minute a change in I-hour was announced and the shot was planned to be fired 30 min before dawn. As a result of this change, however, no change was made in the plan to record the ionospheric conditions during the test.

A review of the graph and photographs indicates that a very unusual condition existed from I−32 until I+45 min, during which period there was a total absence of reflections from the F-layer, and the reflections from the E-layer had many repetitious recurrences. These conditions would seem to indicate a state of turbulence of the F-layer during this period and an extremely stable condition of the E-layer. There is little effect, as indicated on the graph, that can be ascribed to radiation from the detonation of the weapon. However, in light of observations during previous tests, attention was drawn to the fact that no change occurs as the shock-wave front is passing

through the E-layer itself, but there have been charted increases in frequency response of the E-layer taking place at I+5.75, I+8, I+13.5, I+16.5, and I+19 min. If the first of these increases is discounted, the repetition rate of subsequent changes follows fairly closely the pattern noted in previous tests, and the initial effect takes place when the shock-wave front has reached an altitude of about 185 km, and the subsequent transients follow about the same period of damping as noted in previous remarks with respect to the E-layer.

Chapter 4

Discussion

With the exception of George Shot, all ionospheric recordings were made in a period which is known to be a very transitory one for ionospheric phenomena. Furthermore the latitude of Eniwetok Atoll is so low that it is in a belt of equatorial changes in the ionosphere where maximum instability is normal. This is the initial use of the ionospheric recorder in connection with atomic weapon tests. Results have been achieved which can be ascribed to the blast of the shock-wave front, and it is to be noted that this is probably the first instance in which the effect of a man-made disturbance on the ionosphere has been recorded and observed. The results seem to follow a pattern and indicate that some effect is probably felt on the ionosphere as the result of action on the medium residing in the neighborhood of 160 to 185 km elevation at the latitude of Eniwetok and that this disturbance subsides with a damped oscillation having a period of 8 min, 4 min, etc. This would seem to indicate that the effects noted are the result of displacement of the earth's magnetic field and that the F-layer resides beyond it and the E-layer with it and that whatever change occurs in the magnetic field is reflected in a corresponding behavior of the ionospheric layers. The ionospheric layers and the magnetic field exist in a very rarified atmosphere, and if it were possible to displace them, a period of damped oscillation during their return to the normal state would normally be expected. This expectancy is quite definitely verified by the results noted.

The ideal conditions for ionospheric recordings of the effects of atomic weapons are to be achieved when the weapon is detonated at a latitude and at a time when there is a maximum stability of the ionosphere. These conditions would be more nearly satisfied by observation at the Nevada Proving Grounds, which is approximately 20° greater in latitude than that of Eniwetok and where land masses would probably make it possible to place the ionospheric recorder in closer proximity to the site of the detonation. Furthermore, if the weapon is detonated any time between 0900 and sunset, it is quite possible that the ionospheric changes caused by nature will be at a minimum and that observable effects on the ionosphere can be almost wholly ascribed to the detonation of the weapon.

By establishing a second ionospheric-recording station 100 or 200 miles away from that observing the effects of the atomic weapon and having this second station record at the same times as the first station, it would be possible to obtain two simultaneous recordings for comparison. One recording would reveal natural conditions and the other recording would show how those natural conditions have been affected by the detonation of the weapon. Since transient effects in the ionosphere will normally be expected to move in an east-west direction, the second recording station should be established as nearly as possible on the same meridian as the first station, and both stations should, of course, be synchronized as to timing. At the ionospheric-recording station established for observation of the weapon, it could readily be arranged to impose on the recording an instantaneous impulse received from a photoelectric pickup of the illumination from the detonation of the weapon and thus impose a narrow vertical line on the recording to indicate the exact moment of the detonation.

Since the sweep time of the ionospheric re-

corder covers a period of 7.5 sec, the device is not suitable for the determination of instantaneous effects. During the 7.5-sec sweep the device will record an effect transpiring at the frequency to which the equipment is at that moment tuned and will show a phenomenon of transpiring within a period of about $\frac{1}{40}$ sec at that frequency. If it is desired to record effects on the ionosphere occurring in very brief periods, in the order of microseconds, it will be necessary to establish transmitting and recording stations equidistant from the point of detonation and on reciprocal courses as seen from the point of detonation. One of these stations would be required to transmit continuously on a fixed frequency a continuous wave signal which would be received at the other station continuously and recorded on a high-speed magnetic tape or continuous photographic record. The antenna systems of each of the stations would have to be so designed that there would be no surface-wave interaction between the two. There would be an additional requirement for a synchronizing signal to correlate the transmission and the reception. Such an arrangement is not difficult to provide. However, the results obtained from it would probably have little practical value. The contribution which these results would make in the advancement of knowledge with respect to the ionosphere itself is questionable.

The phenomenon revealed by the ionospheric recorder appears to have little observable effect which can be ascribed to radiation, and the phenomenon due to the blast effect of the shock-wave front has very little practical value with respect to the ability to affect radio transmission at the time of the test. It would appear that the maximum effect on radio transmission that would be noted as the result of a blast would probably not cause a blackout on the transmissions. The ionospheric recording of the effect of the atomic weapon has contributed a great deal to the advancement of the basic science. Present concepts of the ionosphere, its behavior, and its composition are largely conjectural and are based on observation of phenomena noted from the ground or at relatively low altitudes. The data obtained from these experiments are, as has been mentioned, the first that have been obtained as the result of a known man-made disturbance of the ionosphere. From a succession of repetitions of these experiments, ionospheric investigators would be provided with very valuable factual and accurate data with which to analyze further ionospheric conditions. It is believed that the ionospheric investigations as a corollary to atomic weapon testing will provide scientists with very valuable information which they could not otherwise obtain.

Section 2

UPPER-AIR TRANSMISSIONS

Chapter 5

Experimental Procedures

5.1 GENERAL PLAN OF OPERATION

A search of the Pacific area, as indicated in Fig. 1.1, revealed that, if a transmitter on the southern part of Okinawa would send on proper frequency, the signal could be received on Kwajalein and Majuro. Map analysis revealed that the path of these transmissions would pass within about 25 miles of Eniwetok Atoll. Propagation studies revealed that for the time of day the frequency should be about 13 Mc. It was found that a frequency of 12,390 kc was assigned to AACS at Okinawa, and it was decided to utilize this frequency. Inspection of the map with reference to these transmissions revealed that the Okinawa-Kwajalein transmissions would probably reflect from the F-layer of the ionosphere at about 18° north latitude and 148° 20′ east longitude and that the Okinawa-Majuro transmissions at about 18° north latitude and 150°45′ east longitude. Considering the F-layer to have an approximate altitude of 160 miles at the time of day under consideration, it was estimated that the height of these transmission paths over the vicinity of Eniwetok Atoll would be about 120 and 90 miles, respectively. The direct distance to the probable point of reflection, as indicated in Fig. 5.1, would be about 1,000 and about 830 miles, respectively, west of Eniwetok. These computations involve many assumptions and are therefore only approximations. However, their

accuracy is within the needs of this problem.

Similar consideration of the radio transmissions from the Truk Navy Radio Station to Honolulu on 11,590 kc reveals that the probable point of reflection would be about 15°45′ north latitude and 176° east longitude and that the path would pass within about 10 miles of the Eniwetok Atoll at a height of approximately 85 miles. The direct distance to the probable point of reflection would be about 900 miles east of Eniwetok.

In the planning and the execution of the program, considerable emphasis was placed on arrangements to observe the effects on the paths of transmissions as the signals passed the proximity of blast area, and little cognizance was taken of what might happen at the points of reflection. From a review of the results it appears that little, if any, effect results from action on the signal while its path is in the blast area. On the other hand, it now appears that there is considerable probability that the signal might be affected at the point of reflection at the time the shock wave produces an effect on the ionosphere in that region. The points of reflection of the signal transmitted for Project 8.3B upper-air transmissions were too remote from the point of detonation to have had much effect even if the periods of observation had been extended to observe the phenomena adequately.

The same assumptions and similar compu-

tations reveal that transmissions from the Navy Radio Station at Yap to a receiving station on Bikini Island on 10,710 kc would have a probable point of reflection at about 11° north latitude and 152°15' east longitude and would pass within 25 miles of Eniwetok at a height of about 35 miles. The distance to the probable point of reflection would be about 670 miles west of Eniwetok.

The transmissions from Okinawa were cleared through Hq, AACS, Washington; Hq, 1808 AACS Wing, Tokyo; and Hq, 1811 AACS Group, Okinawa. They were arranged as a result of a conference between the Project Officer and the Commanding Officer, 1962 AACS Squadron on Okinawa. The transmitter used was a Wilcox 96C. The transmissions from Yap and Truk were cleared by the Project Officer with Office of the Chief of Naval Operations, Washington, the Communications Officer, CinCPac, and the Communications Officer, Marines at Guam, and were arranged by conferences between representatives of the Project Officer and the officers in charge of the Navy Radio Stations at Truk and Yap, respectively. At both stations a Navy TCK transmitter was used. The instructions for the transmissions (Appendix A) were discussed at all stations. The necessity for a steady signal was stressed.

Reception at Hawaii was arranged, and the recording equipment was delivered by a representative of the Project Officer in contact with the Commanding Officer, ASA, Hawaii. Reception at Kwajalein and Majuro was cleared by the Project Officer with TG 3.4 and that at Bikini with TG 3.1. The recording equipment was delivered, and the details of operation were discussed by a representative of the Project Officer. In Hawaii the signal was received on an SX 28 receiver and recorded on a Stancil-Hoffman R4 recorder. At Kwajalein the signal was received on a super pro receiver and recorded on an R4 recorder. At Majuro the signal was received on an SX 28 receiver and recorded on Stancil-Hoffman Minitape recorders. At Bikini an S79 receiver was used, and recording was on Minitape recorders. The instructions for reception and recording are given in Appendix B. The instructions stressed voice-cuing of the tapes and heterodyne of the BFO to produce a steady note. Through oversight the receiving personnel were not cautioned against correcting for variations in

intensities of the signal by adjustment of the volume control.

In spite of the simple code provided, some difficulty was experienced in getting messages through in time covering changes in scheduled transmissions and receptions to correspond with changes made in test times and test dates. Much of this difficulty was due to personnel not connected with the program who did not know what to do with the traffic, both at relay points and at destinations.

5.2 TEST RESULTS

Tests were run for Dog, Easy, and George Shots only. Because of carelessness on the part of the personnel in the monitoring station at Eniwetok who were charged with preserving the tape records, some were erased for other use. There remain recordings of Easy Shot as received at Bikini and of George Shot as received at Honolulu. There is a record of reception at Majuro taken the day of Easy Shot, but the operator began 3 min too late and copied the wrong frequencies. On the Bikini tapes which began at 0622 there is an effect revealed at 0626, as shown on Fig. 5.2. This effect is a 1-db reduction in a signal strength. This change may have been due to change in adjustments at either the transmitter or the receiver. On the Honolulu tapes there is no cue, and the times are reported as 0915 to 1005. There is no recognizable effect that can be ascribed to the detonation of the weapon.

5.3 DISCUSSION

Neither of the tapes discussed nor any others made during the program record long enough to reveal the effect of the blast on the F-layers similar to those effects indicated by the ionospheric records. In order to obtain records of this type having any value, the transmissions should be modulated at a steady audio frequency (about 1,000 cycles) and should be as nearly as possible a pure sine wave. The transmitter should be very stable. To cover the entire period of possible effects, the durations of the transmissions should have the following minimum lengths: Okinawa-Kwajalein and Okinawa-Majuro, 85 min; Yap-Bikini, about 60 min; and Truk-Honolulu, about 80 min. The receiver

should be of a very stable type, and the signal should be received without local heterodyne. Recordings should be voice-cued at the beginning and have an accurate timing signal imposed at the start. If more than one reel is used, the second reel should be voice-cued before beginning recording. A timing signal should be cut on both tapes at changeover time, and then the end of the first reel should be given a voice cue after being cut out of the receiving circuit. Few of the foregoing conditions were present for the off-island transmissions, and the best that can be said for the results achieved from them is that they revealed methods and practices for future conduct of similar tests. The sites selected for transmission and reception were the best available in the Pacific area, but the points of reflection in each case are so distant from Eniwetok that it is questionable whether the result would have been noticed even if the duration of the transmitting periods had been sufficiently prolonged for the receiving stations to record the signal at the time the shock-wave front reached the point of reflection. There is, however, enough possibility of there being recordable disturbances at the points of reflection to warrant planning, at least on repetition of the off-island transmissions, in connection with a future weapons test at Eniwetok. If such tests are to be undertaken, it is recommended that the personnel, both at the transmitter and the receiver, be specifically assigned to the station for the tests and that in a period preceding their arrival on station they be assembled at Eniwetok, Kwajalein, or Honolulu and be given an organized course of training by the Project Officer, going through periods of transmission and recording at reduced distances. It is further recommended that, during the preliminary training period and in the period prior to, and during, test operations, classified communications with the personnel be transmitted in one-time pad systems instead of a code of the type recently used.

It is through upper-air transmissions of the type employed in this phase of the program that practical results, if any, will be achieved as to determination of the effect of a detonation of an atomic weapon on radio transmission. In addition to the practical benefit from this phase of the problem the results are more or less confirmatory of those of a purely scientific application obtained from ionospheric recordings. In both the scientific and the practical aspects the upper-air-transmission phase should closely correlate with the results obtained from the ionospheric recording phase. For the same reasons that it has been recommended that the ionospheric investigations be repeated, particularly in the Nevada area, it is also recommended that the upper-air transmissions be repeated in that area. The problem of situating transmitting equipment and receiving equipment over land areas is very simple compared to that of finding suitable locations for transmitters and receivers over water areas. In the vicinity of the Nevada area there are several Air Force stations where fixed radio equipment is available for the transmissions, and there are military reservations where portable radio transmitters could be established if desired. When the desired transmitter locations have been found it is then a relatively simple matter to make computations which will indicate the desired location of receiver sites at which these transmissions would be received and recorded. The equipment required for a receiving and recording station is readily portable. Therefore these stations should be located so that the point of reflection of the transmissions will appear directly over the point of detonation or at any predetermined distance from it. The Signal Corps has recently organized at Fort Monmouth an Electronics Warfare Unit, and its mission is to receive and analyze both friendly and enemy transmissions. The problem dealing with upper-air transmissions is so closely akin to the primary mission of this newly organized unit that it would afford this unit excellent training to participate as the field forces under the Project Officer in experiments on this phase of the problem.

Section 3

SURFACE TRANSMISSIONS

Chapter 6

Experimental Procedures

6.1 GENERAL PLAN OF OPERATION

It was originally planned that simultaneous transmissions be made from an aircraft and from a ship through the blast to Eniwetok during the period H−5 to H+5 min for each test. The lack of available aircraft made it impractical to assign an airplane for this mission. However, through arrangements with TG 3.3 a destroyer was assigned for the mission, and it was established that during the period of transmission the destroyer would travel toward the blast on a course which was a reciprocal of the bearing of the blast from the Eniwetok receiver station. From an initial point approximately 30 miles distant from the blast at H−5 min the destroyer was to proceed on course for a minimum of 10 min. While proceeding on the course the destroyer was to transmit a CW carrier with regularly installed equipment on 434 and 145.2 Mc and to transmit on radar with normal PRF on 9,150 Mc. This was done for Dog and Easy Shots. At the time of George Shot the additional requirement was imposed for a CW carrier transmission on 1,222 kc. There was no participation in this phase of the program for Item Shot.

Difficulty was experienced at the Eniwetok receiver station with reception of the 145.8- and the 9,150-Mc transmissions, and no satisfactory reception and recording of these signals was made. The following receiving equip-

ment was used: for 434 kc, an NC100; for 1,222 kc, an SX28; for 145.8 Mc, an AN/SPR9; and for 9,150 Mc, an AN/SPR2. All recordings were on a Stancil-Hoffman CRM15 multichannel recorder and were rerecorded on a Stancil-Hoffman R4 recorder for analysis.

6.2 TEST RESULTS

Figure 6.1 is a graph of the rerecording of the 434-kc transmission from the destroyer during Dog Shot. The wave transmitted was a CW carrier heterodyned with a BFO at the point of reception. This recording covered a period of 7 min 15 sec and was preceded by a voice cue. The graph of the recording reveals no significant phenomena as a result of either radiation or the shock wave. Figure 6.2 is a similar rerecording for a period of 5 min of the transmissions on 2,122 kc during George Shot. These transmissions were CW carriers, modulated with a 1,000-cycle VFO and preceded by a voice cue. Figure 6.3 is a similar rerecording for a period of 4 min 40 sec of transmission from the destroyer of a CW carrier on 434 kc, heterodyned at the receiver station with a BFO. This signal also was preceded by a voice cue. In none of these recordings is there any observable effect which can be attributed to either radiation or the blast action of the shock wave.

6.3 DISCUSSION

The results of this program are fragmentary, but there are enough data available to reveal that the method of approach to this phase of the problem was not satisfactory. In order to conduct a repetition of this phase properly, it would be necessary to have the destroyer or nearby radio transmitter transmit on a tone-modulated CW signal for all except the radar frequency where the PRF presents a suitable audio note. It would likewise be necessary to give the receiving-station personnel preliminary training in the reception and recording of these signals. At the recording station the signal could be received on a specially constructed high-speed tape recorder, which could later be rerun at reduced speed or on a multi-channel (four channel) recording-type mirror oscilloscope with recording paper, run at sufficient speed to detect phenomena of the order of 1 μsec. If the problem were to be rerun in this manner, it is believed that the results achieved would be purely academic and contribute little, if anything, of practical value. They would make no contribution to the scientific aspects unless it were possible to measure the amount of energy reflected to the ship-borne radar scope and likewise to measure accurately that energy received at the land receiving-recording station. Then by a comparison with the known output of the transmitter, the sum of energy received at the ship-borne and the land station would differ by the amount of energy lost in absorption both in the transmitting medium and in the atomic cloud. It is doubtful that it would be practical to effect such measurements with precision, and, if they were made, it is furthermore doubtful that they would contribute anything to the advancement of science or practical application.

Section 4

EVALUATION

Chapter 7

Conclusions

The following conclusions were reached:

1. From the results of Project 8.3B it would appear that there is no appreciable effect on radio propagation due to radiation from the detonation of an atomic weapon.

2. The results of ionospheric recordings of Project 8.3B indicate effects on the ionosphere which appear to be due to the blast of the shock wave on a medium, believed to be the earth's magnetic field, lying at an elevation of from 160 to 185 km at about 11° north latitude.

3. The disturbance of the ionosphere is possibly commensurate with the strength of the weapon, but the period of recurrence appears to be a function of the medium and not of the weapon.

4. The above-noted effect should affect radio propagation of signals which would normally be reflected in the distributed area. This should be confirmed by subsequent observations in Nevada where conditions are more suitable than those in the Pacific area.

5. It is impossible to determine from the data available whether the effect on radio propagation could be used at selected sites by agents of foreign powers to determine a measure of the intensity of the weapon.

6. Project 8.3B produced some practical results. In view of the fact that this is the initial attempt to conduct such a project, it is believed that the results are such as to indicate the desirability of repetitions of this Project both at Eniwetok and in Nevada. There were several aspects overlooked in the planning phase that were revealed in the execution of the Project to be necessary and fundamental. Profiting by these oversights and from the results achieved in the execution of the problem in connection with Operation Greenhouse, subsequent tests should produce more nearly complete and more accurate results. Even the results achieved from this problem in Operation Greenhouse, when compared with those to be obtained from future problems of a like nature, will possibly reveal information not now deducible from them. Likewise the results of future projects of this nature will either confirm or deny the deductions made from this initial effort. It is not to be expected that perfection can be reached in the first attempt at a problem involving so many hitherto unknown factors.

Chapter 8

Recommendations

Based on the results of the various phases of Project 8.3B, it is recommended that:

1. The ionospheric recording phase be repeated both at Eniwetok and in Nevada and also at higher latitudes whenever and wherever there are atomic bomb tests.

2. The upper-air-transmission phase be repeated in future tests at Eniwetok and in Nevada with the modifications in equipment and procedures as discussed in Sec. 5.3.

3. The surface-transmission phase of this Project not be repeated because little practical value would probably be achieved from it.

4. Personnel of the Signal Corps Electronic Warfare Unit be utilized to provide personnel to man the transmitting and the receiving-recording stations and to analyze the results obtained from the upper-air-transmission phase.

5. CRPL be requested to provide personnel and equipment to make and analyze ionospheric recordings in connection with future tests.

6. Signal Corps and CRPL personnel who will be used in subsequent tests have Q-clearance applications initiated as soon as possible.

7. AFSWP incorporate, in guided-missile experiments, programs which will provide findings that will corroborate those resulting from projects of the same type as Project 8.3B.

8. Data such as are obtained from this and subsequent projects of this type which are not restricted data be released for their scientific value.

Appendix A

Instructions for Special Transmissions

1. It has been approved by CinCPac and AACS that the following stations will transmit continuous CW signals according to the schedule given in item 5 on the frequencies indicated and the azimuths shown:

Location	Agency	Frequency (kc)	Azimuth
Okinawa	AACS	12,390	108°0′
Truk	Navy	11,590	68°29′
Yap	Navy	10,710	83°04′

2. The transmitting antenna will be a half-wave doublet properly oriented as above. Each antenna will be erected by local personnel from material available on site.

3. It is desired that operation be performed by present station complement. Wilcox 96C transmissions will consist of unmodulated voice carrier only. TCK-4 transmissions will be with closed key in the CW position. (In order to operate a TCK-4 continuously for periods up to 1 hr, no damage will result if, after the transmitter is tuned and loaded in accordance with the instruction book, the operator, with key closed, reduces the plate voltage to 1500 v. This will reduce the plate current to about 300 ma, permitting the power amplifier tubes to work within their rated capacity with little reduction in power output.)

4. The precedence of these transmissions is urgent, and the schedule will be maintained with priority over all other traffic, except operational priority involving combat.

5. The schedule of operation is as follows:

Date	Code	Time Begin	Time Stop
27 March	Mire	1830Z	1855Z
30 March	Dirt	1920Z	2010Z

Date	Code	Time Begin	Time Stop
2 April	Yore	1800Z	1840Z
6 April	Brown	1830Z	1920Z
10 April	Lark	1900Z	1925Z
14 April	Open	1850Z	1930Z
17 April	Cite	1825Z	1915Z
20 April	Wept	1830Z	1845Z
24 April	Kepi	1740Z	1805Z
28 April	Pool	1710Z	1725Z
2 May	Bean	2000Z	2025Z
4 May	Vice	1810Z	1850Z
8 May	Jail	1815Z	1905Z
12 May	Cone	1810Z	1835Z
15 May	Undo	1820Z	1910Z
18 May	Quoit	1940Z	2005Z
21 May	Idea	1700Z	1740Z
24 May	Dove	1900Z	1915Z
26 May	Tile	1810Z	1900Z
30 May	Hare	1900Z	1940Z
1 June	Ripe	1800Z	1850Z
5 June	Asta	2000Z	2025Z
8 June	Esau	1800Z	1840Z
11 June	Grip	1700Z	1725Z
15 June	Soda	1900Z	1940Z
18 June	Zone	2000Z	2025Z
21 June	File	1900Z	1925Z

6. The schedule given in item 5 will be rigidly and accurately followed unless altered by one of the following messages (the first group is the action ordered and the second group is the code of the transmission).

Advance this transmission 24 hr only:
    Hebe, Hera, Juno, Kato

Advance this transmission 1 hr earlier:
    Thor, Time, Talo, Doho

Advance this transmission 2 hr earlier:
   Apex, Bean, Bike, Andy
Delay this transmission 24 hr late:
   Enos, Ezra, Foal, Fido
Delay this transmission 48 hr late:
   Loci, Lazy, Lime, Mike
Delay this transmission 1 hr late:
   Plat, Prim, Polo, Rice
Cancel this transmission:
   Goal, Grid, Glad, Give, Gape

This transmission not heard; check transmitter and antenna:
   Coda, Coco, Deal, Drop

Discontinue all further transmissions of this series, thanks for your cooperation:
   Nipa

7. The messages in item 6 will be received by Okinawa through normal AACS channels and at Truk and Yap through normal Navy channels.

Appendix B

Instructions for Reception of Special Transmissions

1. It has been approved by Hq, JTF-3, that the following stations receive and record CW signals transmitted to them according to the schedule contained in item 5. These transmissions will be received on the following frequencies and on the bearing indicated:

Location	Operated by	Frequency (kc)	Bearing	Recorder
Kwajalein	TG 3.4	12,390	301°10'	R4
Majuro	TG 3.4	12,390	301°10'	Minitape
Bikini	TG 3.2	10,710	268°12'	Minitape
Honolulu	ASA	11,590	261°55'	R4

2. The receiving antenna will be a half-wave doublet properly oriented as above. Each antenna will be erected by local personnel from material available on site.

3. The receiver will be turned on and left in operation 15 min before the scheduled transmission. The received signal will be heterodyned to produce a strong note of from 1,000 to 2,000 cycles. After being tuned in and adjusted to reception, it will be recorded continuously at 7.5 ft/min. Whenever recording is by Minitape, there shall be a 1-min overlap, during which period there will be a voice synchronizing signal.

4. The recorded tapes will be marked to indicate the date and time begun and the time finished and will be sent by earliest transportation to J-5 Division, Hq, JTF-3, APO 187 (HOW), c/o Postmaster, San Francisco, Calif., by mail or special messenger.

5. The schedule of transmissions to be received is as follows:
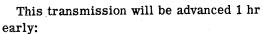
Date	Code	Time Begin	Time Stop
27 March	Mire	1830Z	1855Z
30 March	Dirt	1920Z	2010Z

Date	Code	Time Begin	Time Stop
2 April	Yore	1800Z	1840Z
6 April	Brown	1830Z	1920Z
10 April	Lark	1900Z	1925Z
14 April	Open	1850Z	1930Z
17 April	Cite	1825Z	1915Z
20 April	Wept	1830Z	1845Z
24 April	Kepi	1740Z	1805Z
28 April	Pool	1710Z	1725Z
2 May	Bean	2000Z	2025Z
4 May	Vice	1810Z	1850Z
8 May	Jail	1815Z	1905Z
12 May	Gone	1810Z	1835Z
15 May	Undo	1820Z	1910Z
18 May	Quoit	1940Z	2005Z
21 May	Idea	1700Z	1740Z
24 May	Dove	1900Z	1915Z
26 May	Tile	1810Z	1900Z
30 May	Hare	1900Z	1940Z
1 June	Ripe	1800Z	1850Z
5 June	Asta	2000Z	2025Z
8 June	Esau	1800Z	1840Z
11 June	Grip	1700Z	1725Z
15 June	Soda	1900Z	1940Z
18 June	Zone	2000Z	2025Z
21 June	File	1900Z	1925Z

6. The schedule given in item 5 will be rigidly and accurately followed unless varied by one of the following messages (the first group is the action ordered and the second group is the code of the transmission).

This transmission will be advanced 24 hr early:

Hebe, Hera, Juno, Kato

This transmission will be advanced 1 hr early:
   Thor, Tine, Tale, Doho
This transmission will be advanced 2 hr early:
   Apex, Bean, Bike, Andy
This transmission will be delayed 24 hr late:
   Enos, Ezra, Foal, Fido
This transmission will be delayed 48 hr late:
   Loci, Lazy, Lime, Mike
This transmission will be delayed 1 hr late:
   Plat, Prim, Pole, Rice
This transmission has been canceled:
   Goal, Grid, Glad, Give, Gape

This transmission need not be recorded; if recorded, retain tapes and erase for future use:
   Veal, Wing, Vote, Went, Vase, Wear, Open, Olaf, Ower
Tests have been discontinued, thanks for your cooperation, arrange to send equipment to JTF-3 as planned:
   Nipa
7. In case any transmission is not received, report by message to Hq, JTF-3, by two groups, the first of which is the code word of transmission followed by one of the following code words:
   Coda, Coco, Deal, Drop

Appendix C

Sample of Information Furnished Task Group 3.3 for Inclusion in Each Operations Order

HEADQUARTERS
JOINT TASK FORCE THREE
APO 187

AG 311   25 April 1951

SUBJECT: Task Group 3.3 Participation in Project 8.3B

TO: Commander Task Group 3.3
          c/o FPO, San Francisco, Calif.

1. Reference is made to paragraph 5 of your letter serial 0019 dated 3 February 1951.

2. It is desired that the DDE assigned to assist in the 8.3B Program for GEORGE test conduct the following:

(a) At H minus 5 minutes pass through Point "A" (Bearing 356° T., distance 30 nautical miles from EBERIRU shot tower) on course 176° T., at 15 knots until H plus 5 minutes.

(b) Transmit continuous carrier and/or pulse signals from H minus 10 to H plus 5 minutes on the following frequencies:

Band	Frequency
LF	434 kcs
LF	2122 kcs
VHF	145.8 mcs
RADAR	1329 mcs

3. The above requirement is for GEORGE shot only. Requirement for succeeding tests will be furnished prior to each shot in sufficient time to effect the required coordination.

BY COMMAND OF LIEUTENANT GENERAL QUESADA:

Copy furnished:
  CTG 3.1 ATTN: Col. Jarmon

Appendix D

Velocity of the Shock Wave in Air

In "The Effects of Atomic Weapons"[1] reference is made to Fig. 3.13f as follows: "...the time of arrival of the shock as a function of the distance from the source. It can be seen that, as expected, the slope of this curve approaches the velocity of sound as the shock weakens." Figure 3.13f is a graph of time of arrival of shock, seconds (ordinate) vs distance from bomb, feet (abscissa). On this curve the velocity of the shock wave is more rapid than the velocity of sound until a distance of approximately 9,000 ft is reached at the end of about 6.25 sec. Thereafter, the velocity of the shock wave approximately coincides with the velocity of sound. These characteristics are those of a shock wave in an infinite homogeneous atmosphere and are the result of an air burst.

In considering the velocity of the shock wave, it therefore follows that, since the velocity of shock wave up to 9,000 ft accelerates to a point where it has a lead of about 2,000 ft on a normal sound wave initiated concurrently, it can be considered that the velocity of the shock wave is that of the sound wave plus 2,000 ft. In dealing with the time of travel of shock waves over distances of 50 miles or more, this lead of less than ½ mile becomes insignificant when compared to the accuracy of the means of measuring and scaling these distances in the upper atmosphere.

Since the velocities of sound and of shock wave reach concurrence at a distance of approximately 9,000 ft from Point 0, the velocity of the shock wave from that point on should conform to the velocity of sound as determined from experiment and observation in the upper atmosphere. The accepted velocity of sound at sea level and 0°C is 1,088 ft/sec. It is known that sound velocity varies directly as the square root of the absolute temperatures of the gases through which it passes and inversely as the square root of the densities of those gases, disregarding change in chemical constituents of the gases.

R. J. Havens of the Naval Research Laboratory, Bellview, supplied the data shown in the addendum to this appendix relative to atmospheric conditions up to 220 km and based on information obtained from rocket flights at White Sands, N. Mex. From these and other data, Fig. D.1 of atmospheric densities was plotted. Havens plotted the curves of sound velocity in the upper atmosphere as shown in Fig. D.2 from the same data.

The Project Officer prepared the graph of the time-distance relation of vertically projected sound, shown in Fig. D.3, by using mean velocities up to 160 km and thereafter interpolating data obtained from Havens' table and from the curve and converting from kilometers to miles.

The matter of sound velocity, in general, without specific reference to atomic detonations or to high-intensity explosive effects, was discussed with Daniels of Evans Signal Laboratory, Fort Monmouth, N. J. Daniels stated that he had determined that 190 km was the approximate maximum range for a shock wave from sources which he had considered. He was of the opinion that this maximum range could not be exceeded because of the rarity of the atmosphere at that altitude and beyond. It is not known whether Daniels' concepts were based on an explosion of the order of 10 kt and greater. Under the hypothesis given by Daniels the upper-air limit of sound propagation is approximately 120 miles. It is not known whether or not this would also apply to shock wave, but

it is reasonable to presume that, if a shock wave were to exceed this altitude, it would be of very meager strength.

The data appearing in the addendum were used to compute the progress of shock wave up to and including 120 miles as shown in Fig. D.3. On this graph the travel of shock wave has also been plotted at the constant velocity of sound at sea level. This latter velocity has been employed in computing the graphs of ionospheric recordings for Project 8.3B. It will be noted

that this introduces some error, but this error is of such small magnitude that it is probably less than that made in interpreting the ionospheric records for graphic presentation.

REFERENCE

1. Los Alamos Scientific Laboratory, "The Effects of Atomic Weapons," p 52, U. S. Government Printing Office, Washington, 1950.

ADDENDUM TO APPENDIX D

AVERAGE ATMOSPHERE UP TO 220 KM*

Altitude† above Sea Level (km)	Pressure (mm Hg)	Density (g/m³)	Temperature (°K) M = 29 Km	M = 24 Km	M = 14.5 Km	Scale Height	Sound Velocity (m/sec)	Mean Free Path (cm, N₂)
0	7.6×10^2	1.2×10^3	290			8.5	345	6.5×10^{-6}
10	2.1×10^2	4.2×10^2	230			6.8	310	1.9×10^{-5}
20	4.2×10	9.2×10	210			6.1	295	8.6×10^{-5}
30	9.5	1.9×10	235			6.9	315	4.2×10^{-4}
40	2.4	4.3	260			7.7	325	1.8×10^{-3}
50	7.5×10^{-1}	1.3	270			8.0	330	6.1×10^{-3}
60	2.1×10^{-1}	3.8×10^{-1}	260			7.8	325	2.1×10^{-2}
70	5.4×10^{-2}	1.2×10^{-1}	210			6.3	295	6.6×10^{-2}
80	1.0×10^{-2}	2.5×10^{-2}	190			5.7	280	3.2×10^{-1}
90	1.9×10^{-3}	4.0×10^{-3}	210			6.3	295	2.0
100	4.2×10^{-4}	8×10^{-4}	240			7.2	315	10
110	1.2×10^{-4}	2.0×10^{-4}	270	220		8.2	330	40
120	3.5×10^{-5}	5×10^{-5}	330	270		10	370	1.5×10^2
130	1.5×10^{-5}	2×10^{-5}	390	320		12	400	4×10^2
140	7×10^{-6}	7×10^{-6}	450	370	230	14	430	1×10^3
150	3×10^{-6}	3×10^{-6}		420	250	16	460	2.5×10^3
160	2×10^{-6}	1.5×10^{-6}		470	280	18	480	5×10^3
220		1×10^{-7}	‡	‡	‡	30	600	

*Data supplied by R. J. Havens and H. E. LaGow, Naval Research Laboratory, October 15, 1951.

†The figures at altitudes above 40 km are based entirely on pressure and density data obtained on 10 rocket flights at White Sands, two of which reached 160 km and one of which reached 219 km above sea level.

‡Tentative.

Appendix E

Height of the Ionospheric Layers

The ionospheric recorder produces an image of the virtual height of the ionospheric layers. The determination of the true heights of these layers has been the subject of investigation by CRPL, NBS. White and Watchel[1] reveal that there is a slight disparity of true heights of the ionospheric layers and of the virtual heights as recorded, ranging from 5 to 25 km without regard to sign. These variations are of such low order compared to the distances involved that it is concluded that they may be disregarded, and for all practical purposes of this program the virtual height as recorded may safely be accepted as the approximate actual height.

REFERENCE

1. Gladys R. White and Irma S. Watchel, True Heights of the F-2 Layers, J. Geophys. Research, 54:239-242 (1949).
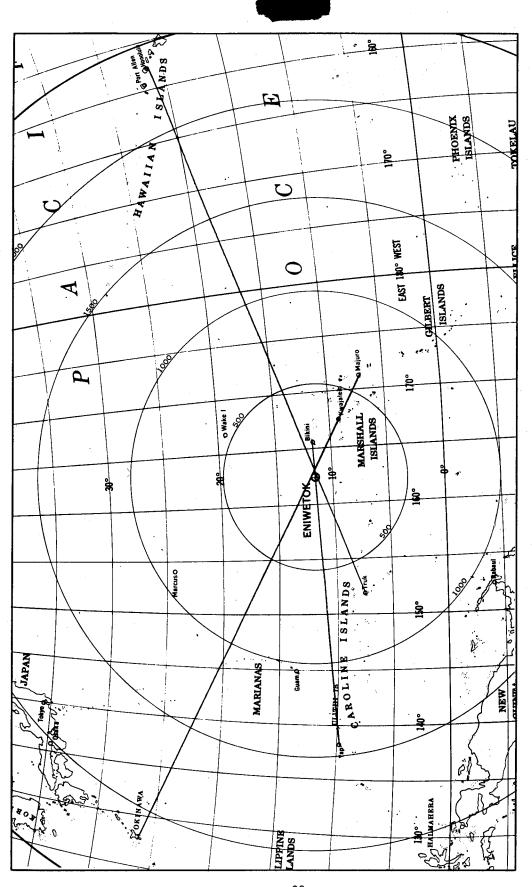
Fig. 1.1 Great Circle Distances and Azimuths from Eniwetok Atoll, Showing Upper-air-transmission Paths (Prepared by Navy Hydrographic Office) (See Page 61)
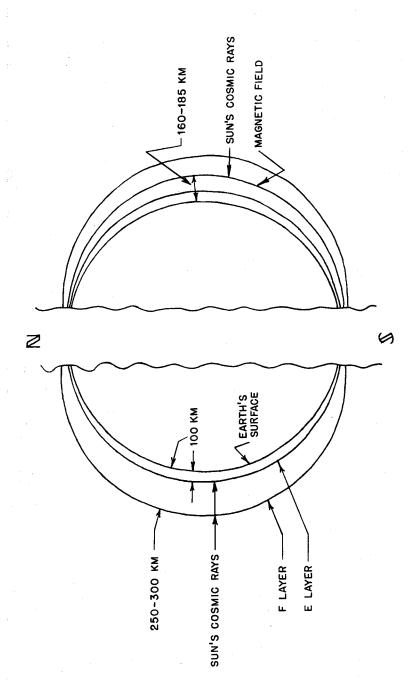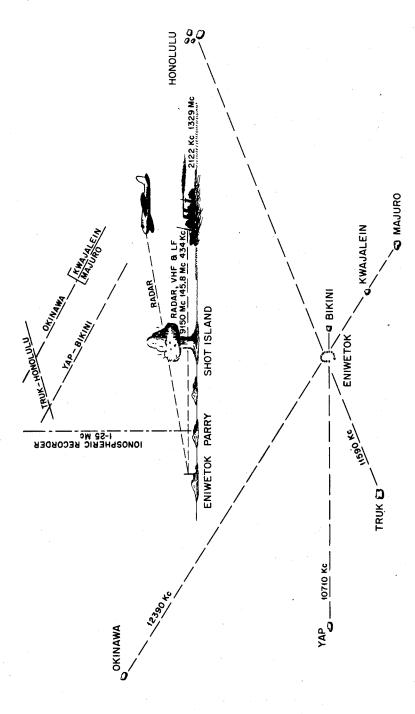
Fig. 1.2 Sketch of Ionospheric Concepts. The left portion illustrates the ionization theory; the right portion illustrates the electrostatic–field theory. (See page 62.)

Fig. 1.3 Schematic Diagram of Planned Operations, Project 8.3B
(See Page 62)
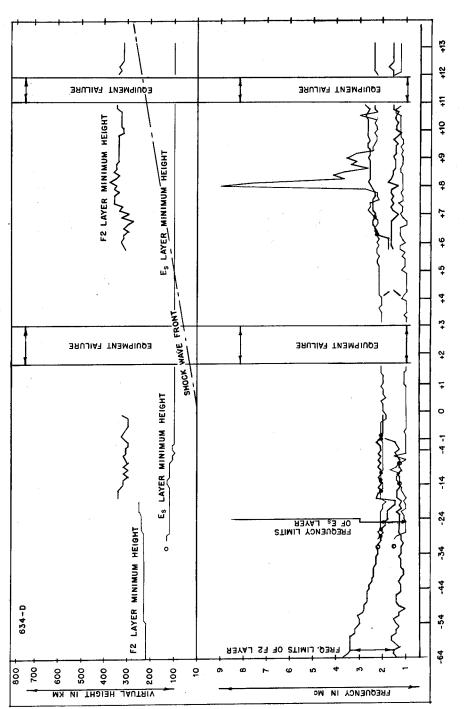
Fig. 3.1 Ionospheric Conditions, Dog Shot, D−64 to D + 13 Min

(See Page 67)
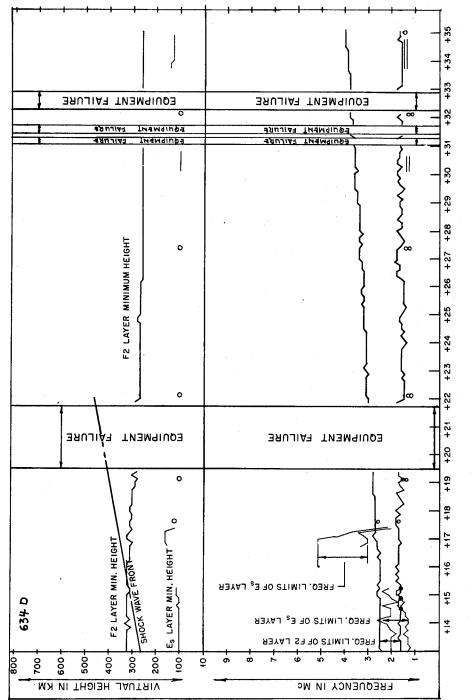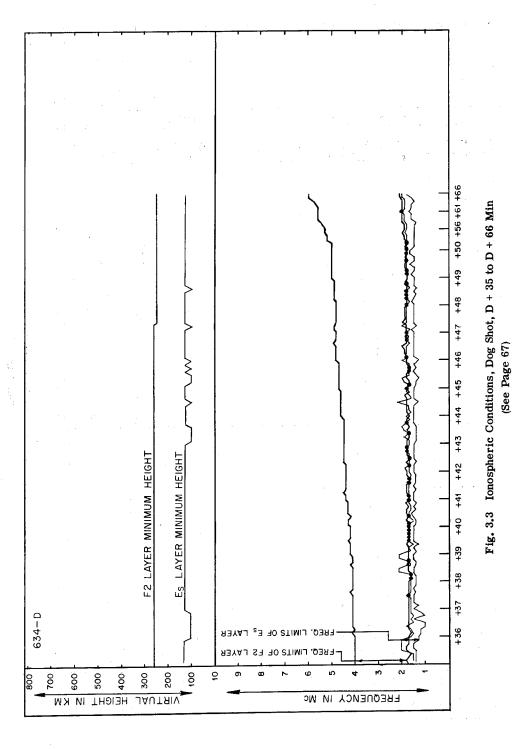
Fig. 3.2   Ionospheric Conditions, Dog Shot, D + 13 to D + 35 Min

(See Page 67)

Fig. 3.3 Ionospheric Conditions, Dog Shot, D + 35 to D + 66 Min
(See Page 67)
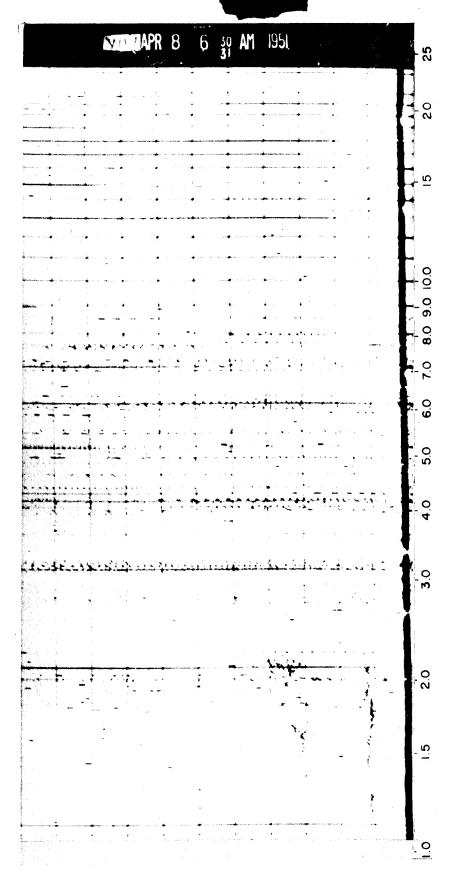
Fig. 3.4 Ionospheric Record of Conditions at D−4 to D−3 Min 52.5 Sec. There is a slight showing of the E-layer, and the F-layer is forming between 300 and 400 km. (See page 67.)

95
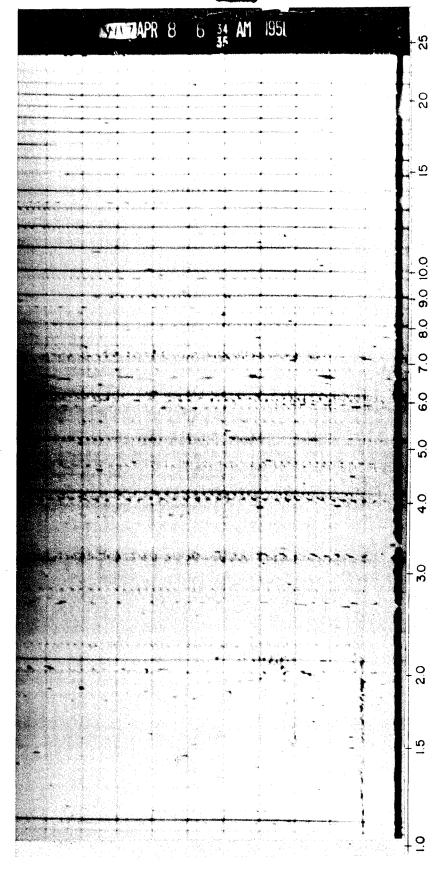
Fig. 3.5   Conditions at D-hour to D + 7.5 Sec.   The E-layer is about 2 km lower in altitude, and the F-layer is less pronounced.   (See page 67.)
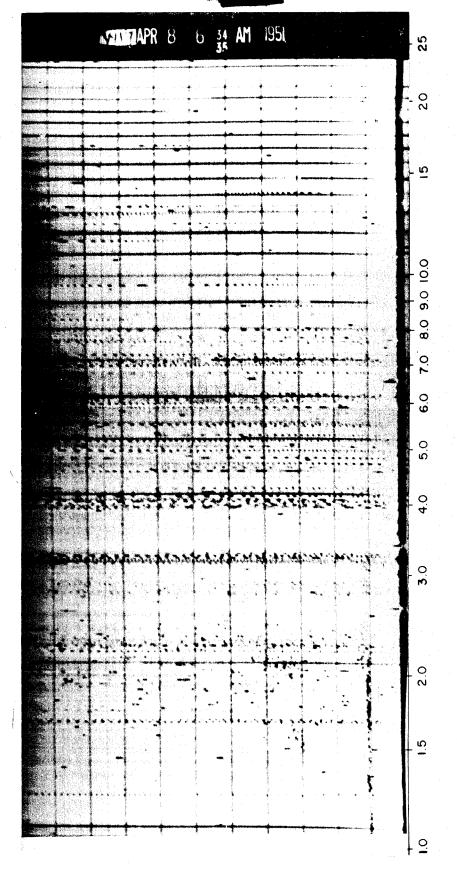
Fig. 3.6   Conditions at D + 7.5 to D + 15 Sec.   The E-layer is increasing in frequency, and the F-layer has disappeared.   (See page 67.)
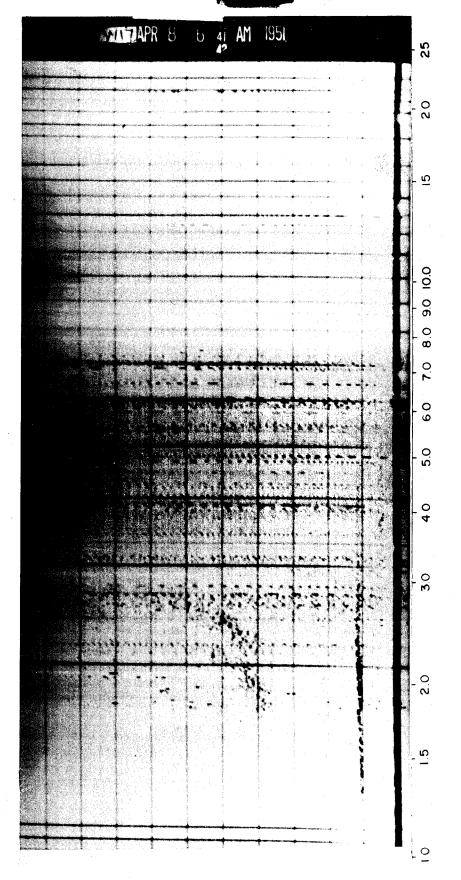
Fig. 3.7 Conditions at D + 7 Min 52.5 Sec to D + 8 Min. The E-layer is increasing in minimum frequency and altitude, and the F-layer is returning at higher altitude. (See page 67.)
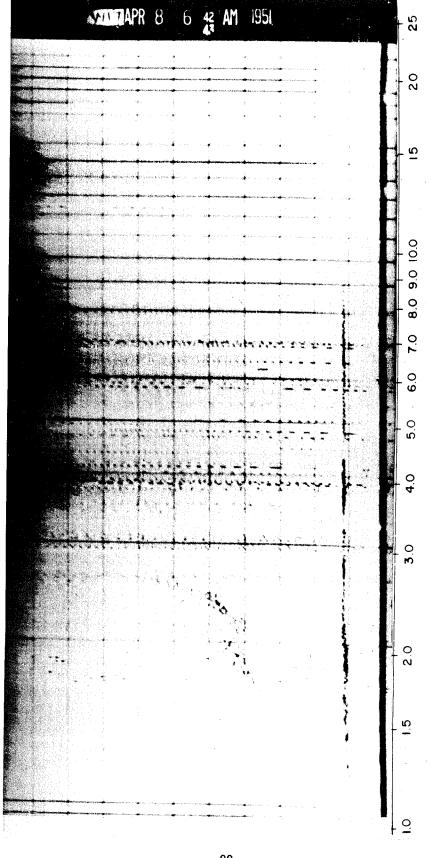
Fig. 3.8   Conditions at D + 8 to D + 8 Min 7.5 Sec. The E-layer is extending to much higher frequency, and the F-layer is forming distinct traces. (See page 67.)

APR 8 6 42 AM 1951
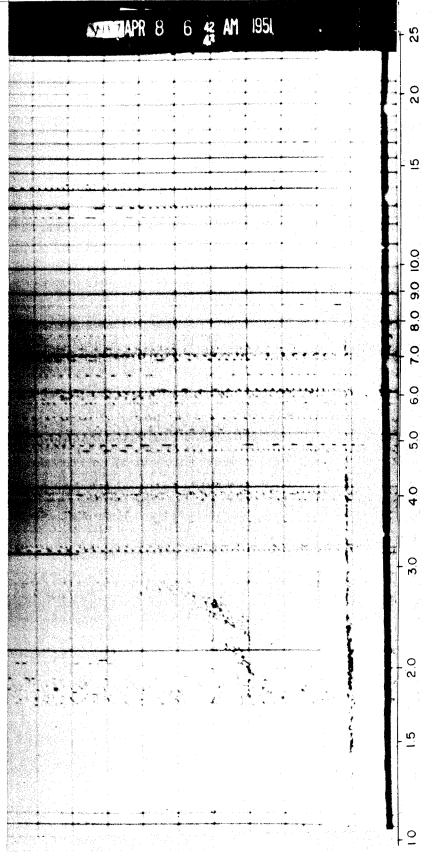
Fig. 3.9 Conditions at D + 8 Min 7.5 Sec to D + 8 Min 15 Sec. Little change from the conditions in Fig. 3.8 is shown. (See page 67.)
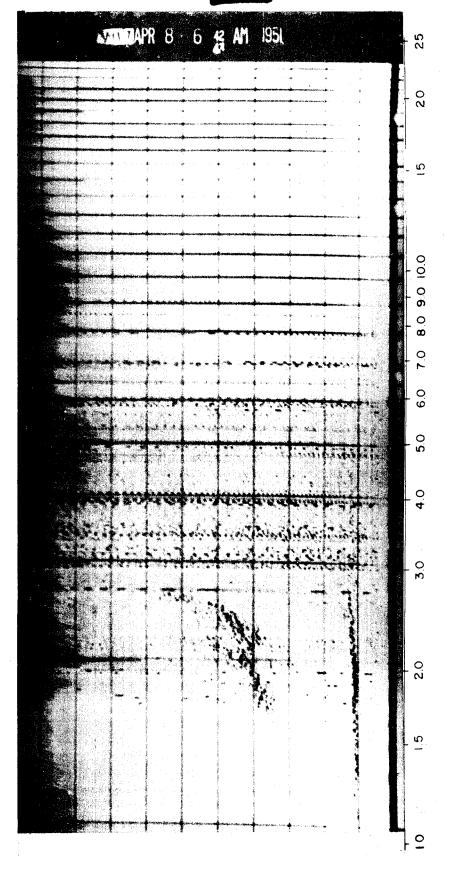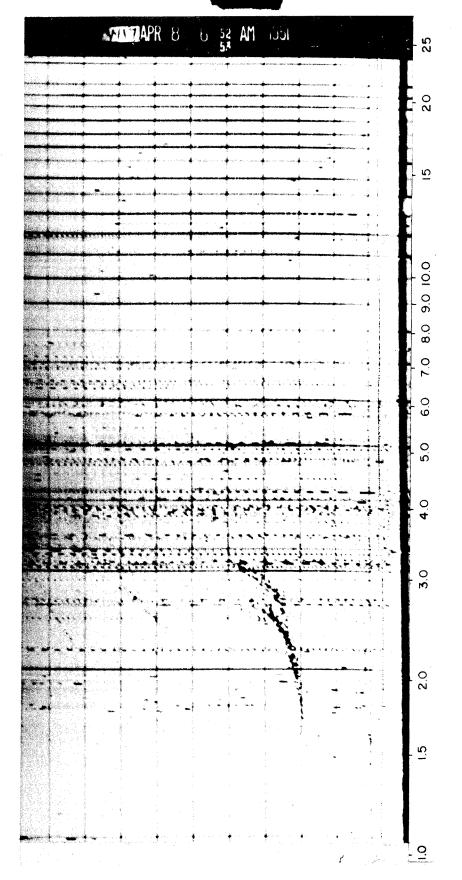
Fig. 3.10 Conditions at D + 8 Min 37.5 Sec to D + 8 Min 45 Sec. Still little change is noted. (See page 67.)

Fig. 3.11 Conditions at D + 8 Min 52.5 Sec to D + 9 Min. The E-layer is practically gone, and the F-layer is more distinct. (See page 67.)
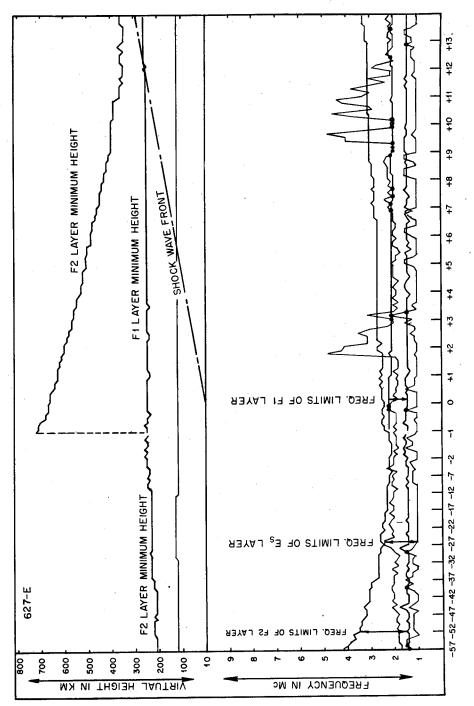
Fig. 3.12 Ionospheric Conditions, Easy Shot, E − 57 to E + 14 Min
(See Page 67)
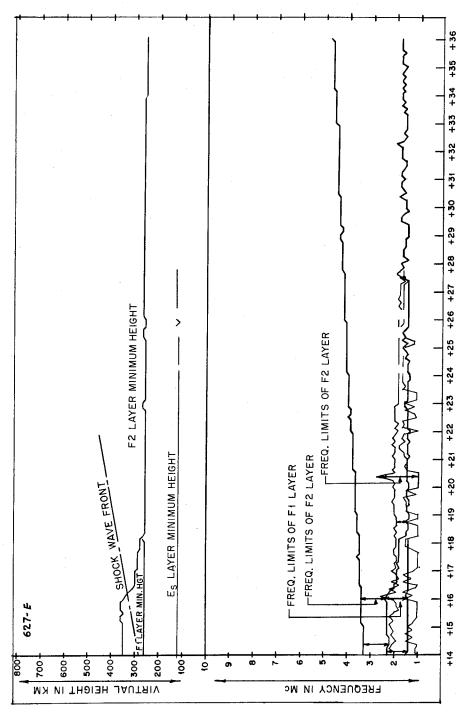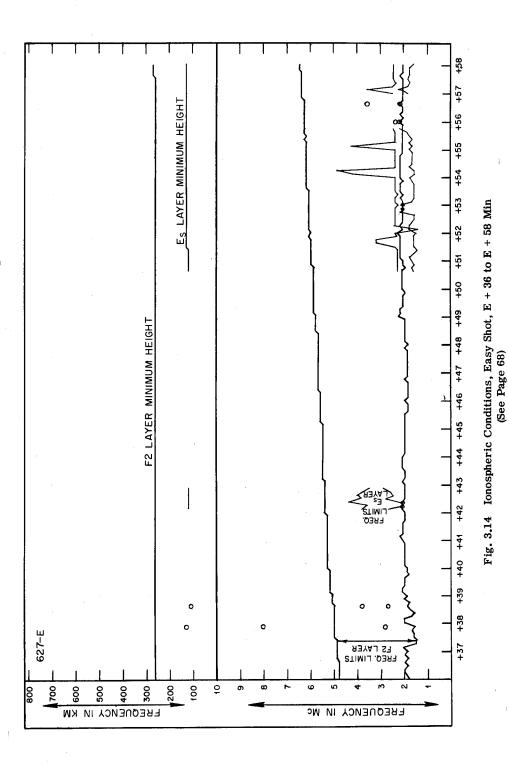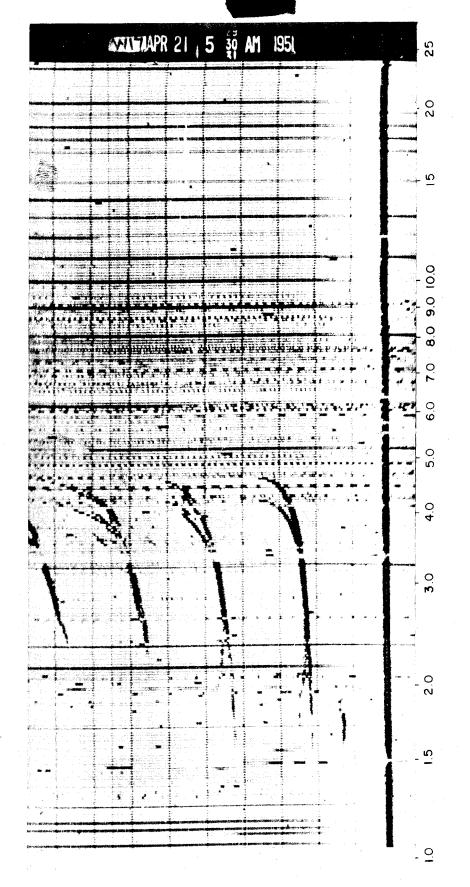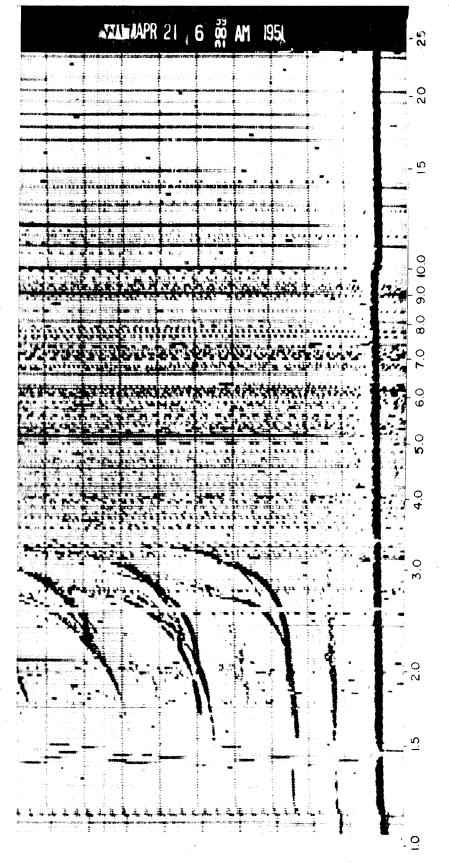
Fig. 3.13 Ionospheric Conditions, Easy Shot, E + 14 to E + 36 Min
(See Page 67)

Fig. 3.14 Ionospheric Conditions, Easy Shot, E + 36 to E + 58 Min
(See Page 68)

Fig. 3.15 Conditions at E—57 Min. This is an early morning record, showing the F-layer and some E_s-layer. (See page 68.)

APR 21 6:00 AM 1951

Fig. 3.16 Conditions at E−27 Min. This is a normal presunrise record with the F-layer and E$_s$-layer appearing. The critical frequency of the F-layer has decreased. (See page 68.)

107
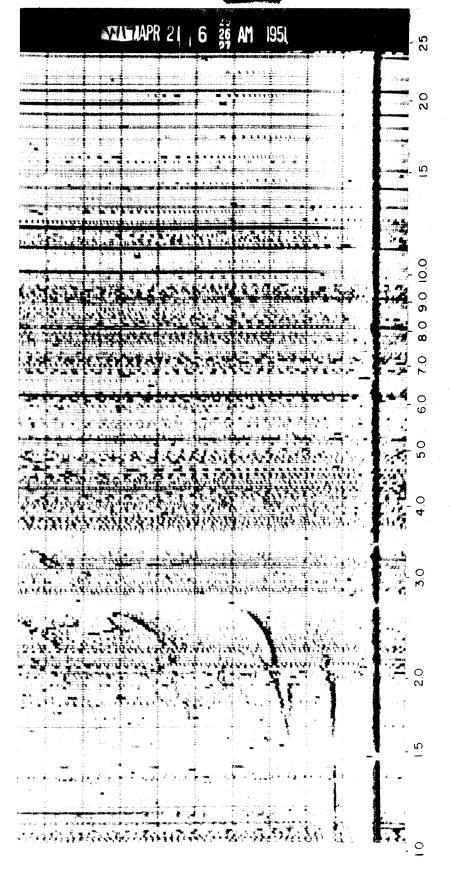
Fig. 3.17 Conditions at E−1 Min. A normal presunrise record of the F-layer with traces of the F-2 layer forming at about 700 km. (See page 68.)

The record shows "APR 21 6 AM 1951" with timing marks, and a horizontal scale reading 1.0, 1.5, 2.0, 3.0, 4.0, 5.0, 6.0, 7.0, 8.0, 9.0, 10.0, 15, 20, 25.
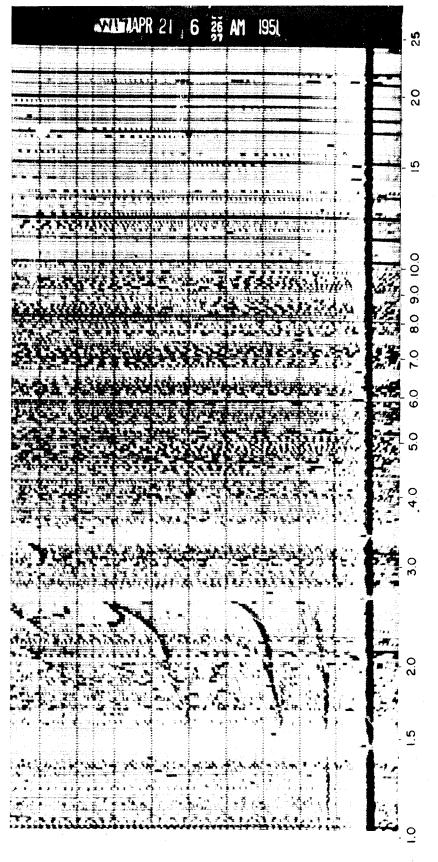
Fig. 3.18 Conditions at E−7.5 Sec. A normal presunrise record of the F-layer. The F-2 layer is more definite and has dropped to about 670 km. (See page 68.)
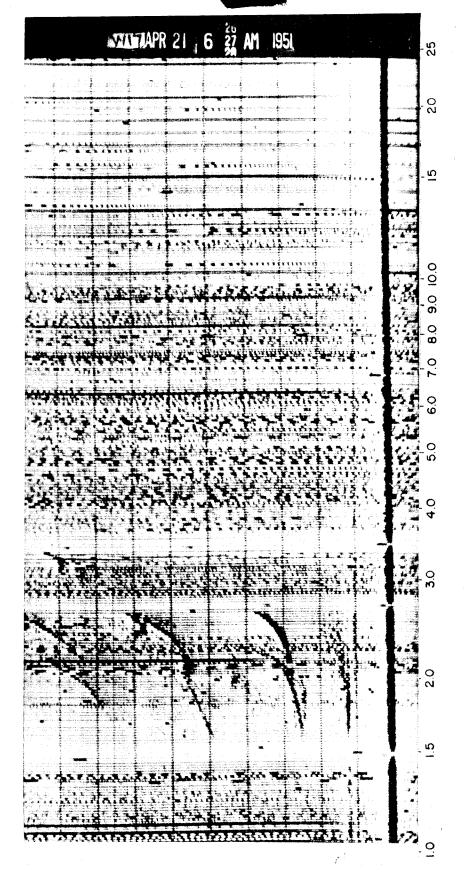
Fig. 3.19 Record Taken at E−0 Time. There are no abrupt changes; the F-2 layer is forming. (See page 68.)
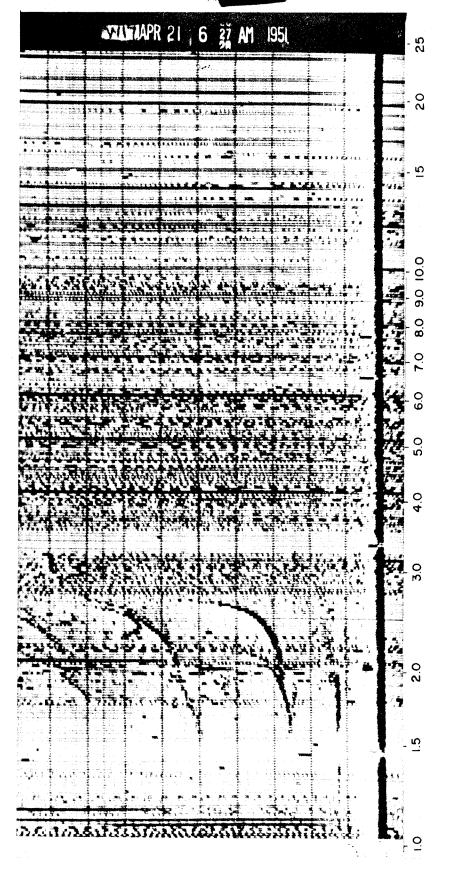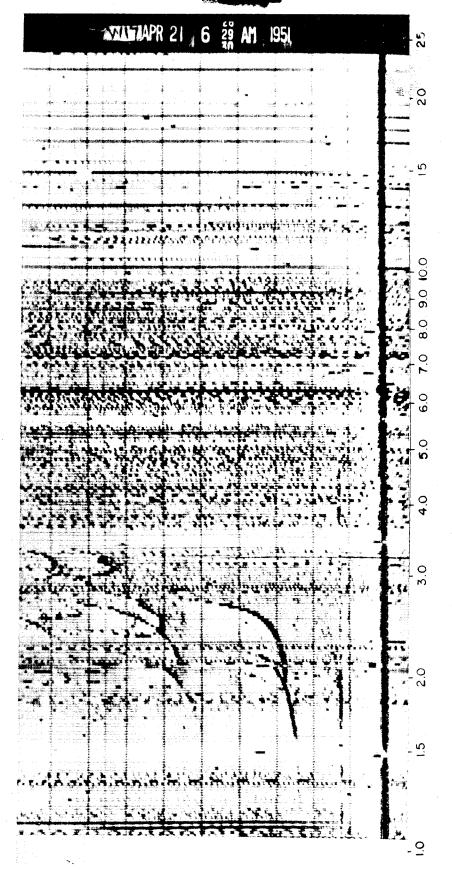
Fig. 3.20   Record Taken at E + 22.5 Sec.   There are no abrupt changes; the F-2 layer is more definite.   (See page 68.)

Fig. 3.21 Record Taken at E + 2 Min. The F-2 layer, at 600 km, is quite definite. (See page 68.)
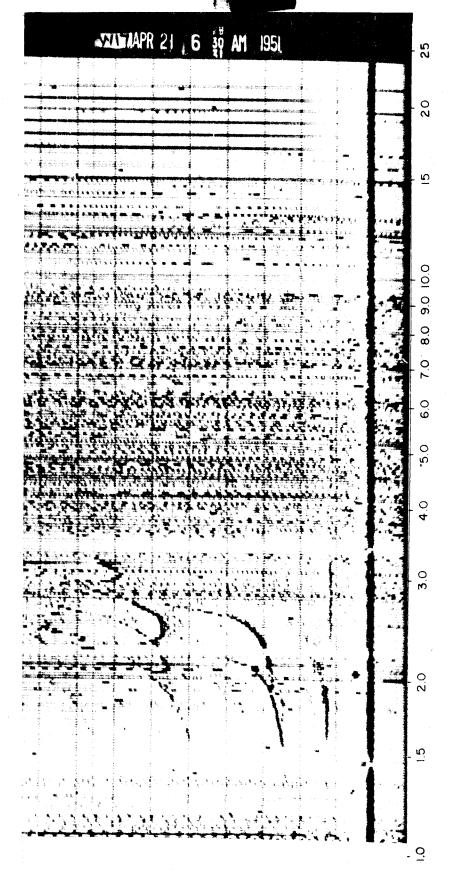
Fig. 3.22 Record Taken at E + 3 Min. The F-2 layer is dropping in height and is at 560 km. Intermittent traces of the E_s-layer are recorded up to 31 Mc. (See page 68.)

113
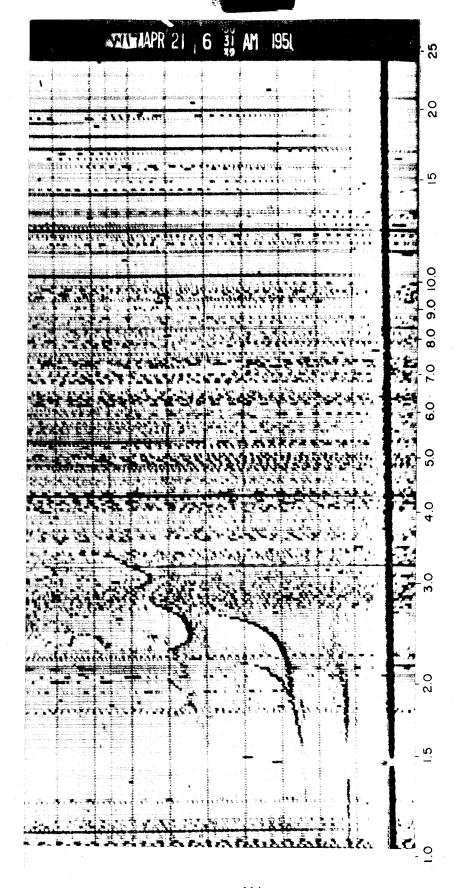
Fig. 3.23 Record Taken at E + 4 Min. The F-2 layer has dropped to 530 km. (See page 68.)

114
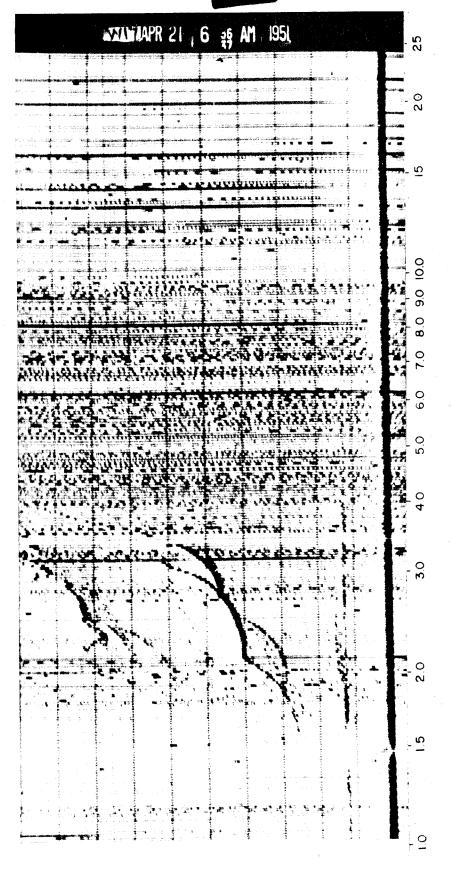
Fig. 3.24   Record Taken at E + 9 Min.   The F-2 layer has dropped to 400 km and is merging with the F-1 layer.   The Es-layer appears up to 4 Mc.   (See page 68.)

Fig. 3.25 Record Taken at E + 9 Min 45 Sec. The F-2 and F-1 layers are merging, with intermittent traces of the E$_s$-layer up to 4.8 Mc. (See page 68.)
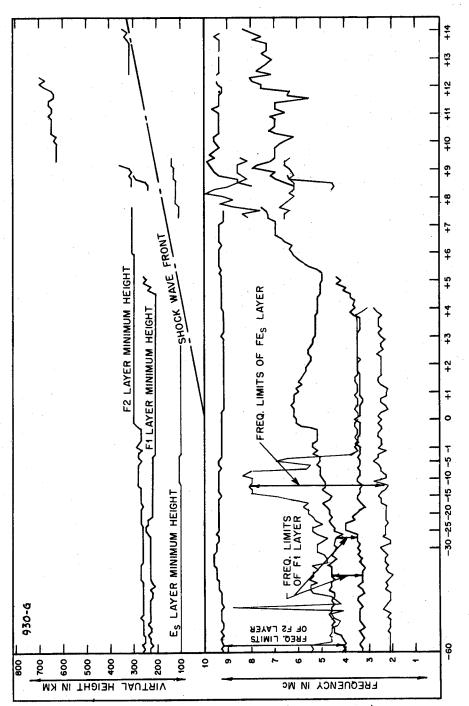
Fig. 3.26 Ionospheric Conditions, George Shot, G−60 to G + 14 Min
(See Page 68)

117
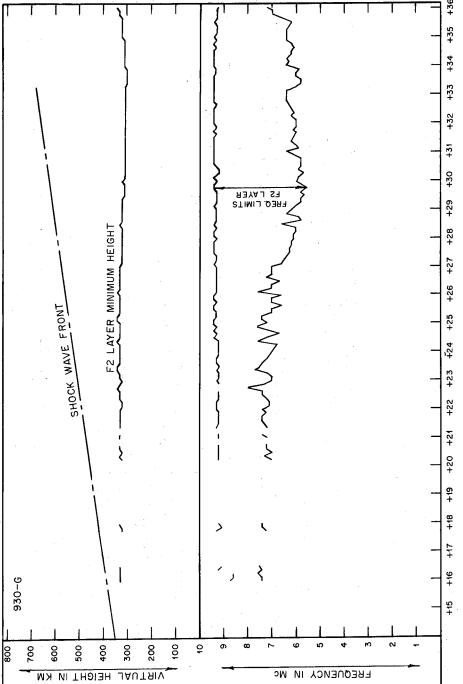
Fig. 3.27 Ionospheric Conditions, George Shot, G + 14 to G + 36 Min
(See Page 68)

118
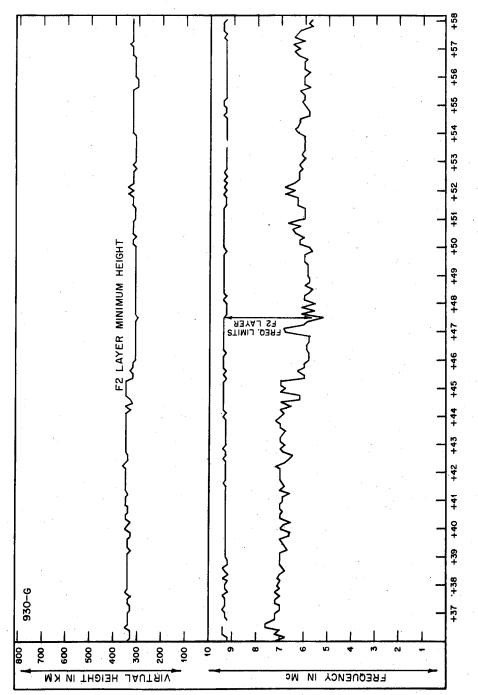
Fig. 3.28 Ionospheric Conditions, George Shot, G + 36 to G + 58 Min
(See Page 68)
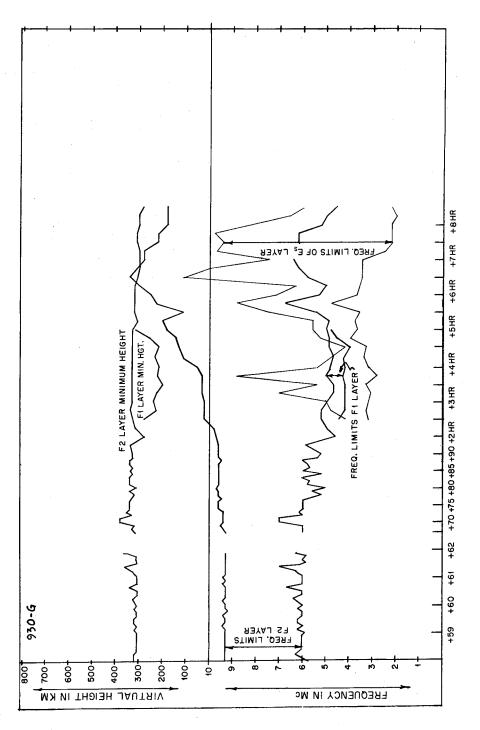
Fig. 3.29 Ionospheric Conditions, George Shot, G + 58 Min to G + 8.5 Hr
(See Page 68)
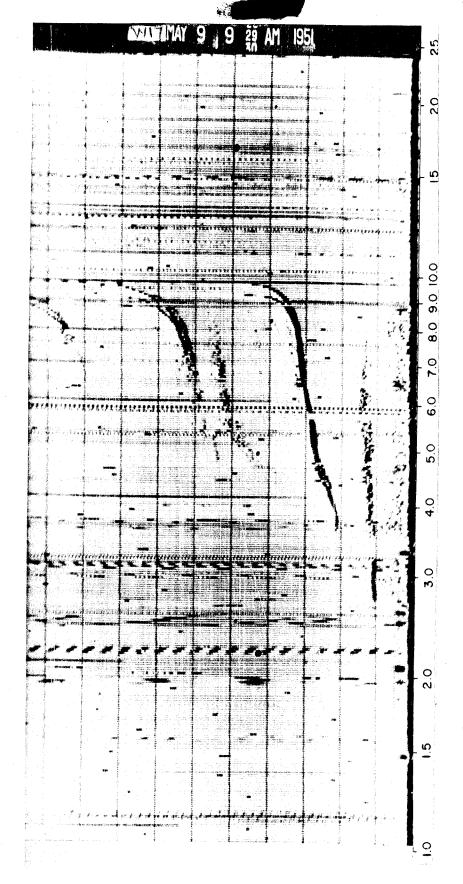
Fig. 3.30   Ionospheric Record Taken at G−1 Min. Normal conditions at that time are illustrated. The E_s-layer has some stratification appearing in the high-frequency portion of the echoes. A normal F-layer trace with two multiples is shown. (See page 68.)

121
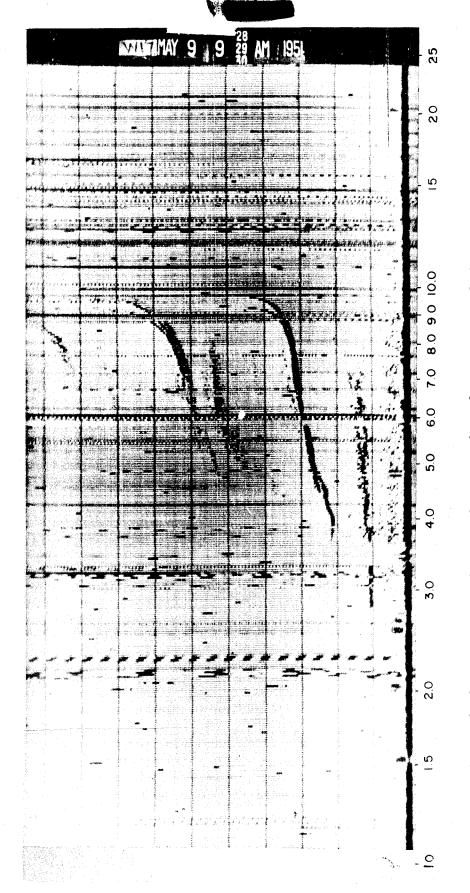
Fig. 3.31 Record Taken at G−7.5 Sec. There is no change in conditions from previous record taken at G−1 Min. (See page 68.)
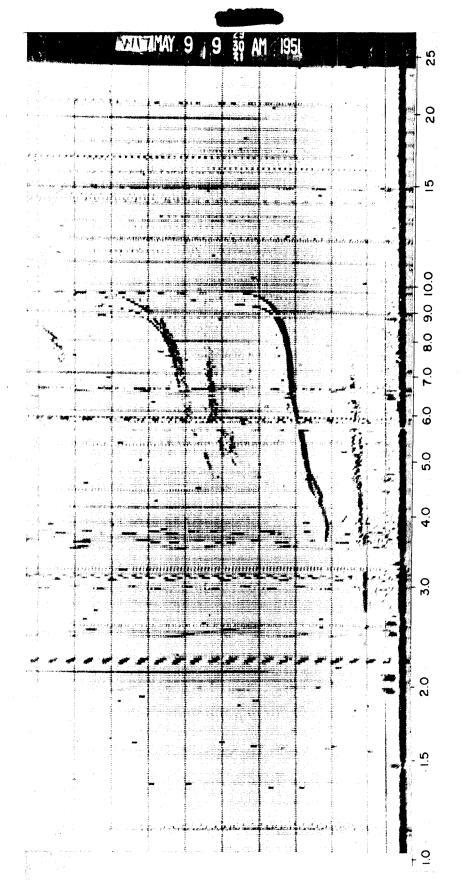
Fig. 3.32   Record Taken at G—0 Time. No instantaneous changes are observed. (See page 68.)

123
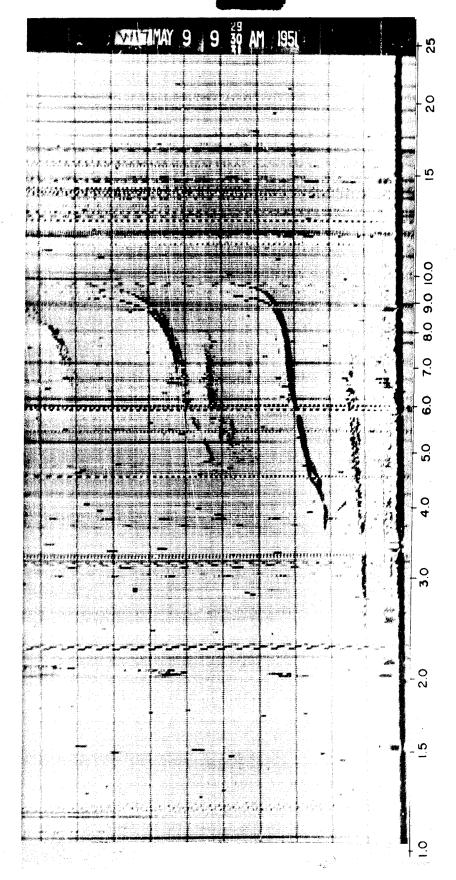
Fig. 3.33 Record Taken at G + 22.5 Sec. Absorption is normal. (See page 68.)
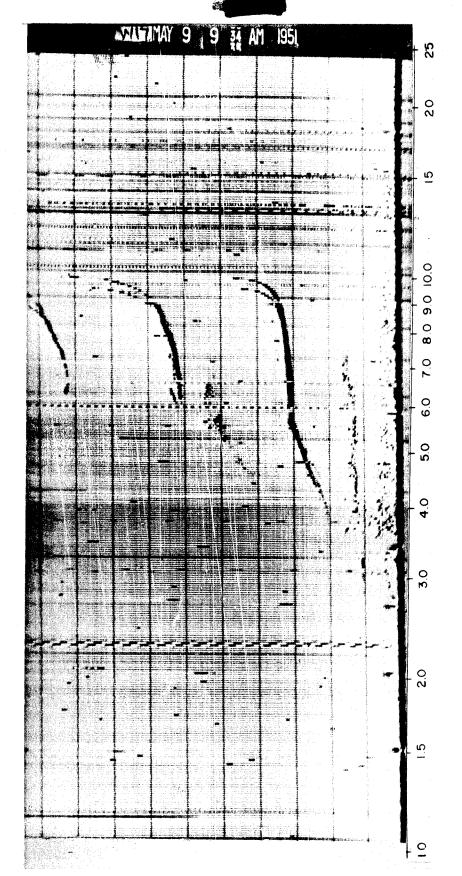
Fig. 3.34 Record Taken at G + 4 Min. The shock-wave front enters the E_s-layer. (See page 68.)

125
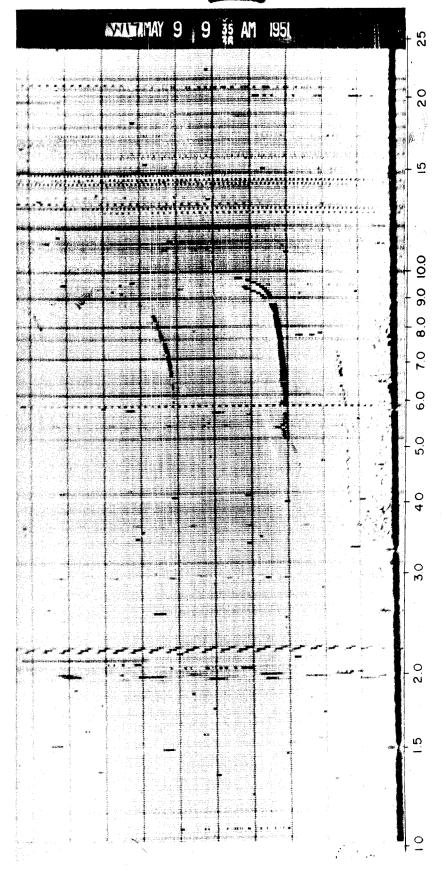
Fig. 3.35 Record Taken at G + 5 Min. The E-layer and the F-1 layer are almost completely absorbed. (See page 68.)
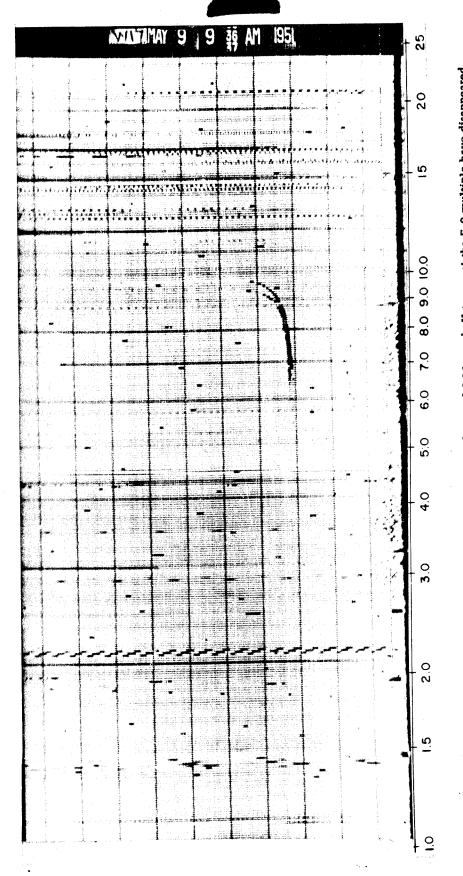
Fig. 3.36 Record Taken at G + 6 Min. Absorption has progressed up to 6.3 Mc, and all traces of the F-2 multiple have disappeared. (See page 68.)
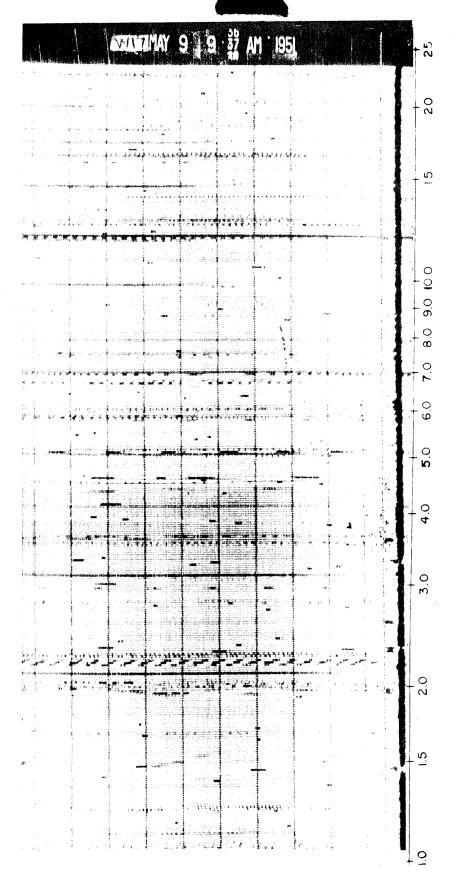
Fig. 3.37   Record Taken at G + 7 Min. Absorption is nearly complete, with intermittent traces of the F-2 layer appearing. (See page 68.)

128
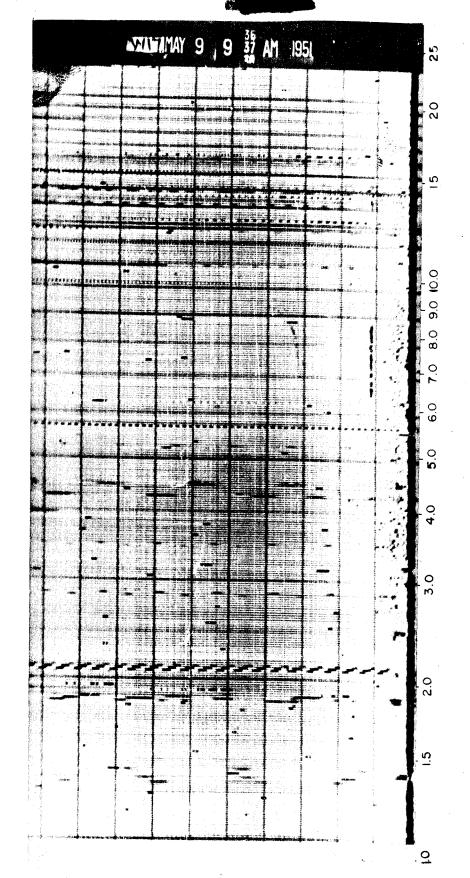
Fig. 3.38 Record Taken at G + 7.5 Min. Heavy absorption is shown. The E_s-layer appears from 6.6 to 8.4 Mc, and traces of the F-2 layer are still visible. (See page 68.)

129
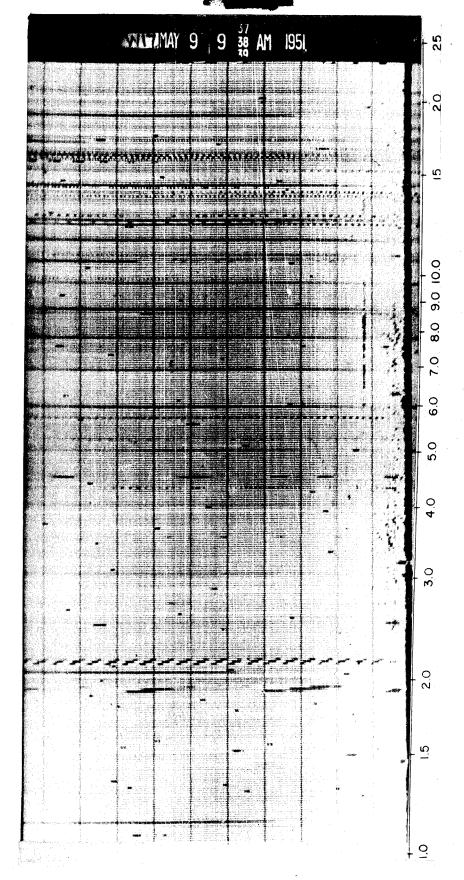
Fig. 3.39 Record Taken at G + 8 Min. Heavy absorption is shown with the E$_s$-layer more absorbed, and all traces of the F-2 layer are gone. (See page 68.)
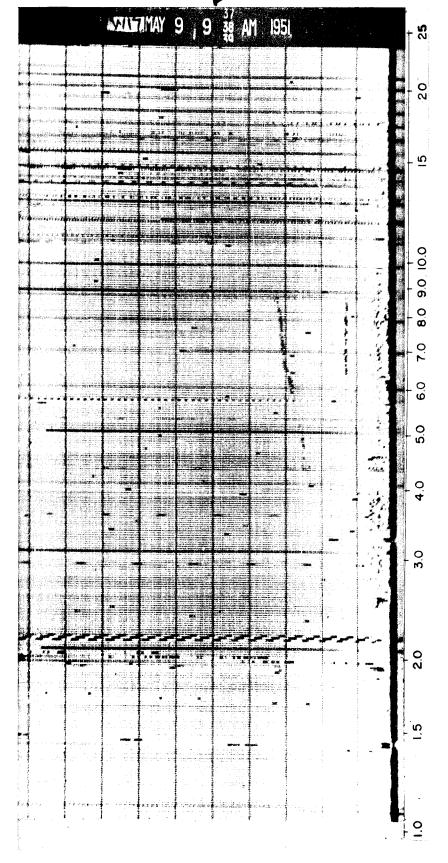
Fig. 3.40 Record Taken at G + 8.5 Min. Heavy absorption of the E_s-layer and a reappearance of the F-1 layer and the F-2 layer are shown. (See page 68.)
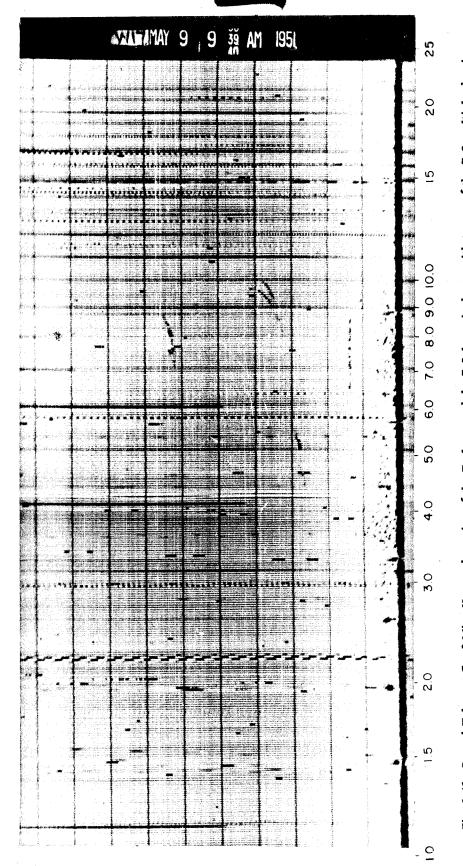
Fig. 3.41 Record Taken at G + 9 Min. Heavy absorption of the E_{Is}-layer and the F-2 layer is shown with traces of the F-2 multiple showing. (See page 68.)
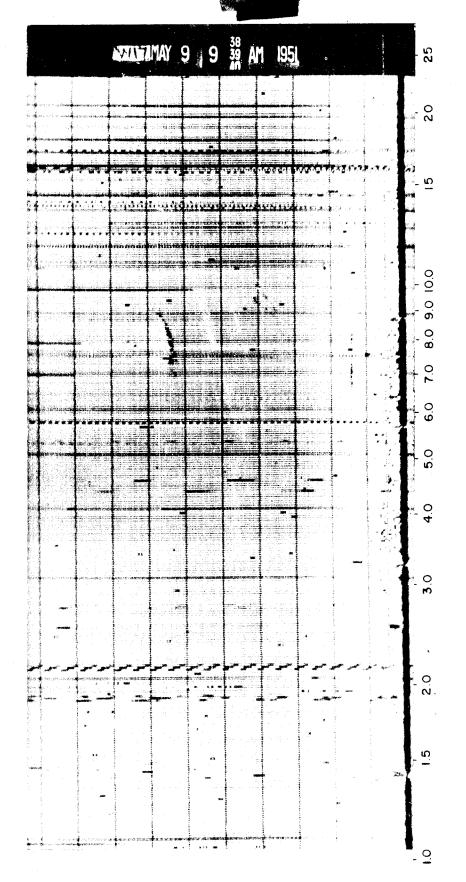
Fig. 3.42 Record Taken at G + 9.25 Min. Heavy absorption of the E$_{ls}$-layer and the F-2 layer is shown. The intensity of the multiple is greater than the fundamental trace. (See page 69.)
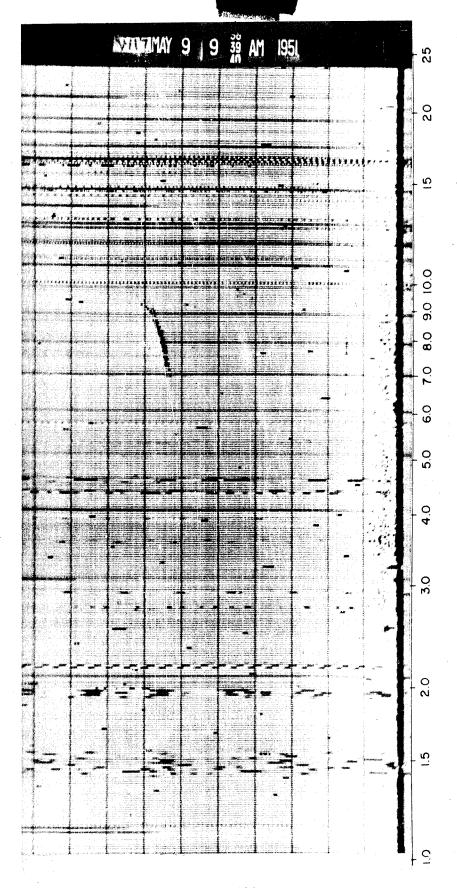
Fig. 3.43   Record Taken at G + 9.75 Min. Heavy absorption of the E_{Js}-layer and the F-2 layer is shown, with only the F-2 multiple showing.

(See page 69.)
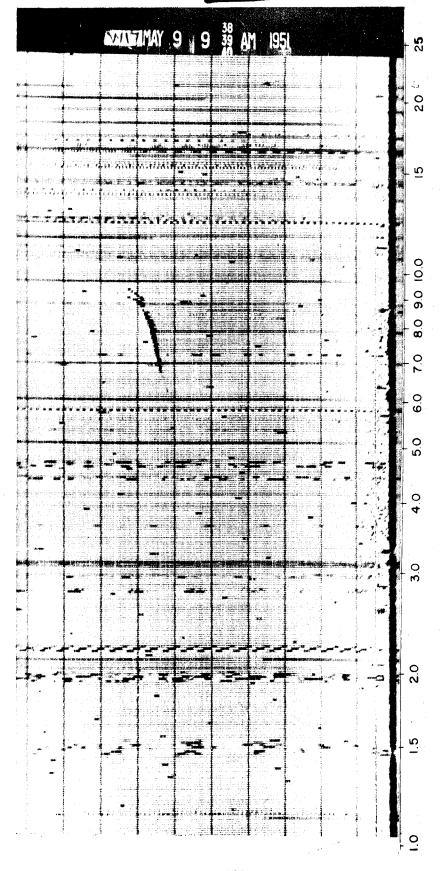
Fig. 3.44 Record Taken at G + 10 Min. The E_s-layer is completely absorbed with only the F-2 layer multiple appearing. (See page 69.)
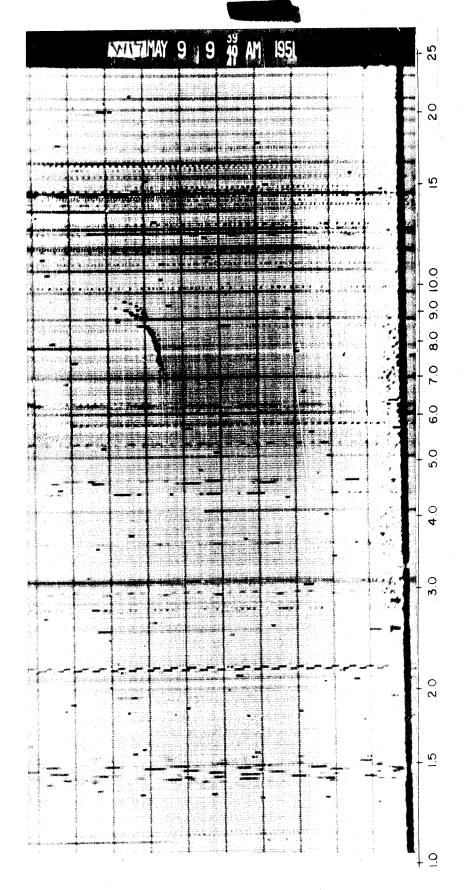
Fig. 3.45 Record Taken at G + 10.5 Min. The E_s-layer is completely absorbed, and the F-2 layer multiple is beginning to disappear. (See page 69.)
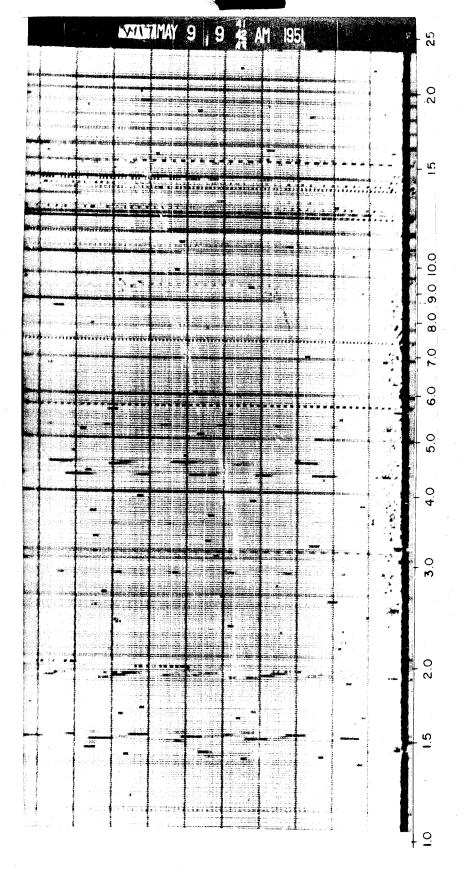
Fig. 3.46. Record Taken at G + 12 Min. Absorption is nearly complete, and only portions of the F-2 multiple trace remain. (See page 69.)

137
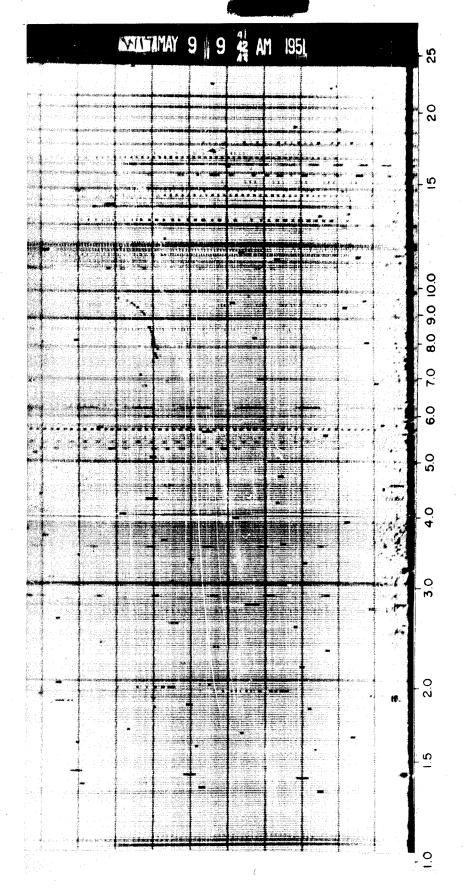
Fig. 3.47 Record Taken at G + 12.5 Min. Heavy absorption is shown, with the F-2 layer multiple absorbed and the F-2 layer beginning to reappear at normal altitude. (See page 69.)
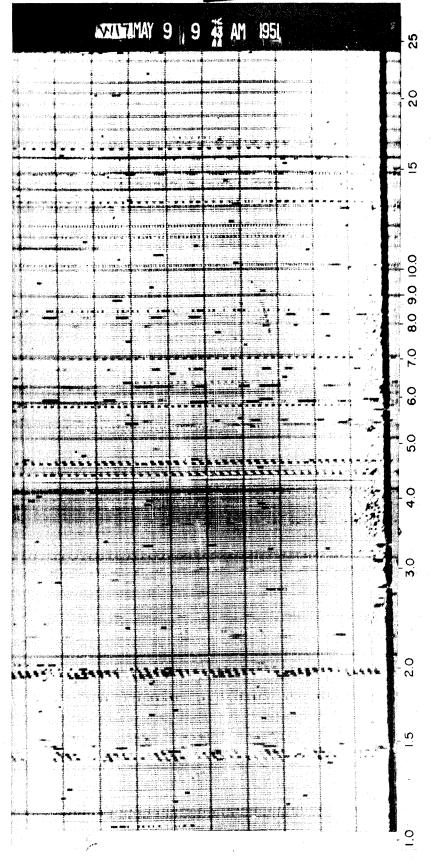
Fig. 3.48   Record Taken at G + 13 Min. Heavy absorption of the F-2 layer at normal altitude is shown. (See page 69.)

139

MAY 9   9 14 AM 1951
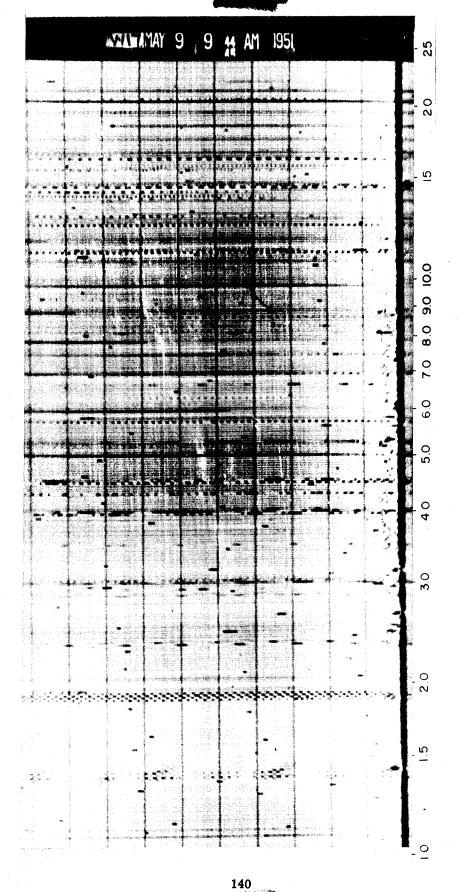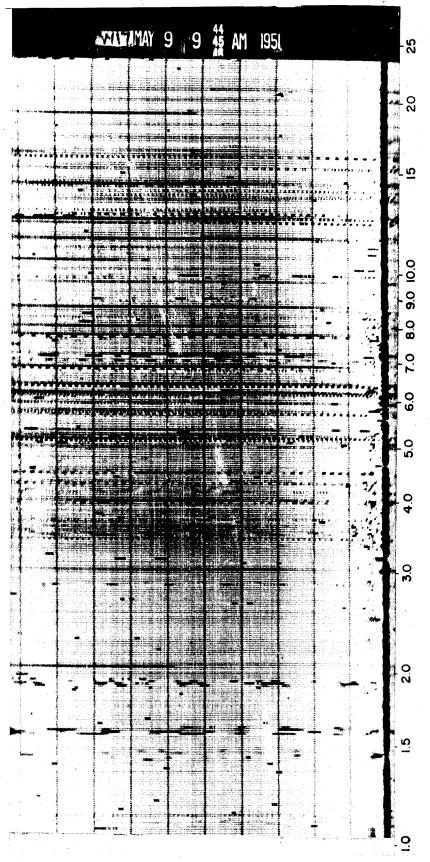
Fig. 3.49   Record Taken at G + 14 Min.   Traces of the F-2 layer are fading.   (See page 69.)

Fig. 3.50 Record Taken at G + 15 Min. There is a complete absence of all traces. (See page 69.)

141
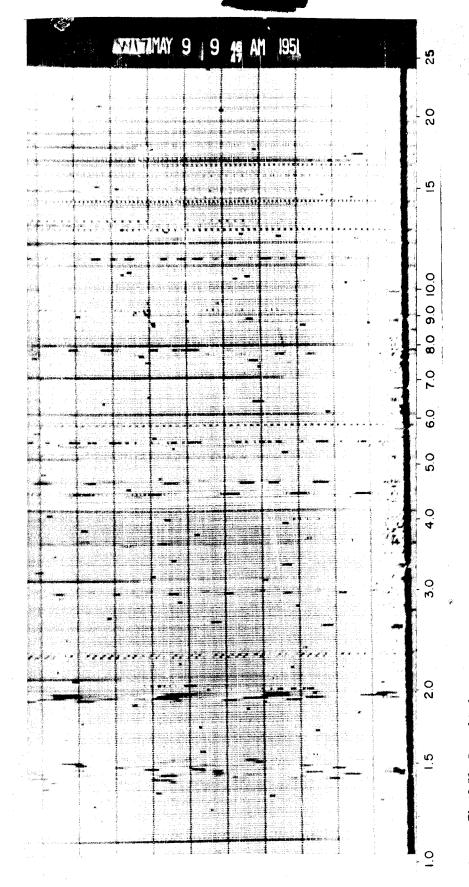
Fig. 3.51 Record Taken at G + 16 Min. Almost complete absorption is shown, with a faint trace of the F-2 layer at 8.5 Mc and the first multiple at 9 Mc. (See page 69.)

MAY 9 9 16 AM 1951
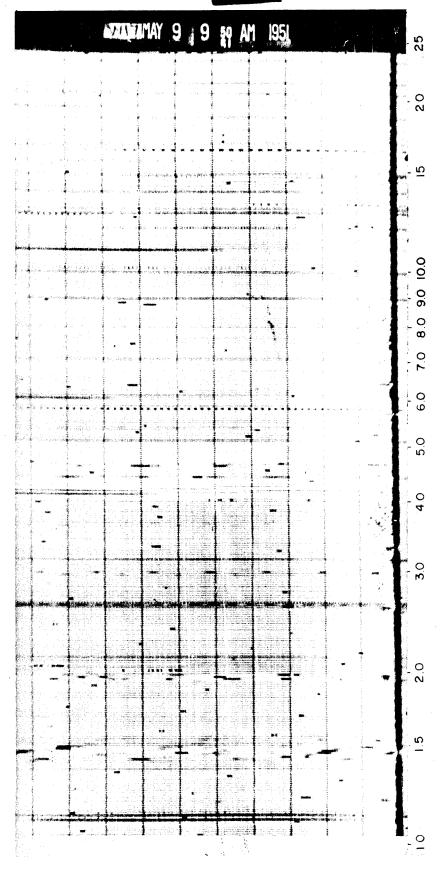
Fig. 3.52 Record Taken at G + 20 Min. There is heavy absorption, with traces of the F-2 layer appearing at normal heights. (See page 69.)
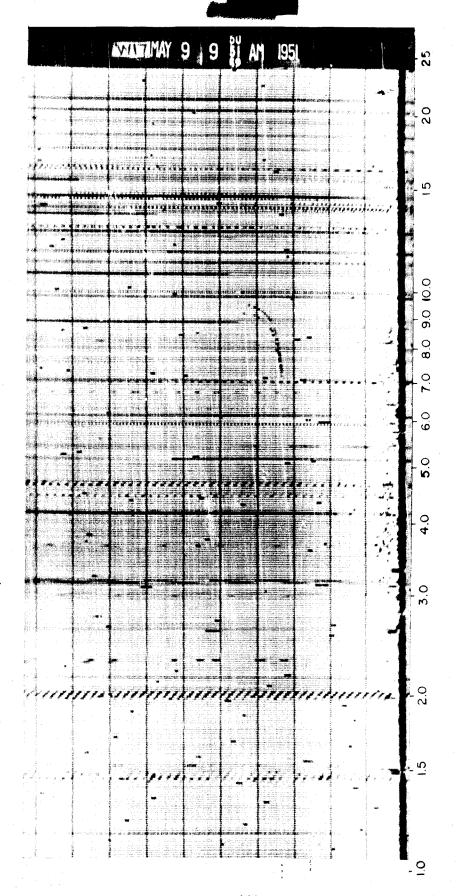
Fig. 3.53 Record Taken at G + 22 Min. The F-2 layer is more pronounced at normal heights. (See page 69.)

144
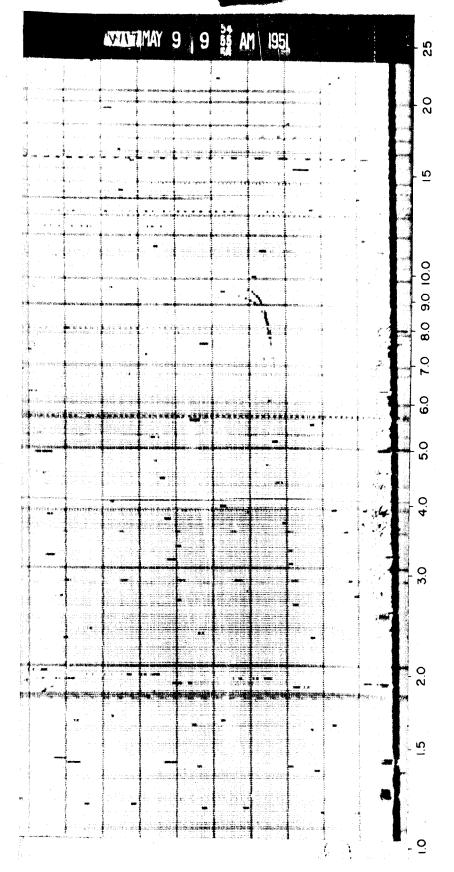
Fig. 3.54   Record Taken at G + 25 Min.   There is increased recovery of the F-2 layer.   (See page 69.)
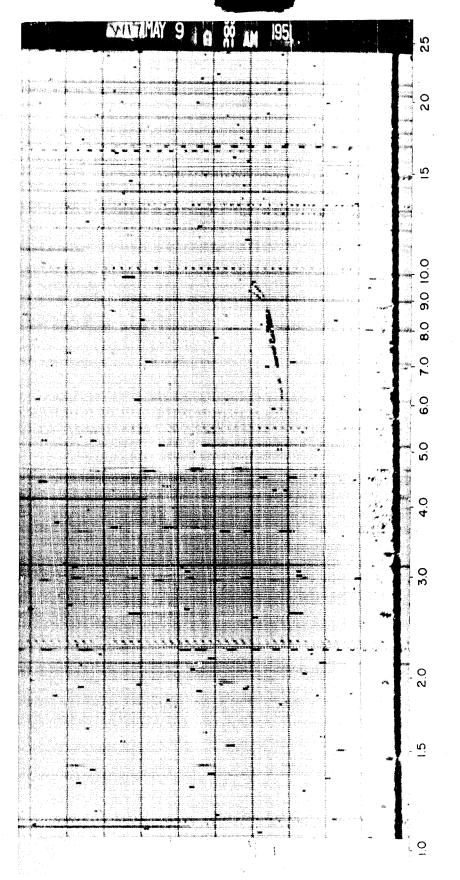
Fig. 3.55   Record Taken at G + 30 Min. Photograph shows further recovery of fade-out, with absorption at 7.2 Mc of the F-2 layer.
(See page 69.)

146
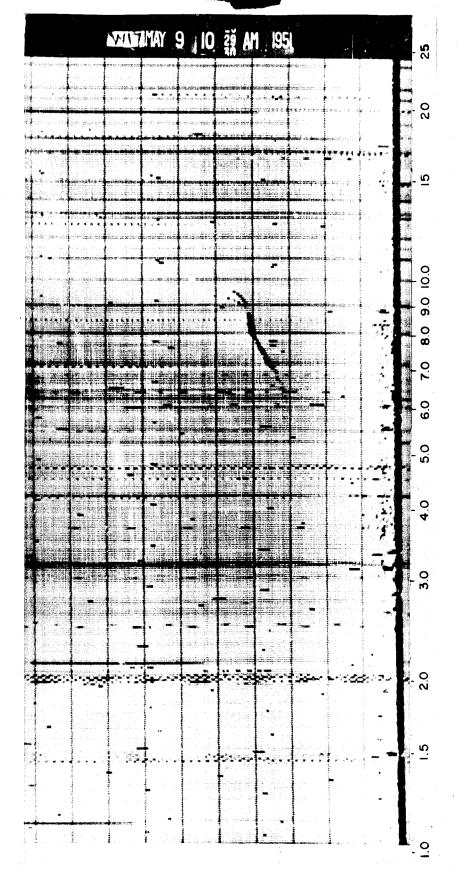
Fig. 3.56 Record Taken at G + 50 Min. There is more recovery of fade-out with absorption of the F-1 and E regions only. (See page 69.)
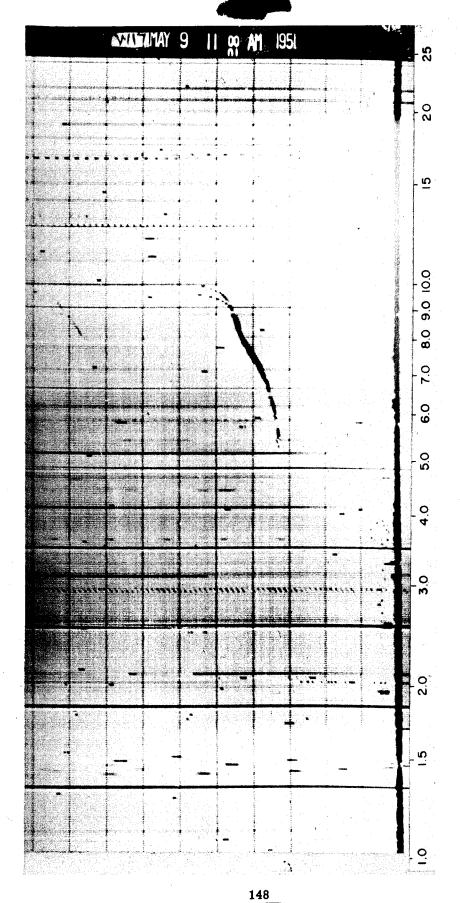
Fig. 3.57 Record Taken at G + 1.5 Hr. Absorption is down to 5.2 Mc in the F-1 region. (See page 69.)
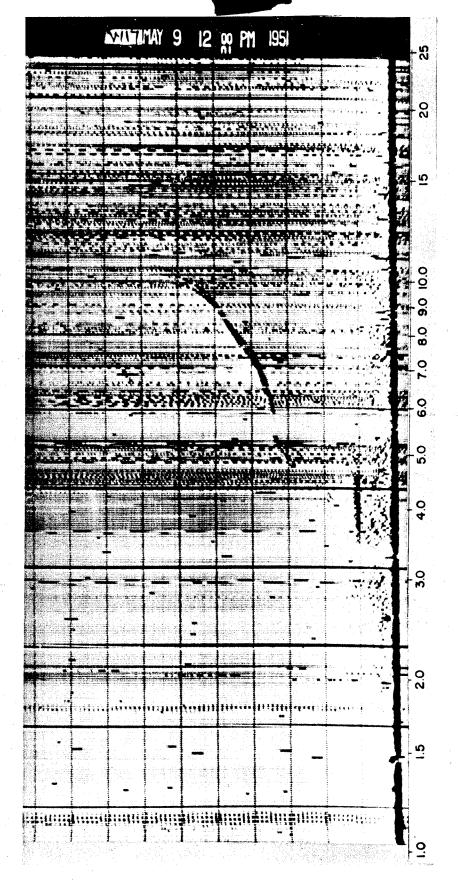
Fig. 3.58 Record Taken at G + 2.5 Hr. Recovery is nearly complete in all layers. (See page 69.)
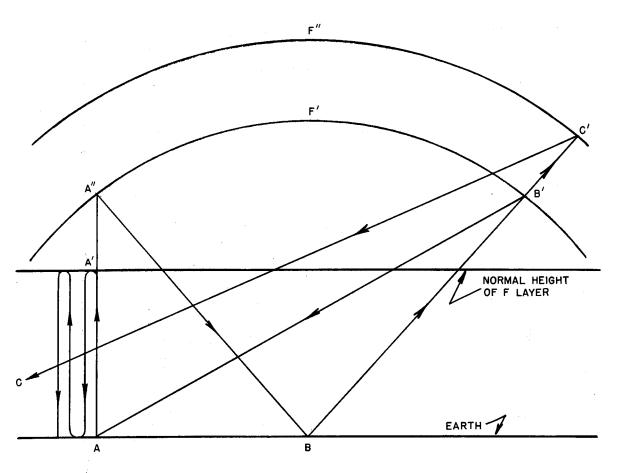
Fig. 3.59   Schematic Diagram Explaining Primary and Multiple Reflections Shown on Ionospheric Recordings
(See Page 69)
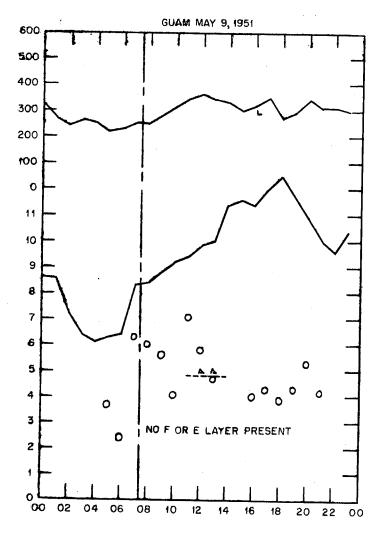
Fig. 3.60 Ionospheric Conditions at Guam, George Day
(See Page 70)
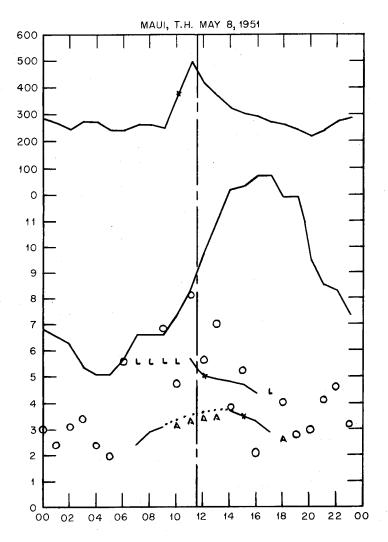
Fig. 3.61 Ionospheric Conditions at Maui, George Day
(See Page 70)
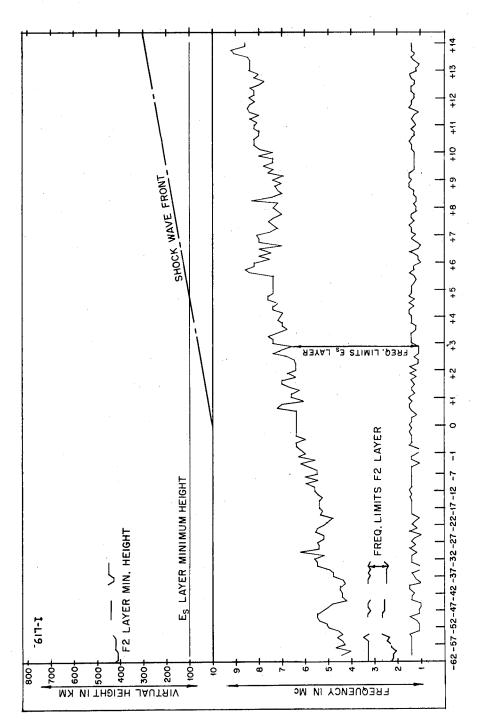
Fig. 3.62   Ionospheric Conditions, Item Shot, I−62 to I + 14 Min
(See Page 70)
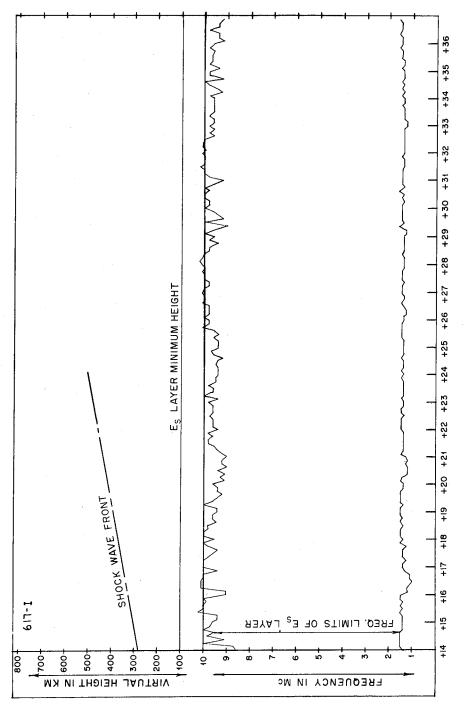
Fig. 3.63   Ionospheric Conditions, Item Shot, I + 14 to I + 37 Min
(See Page 70)
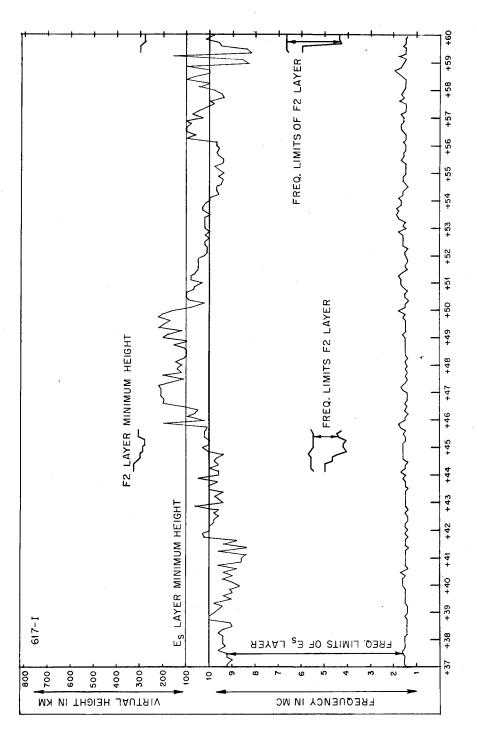
Fig. 3.64 Ionospheric Conditions, Item Shot, I + 37 to I + 60 Min
(See Page 70)
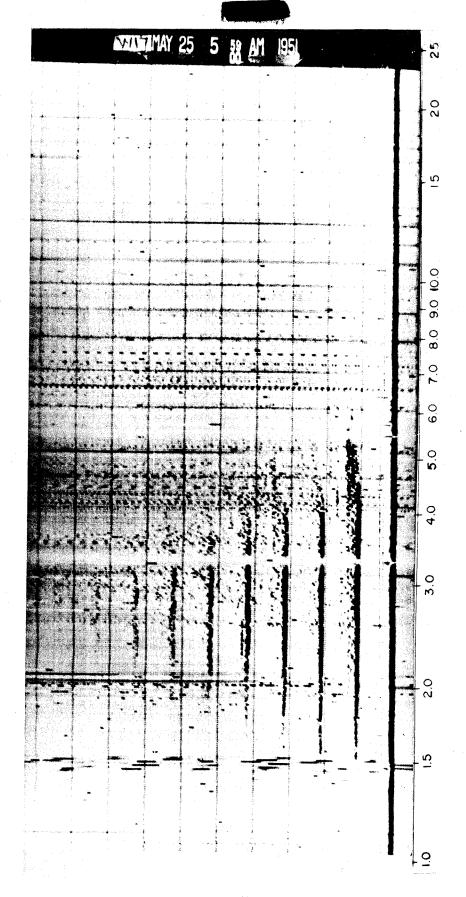
Fig. 3.65 Ionospheric Record of Conditions at 1—19 Min. The E-layer is at 1.5 to 55 Mc with seven reflections. (See page 70.)
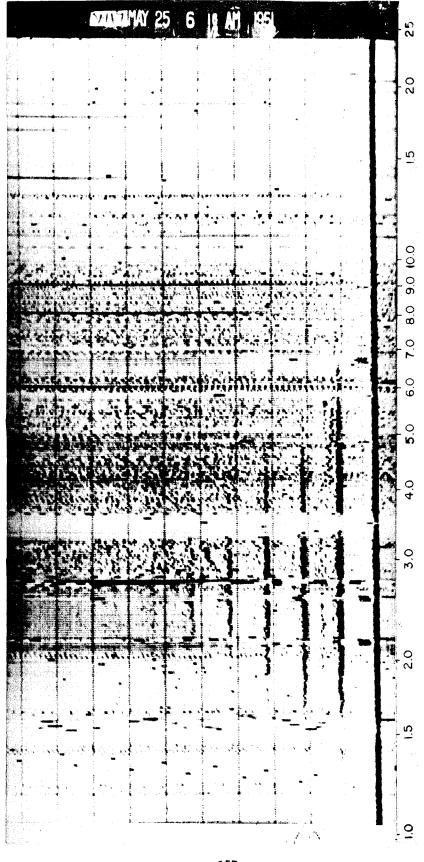
Fig. 3.66   Ionospheric Record of Conditions at 1–1 Min. The E-layer is decreasing in frequency response, and reflections have decreased to five. (See page 70.)
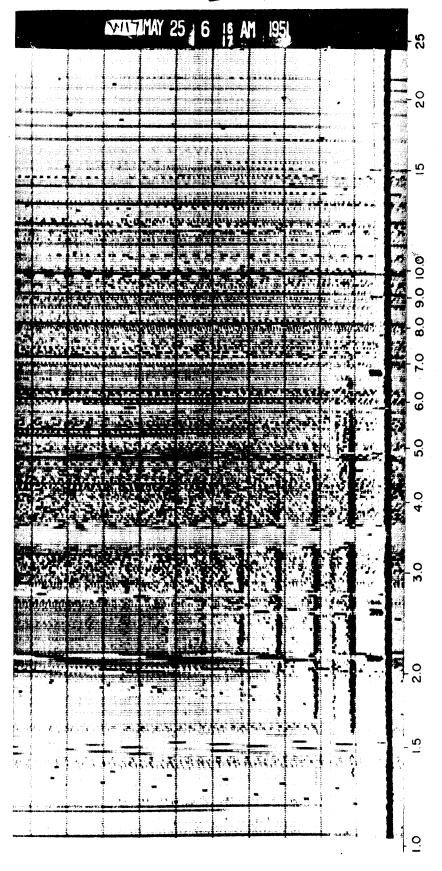
Fig. 3.67 Ionospheric Record of Conditions Immediately Prior to I—0. Little change is noted. (See page 70.)
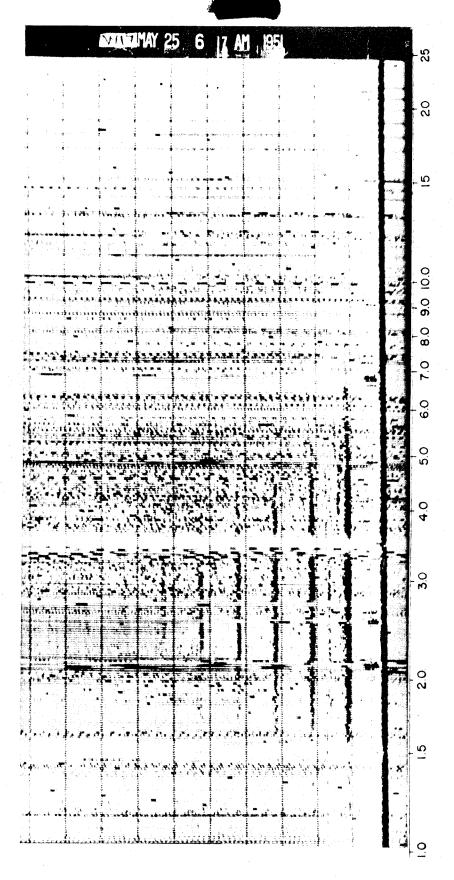
Fig. 3.68 Ionospheric Record of Conditions at I−0. There is practically no change. (See page 70.)

159
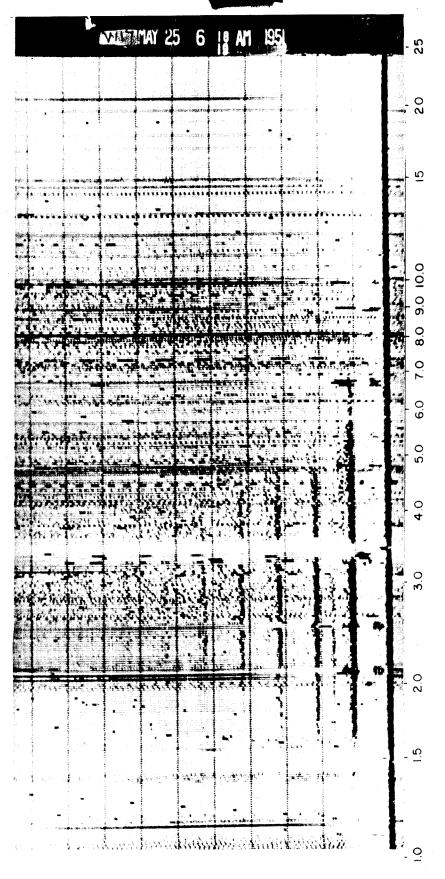
Fig. 3.69 Ionospheric Record of Conditions at I + 1 Min. Little change from conditions in Fig. 3.68. (See page 70.)

160
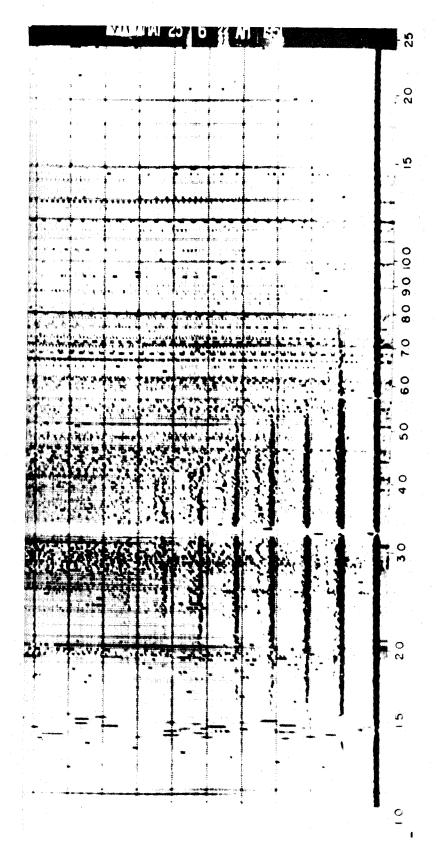
Fig. 3.70 Ionospheric Record of Conditions at I + 5 Min. Little change. (See page 70.)
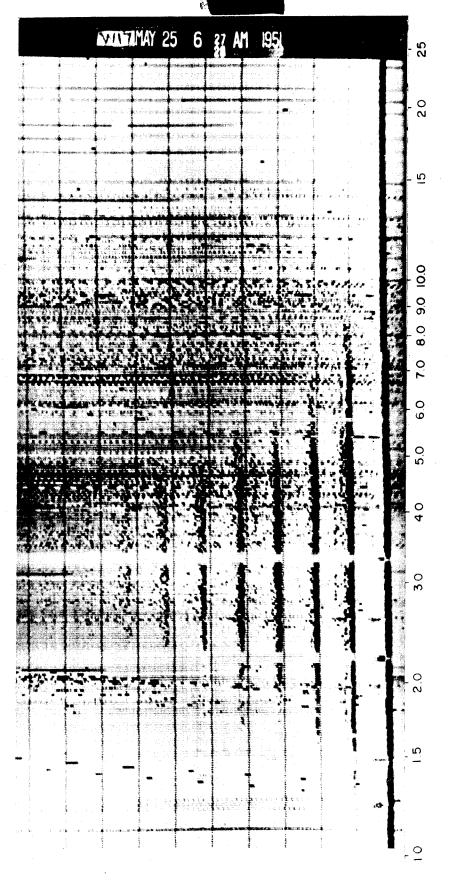
Fig. 3.71 Ionospheric Record of Conditions at I + 10 Min. Little change. (See page 70.)
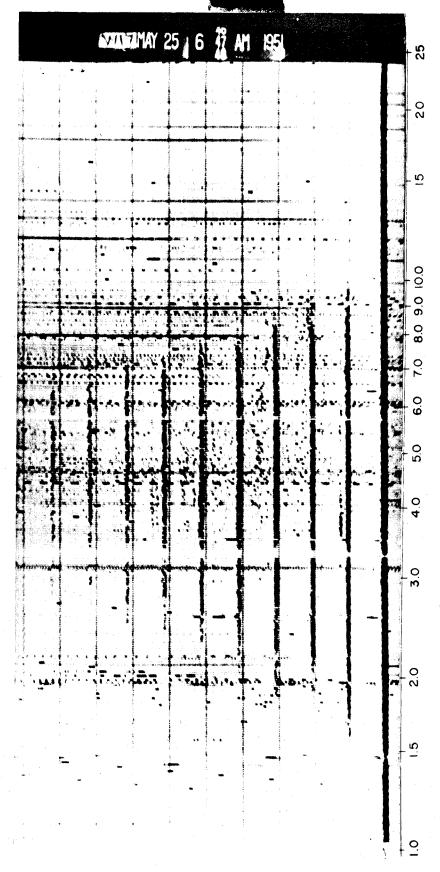
Fig. 3.72 Ionospheric Record of Conditions at I + 30 Min. The E-layer is extending to lower frequency, and reflections have increased to nine. (See page 70.)
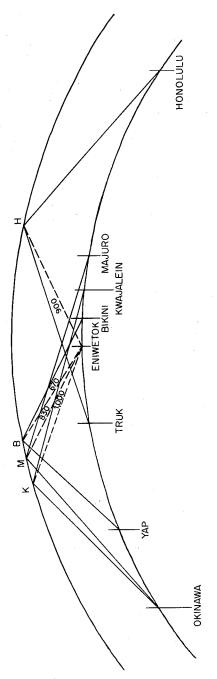
Fig. 5.1   Schematic Diagram of Paths of Transmitted Signals in Upper-air-transmission Phase
(See Page 74)
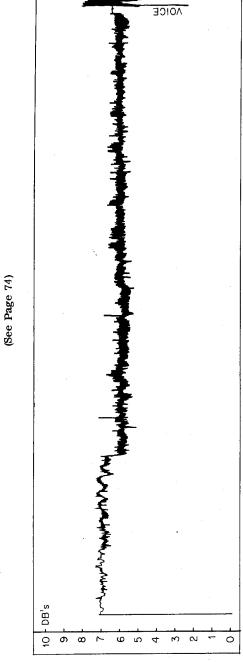
Fig. 5.2   Recording VM Record, Bikini Reception, Easy Shot
(See Page 75)
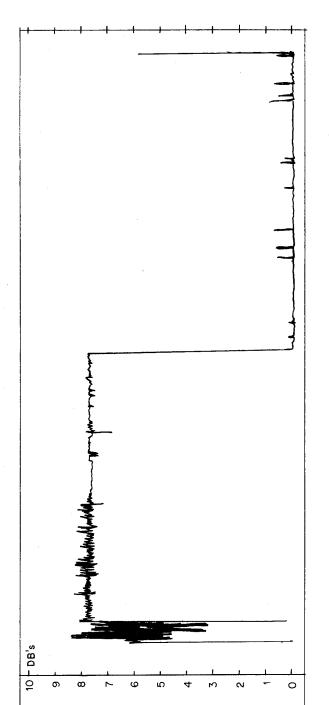
Fig. 6.1   Recording VM Record, Reception Surface Wave, 434 Kc, Dog Shot
(See Page 77)
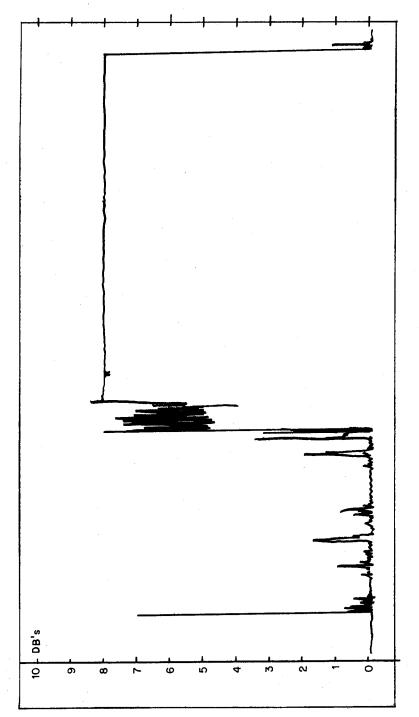
Fig. 6.2 Recording VM Record, Reception Surface Wave, 2,122 Kc, George Shot
(See Page 77)

166
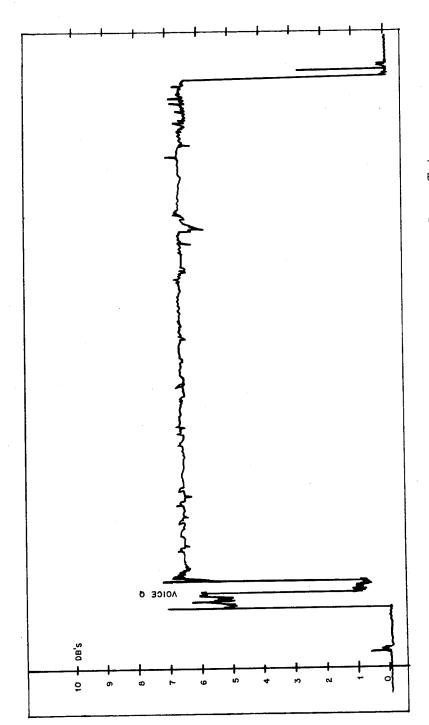
Fig. 6.3   Recording VM Record, Reception Surface Wave, 434 Kc, George Shot
(See Page 77)
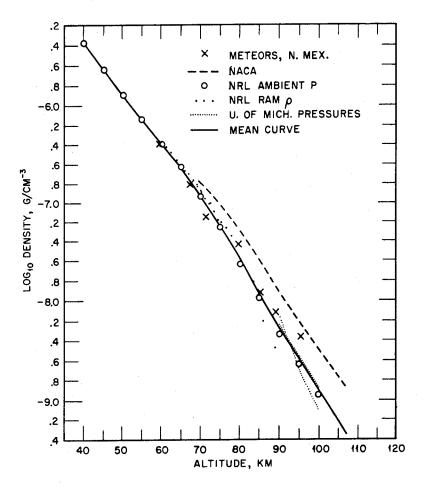
Fig. D.1 Density of the Upper Atmosphere
(See Page 86)
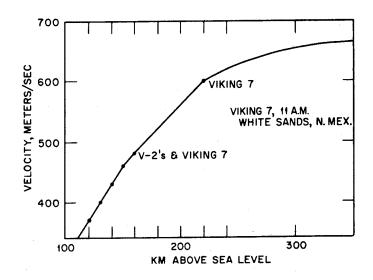
Fig. D.2 Curve of Sound Velocity in the Upper Atmosphere. Data obtained from density on Viking 7
(August 1951) and Viking 2's (March 1947 and January 1948), all day time. (See page 86.)
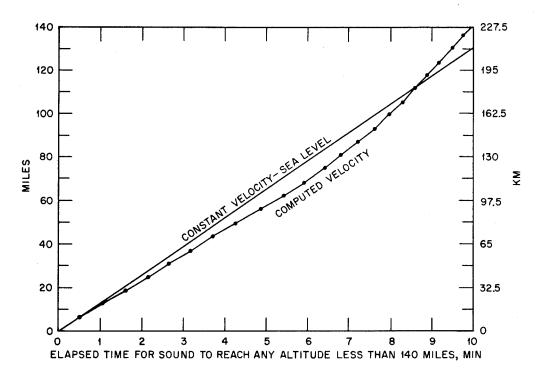
Fig. D.3   Time–Distance Curve of Vertically Projected Sound
(See Page 86)

Part III

PHOTOGRAPHIC ASSESSMENT
OF BOMB DAMAGE

by

EUGENE E. FURNISH

Chapter 1
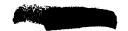
Objective of Project 8.3C

The objective of Project 8.3C was to photograph Air Force structures on Engebi Island, Eniwetok Atoll, to indicate blast damage.

Three phases of photography were to be completed on Easy Shot:

1. Pre-Easy photographs, obliques and verticals, 16 April 1951.
2. Strike photographs, verticals, 21 April 1951.
3. Post-Easy photographs, obliques and verticals, 22 April 1951.

Chapter 2

Types of Equipment Employed

2.1 PHOTOGRAPHIC EQUIPMENT

1. K-17 aerial mapping cameras with 6- and 12-in. cones
2. Super XX Aerographic film, ASA rating 100
3. Minus blue filter, used in conjunction with 6- and 12-in. cones
4. A-11 mount
5. Type A-2 vertical view finder
6. A5A film magazine
7. B-3B intervalometer

2.2 AIRCRAFT

1. B-17 to obtain oblique and vertical photographs
2. B-50D to obtain strike photographs

2.3 CAMERAS, OBLIQUE AND VERTICAL

1. Obliques, K-17 with 12-in. cone
2. Verticals, K-17 with 6- and 12-in. cones
3. Strike photographs, vertical, K-17 with 12-in. cone

2.4 SHUTTER SPEEDS AND DIAPHRAGM OPENINGS

1. Obliques, $\frac{1}{225}$ sec at f/16
2. Verticals, $\frac{1}{225}$ sec at f/11
3. Strike photographs, $\frac{1}{225}$ sec at f/11

Chapter 3

Discussion

There were two phases of the pre- and post-Easy photography, low-altitude oblique and vertical.

3.1 OBLIQUE PHOTOGRAPHY

The low-altitude oblique photographs were obtained with a hand-held K-17 camera with a 12-in. cone at an altitude of 500 ft and ¼ to ½ mile from the target, showing no horizon.

The series of low obliques was taken from the right rear door of the B-17 aircraft. A ⅜-in. rubber tube was run from the normal camera station in the radio room to the rear door to furnish vacuum for the camera. The electrical power was obtained from a 24-v heated-suit outlet. Prior to the mission the rear door was removed.

There were 11 targets to be photographed, and four different headings were required on each individual target (see Fig. 1).

3.2 VERTICAL PHOTOGRAPHY

The vertical photographs were obtained by using a K-17 camera with 6- and 12-in. cones.

There were five flight lines to be accomplished from a vertical angle. These photographic flight lines were to be made from altitudes of 6,000 and 12,000 ft.

For photography at the 6,000-ft altitude a K-17 camera with a 12-in. cone was used, obtaining a scale of 1:6,000. There were two flight lines accomplished at the 6,000-ft altitude.

For photography at the 12,000-ft altitude, two cameras were employed, a K-17 with a 6-in.

cone, obtaining a scale of 1:24,000, and a K-17 camera with a 12-in. cone, obtaining a scale of 1:12,000. Three flight lines were accomplished from this altitude.

A navigator directed the pilot over the pre-designated flight lines and instructed the photographer when to energize the camera.

All vertical flight lines were made with an overlap of 60 per cent. A 60 per cent overlap was used to obtain a stereo effect from the end-result photographs.

3.3 STRIKE PHOTOGRAPHY

Strike photography was performed to determine the feasibility of photographing bomb damage by the actual illumination of the fireball.

Strike photographs were taken from a B-50D aircraft. A K-17 camera with a 12-in. cone was placed in the rear unpressurized portion of the aircraft to photograph the strike operation.

A special mount was fabricated to hold the camera. The mount was placed in the aircraft to shoot back at an angle of 22° from vertical. This special mount was bolted to the floor braces used in the regular camera mount. All vacuum and electrical outlets are standard at this station in the aircraft.

An intervalometer was placed in the bombardier's position and preset in 4-sec intervals so as to automatically energize the camera. The electrical system is so arranged that the intervalometer is automatically energized when the master power and camera door switches are tripped to the on position. These switches are on the right top side of the bombardier's

panel. The photographer threw these two switches to the on position at -15 sec and to the off position at $+60$ sec.

The strike photographs were taken from an altitude of 25,000 ft, and an approximate scale of 1:25,000 was acquired.

No filter was used in the strike photography, and a shutter speed of $\frac{1}{225}$ sec at f/11 was used.

The camera magazine was heated to assist in the camera and magazine operation.

A total of three photographs were taken during this operation.

Chapter 4

Recommendations

It is recommended in all future tests in which oblique photographs are taken that an altitude of no less than 1,000 ft be used when employing a K-17 camera with a 12-in. cone, and in the event a 24-in. cone is to be used the altitude should not be less than 2,000 ft.

When the target is moving at an angle of 90° to the aircraft and at high speed, the highest possible shutter speed is not sufficient to stop motion. The solution to this problem would be to go to a higher altitude, acquire a smaller image, and then enlarge the image to the size of the specified requirements.

It is recommended that all still aerial film be processed as soon as possible after the mission. This would aid in obtaining new photographs in the event that there was malfunction of equipment.

It is also recommended that camera tests be made by flying a mission prior to the actual test. In this manner the pilot, navigator, and photographer would become acquainted with the target area.

A K-24 camera should be employed to obtain strike photographs. Since this camera cycles at three photographs per second while the K-17 camera cycles one photograph in 3 sec, it is possible to obtain nine photographs with the K-24 camera in place of one with the K-17 camera. The use of the K-24 camera would ensure exposures being made throughout the maximum peak of the fireball.

Chapter 5

Photographs

5.1 OBLIQUE PHOTOGRAPHS, 500-FT ALTITUDE

Target area 1:
Refer to Figs. 2, 2A, 3, 3A, 4, 5, 6, 7, 8, 9, and 10

Target area 2:
Refer to Figs. 11, 11A, 12, 12A, 13, 13A, 14, 14A, 15, 16, 17, 18, 19, and 20

Target area 3:
Refer to Figs. 21, 21A, 22, 22A, 23, 23A, 24, 25, 26, 27, 28, 29, and 30

Target area 4:
Refer to Figs. 31, 31A, 32, 32A, 33, 33A, 34, 34A, 35, and 35A

Target area 5:
Refer to Figs. 36, 36A, 37, 37A, 38, 38A, 39, 39A, 40, and 41

Target area 6:
Refer to Figs. 42, 42A, 43, 43A, 44, 44A, 45, and 45A

Target area 7:
Refer to Figs. 46, 46A, 47, 48, 49, 50, 51, 52, 53, 54, 55, and 56

Target area 8:
Refer to Figs. 57, 57A, 58, 58A, 59, 59A, 60, and 60A

Target area 9:
Refer to Figs. 61, 61A, 62, 62A, 63, 63A, 64, and 64A

Target area 10:
Refer to Figs. 65, 65A, 66, 66A, 67, 67A, 68, 68A, and 69

Target area 11:
Refer to Figs. 70, 70A, 71, 71A, 72, 72A, 73, 73A, and 74

5.2 STRIKE PHOTOGRAPHS

Refer to Figs. 75, 76, and 77

5.3 VERTICAL PHOTOGRAPHS

Flight line 1; 12-in. cone, 6,000 ft, scale 1:6,000
Refer to Figs. 78, 79, 80, 81, 82, and 83
Flight line 3; 12-in. cone, 6,000 ft, scale 1:6,000
Refer to Figs. 84, 84A, 85, 85A, 86, 86A, 87, 87A, 88, 89, 90, 91, and 92
Flight line 1; 12-in. cone, 12,000 ft, scale 1:12,000
Refer to Figs. 93, 94, and 95
Flight line 2; 6-in. cone, 12,000 ft, scale 1:24,000
Refer to Figs. 96, 96A, 97, 97A, 98, 98A, 99, 99A, 100, 101, 102, and 103
Flight line 3; 12-in. cone, 12,000 ft, scale 1:12,000
Refer to Figs. 104, 104A, 105, 105A, 106, and 106A

5.4 OBLIQUE PHOTOGRAPHS, 500-FT ALTITUDE

Fig. 107   Looking east
Fig. 108   Looking north
Fig. 109   Looking east
Fig. 110   Looking west
Fig. 111   Tower
Fig. 112   Looking toward crater area

Fig. 1 Flight Lines for Photography
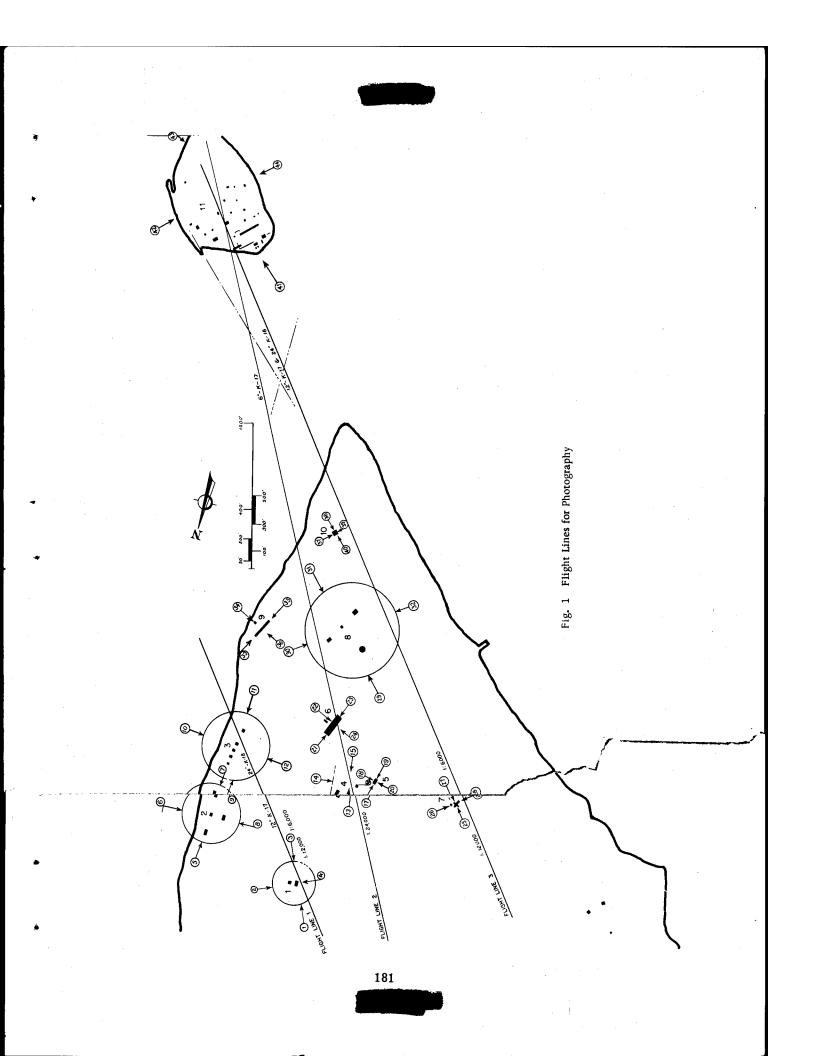
Fig. 2 16 April 51, Oblique, Spot Shot, 12-in. Cone, 500-ft Altitude, Engebi, Target Area 1

Fig. 2A   22 April 51, Oblique, Spot Shot, 12-in. Cone, 500-ft Altitude, Engebi, Target Area 1
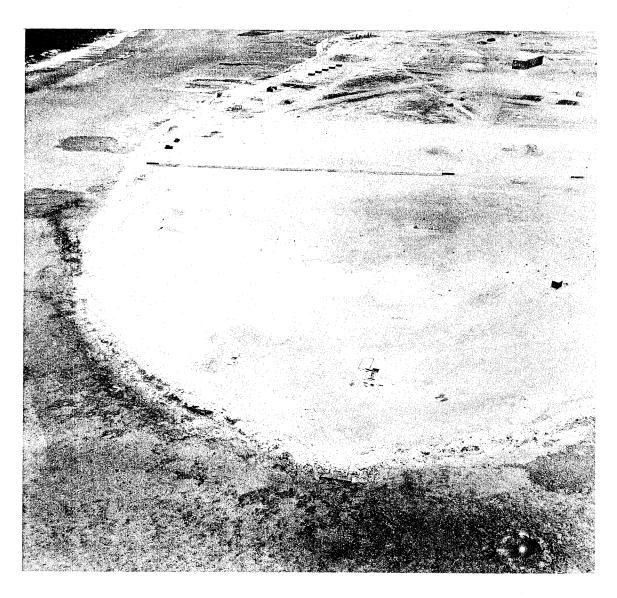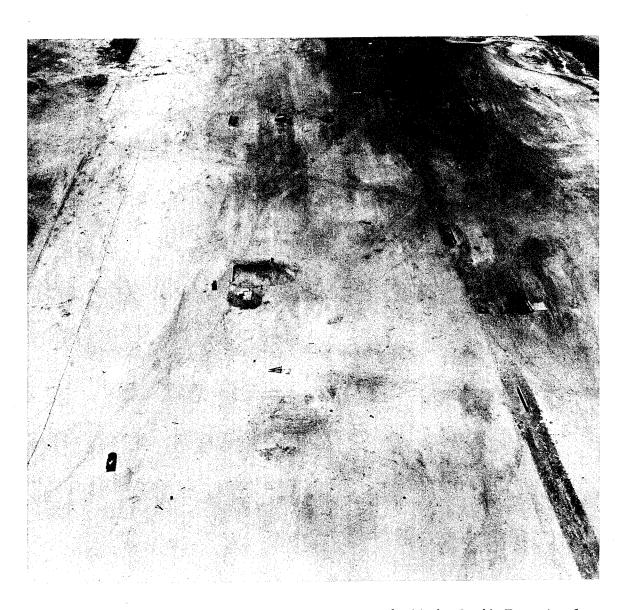
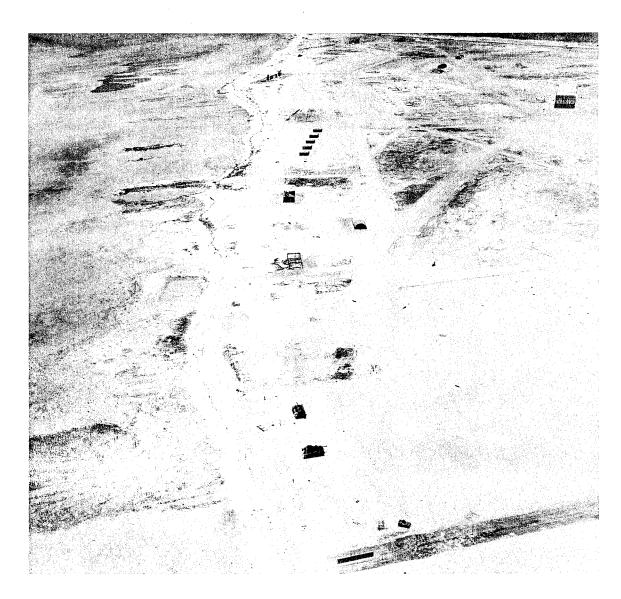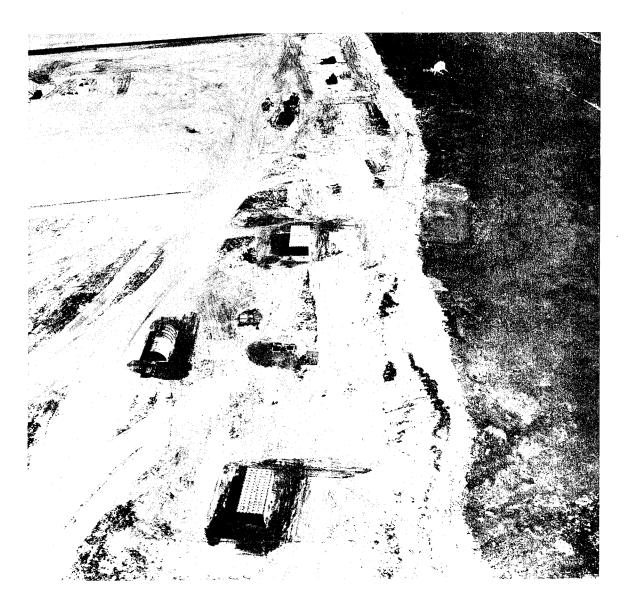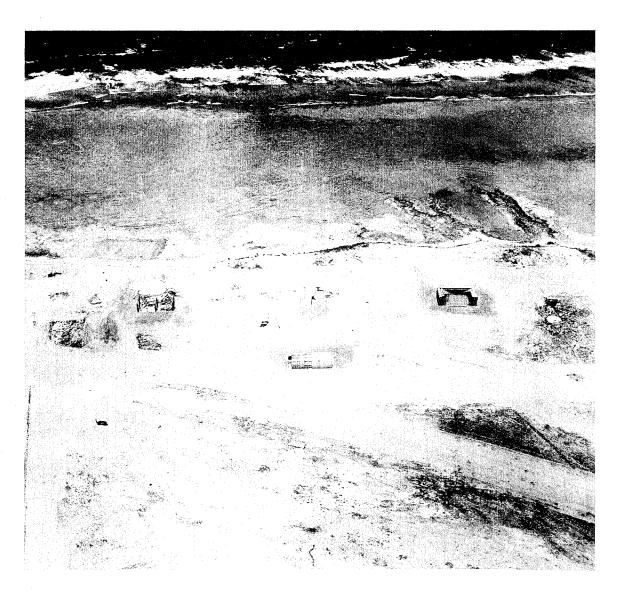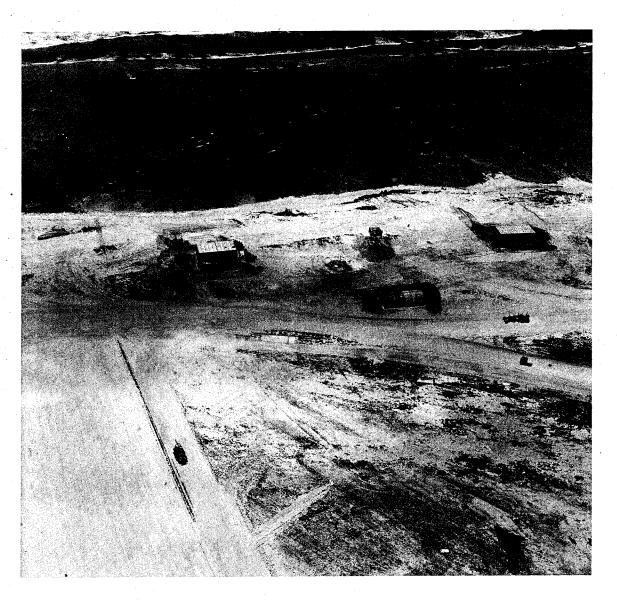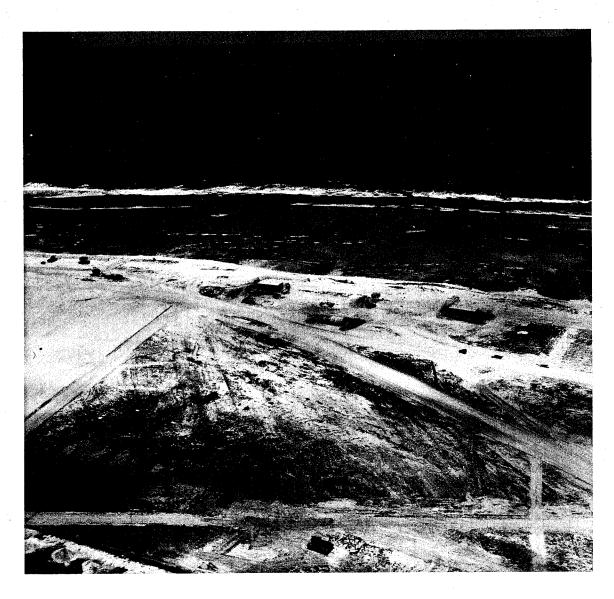Fig. 3   16 April 51, Oblique, Spot Shot, 12-in. Cone, 500-ft Altitude, Engebi, Target Area 1

Fig. 3A   22 April 51, Oblique, Spot Shot, 12-in. Cone, 500-ft Altitude, Engebi, Target Area 1

Fig. 4   22 April 51, Oblique, Spot Shot, 12-in. Cone, 500-ft Altitude, Engebi, Target Area 1
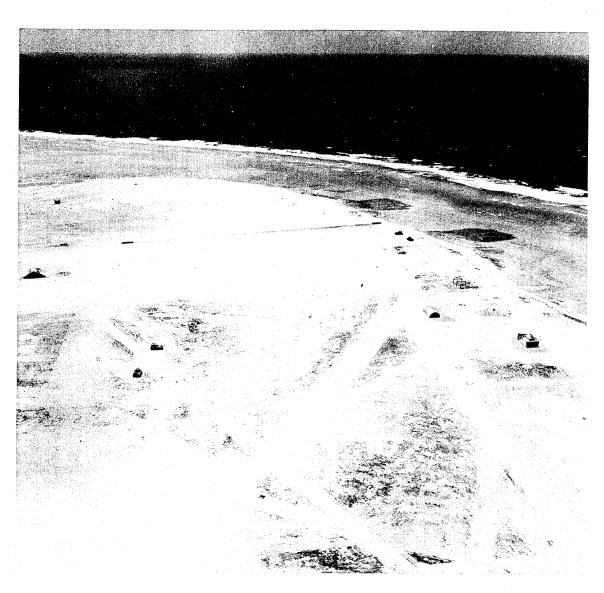
Fig. 5   22 April 51, Oblique, Spot Shot, 12-in. Cone, 500-ft Altitude, Engebi, Target Area 1
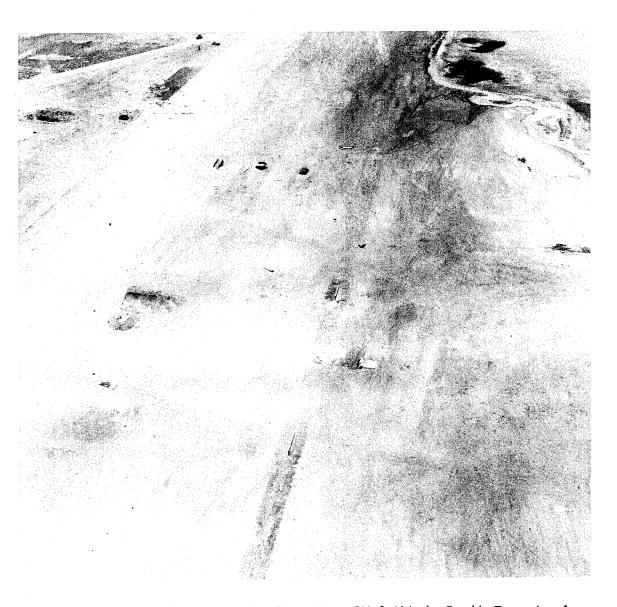
Fig. 6   22 April 51, Oblique, Spot Shot, 12-in. Cone, 500-ft Altitude, Engebi, Target Area 1
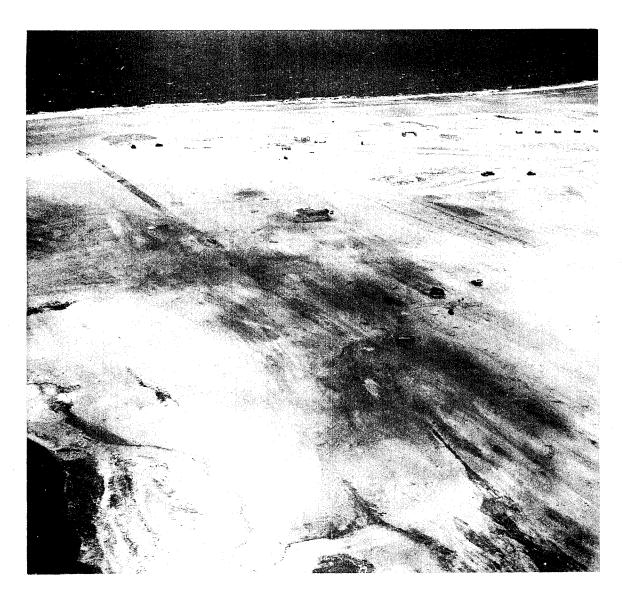
Fig. 7   22 April 51, Oblique, Spot Shot, 12-in. Cone, 500-ft Altitude, Engebi, Target Area 1
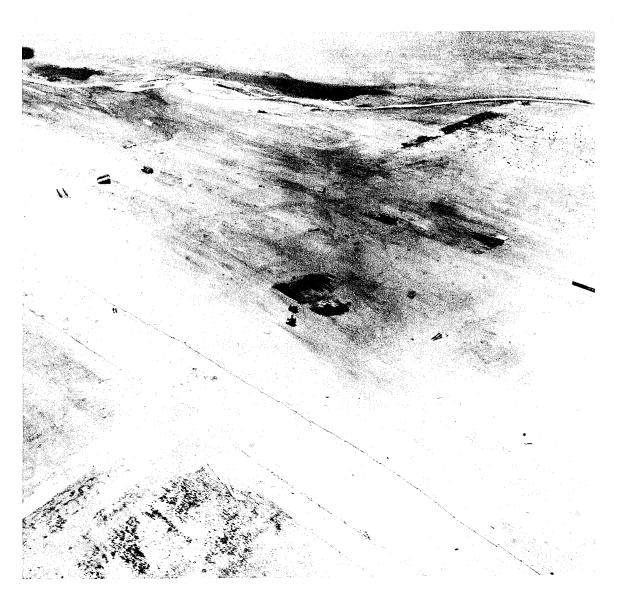
Fig. 8   22 April 51, Oblique, Spot Shot, 12-in. Cone, 500-ft Altitude, Engebi, Target Area 1

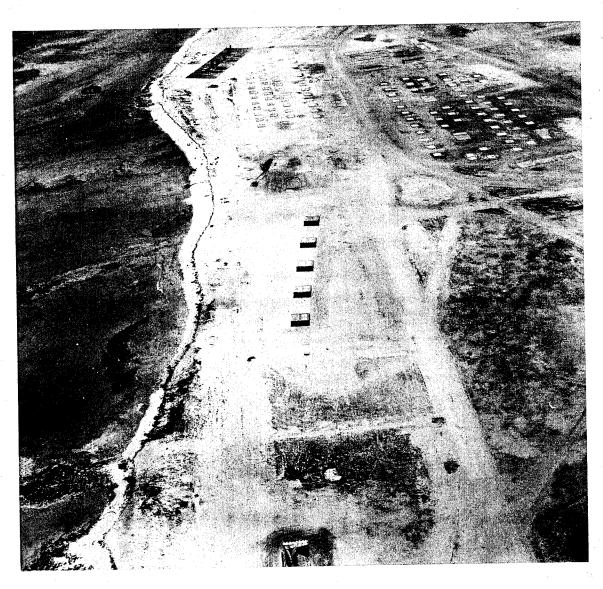Fig. 9   22 April 51, Oblique, Spot Shot, 12-in. Cone, 500-ft Altitude, Engebi, Target Area 1

Fig. 10   22 April 51, Oblique, Spot Shot, 12-in. Cone, 500-ft Altitude, Engebi, Target Area 1

Fig. 11   16 April 51, Oblique, Spot Shot, 12-in. Cone, 500-ft Altitude, Engebi, Target Area 2

Fig. 11A 22 April 51, Oblique, Spot Shot, 12-in. Cone, 500-ft Altitude, Engebi, Target Area 2

Fig. 12   16 April 51, Oblique, Spot Shot, 12-in. Cone, 500-ft Altitude, Engebi, Target Area 2
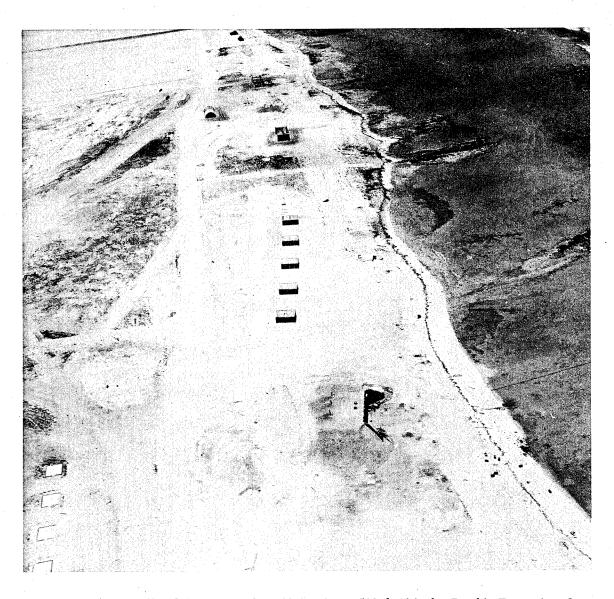
Fig. 12A   22 April 51, Oblique, Spot Shot, 12-in. Cone, 500-ft Altitude, Engebi, Target Area 2

Fig. 13   16 April 51, Oblique, Spot Shot, 12-in. Cone, 500-ft Altitude, Engebi, Target Area 2

Fig. 13A   22 April 51, Oblique, Spot Shot, 12-in. Cone, 500-ft Altitude, Engebi, Target Area 2

Fig. 14   16 April 51, Oblique, Spot Shot, 12-in. Cone, 500-ft Altitude, Engebi, Target Area 2

Fig. 14A 22 April 51, Oblique, Spot Shot, 12-in. Cone, 500-ft Altitude, Engebi, Target Area 2

Fig. 15 16 April 51, Oblique, Spot Shot, 12-in. Cone, 500-ft Altitude, Engebi, Target Area 2
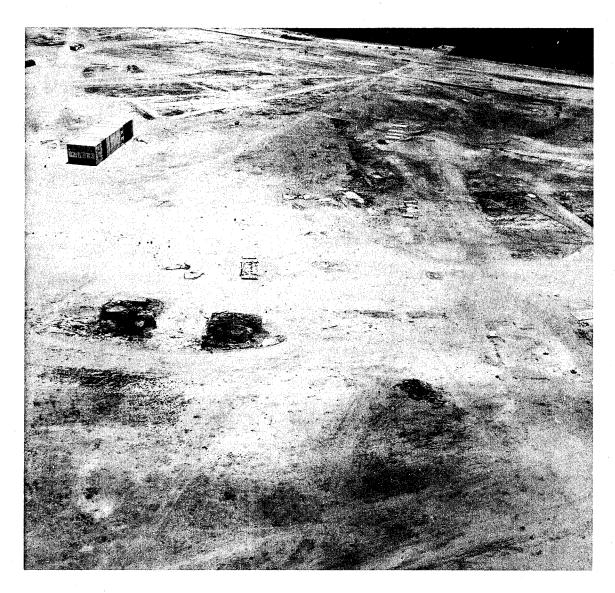
Fig. 16   16 April 51, Oblique, Spot Shot, 12-in. Cone, 500-ft Altitude, Engebi, Target Area 2

Fig. 17   16 April 51, Oblique, Spot Shot, 12-in. Cone, 500-ft Altitude, Engebi, Target Area 2

Fig. 18   16 April 51, Oblique, Spot Shot, 12-in. Cone, 500-ft Altitude, Engebi, Target Area 2

Fig. 19 16 April 51, Oblique, Spot Shot, 12-in. Cone, 500-ft Altitude, Engebi, Target Area 2

Fig. 20   16 April 51, Oblique, Spot Shot, 12-in. Cone, 500-ft Altitude, Engebi, Target Area 2

Fig. 21   16 April 51, Oblique, Spot Shot, 12-in. Cone, 500-ft Altitude, Engebi, Target Area 3

Fig. 21A   22 April 51, Oblique, Spot Shot, 12-in. Cone, 500-ft Altitude, Engebi, Target Area 3
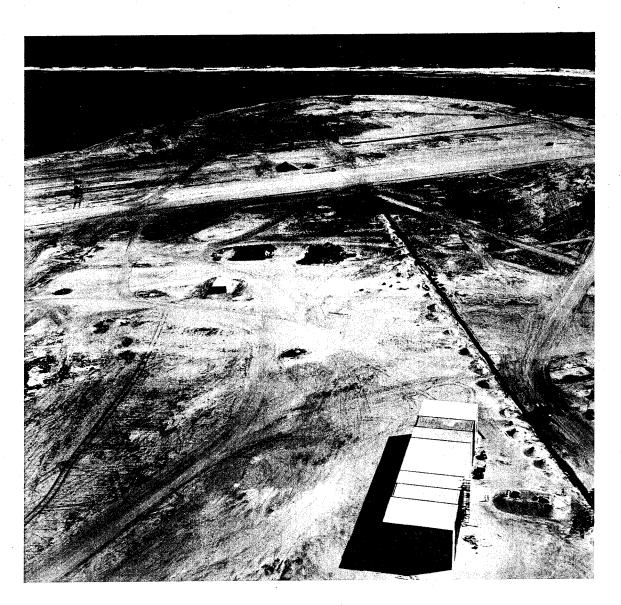
Fig. 22   16 April 51, Oblique, Spot Shot, 12-in. Cone, 500-ft Altitude, Engebi, Target Area 3

Fig. 22A   22 April 51, Oblique, Spot Shot, 12-in. Cone, 500-ft Altitude, Engebi, Target Area 3

211

Fig. 23   16 April 51, Oblique, Spot Shot, 12-in. Cone, 500-ft Altitude, Engebi, Target Area 3

Fig. 23A   22 April 51, Oblique, Spot Shot, 12-in. Cone, 500-ft Altitude, Engebi, Target Area 3

Fig. 24 16 April 51, Oblique, Spot Shot, 12-in. Cone, 500-ft Altitude, Engebi, Target Area 3

Fig. 25 16 April 51, Oblique, Spot Shot, 12-in. Cone, 500-ft Altitude, Engebi, Target Area 3

Fig. 26   16 April 51, Oblique, Spot Shot, 12-in. Cone, 500-ft Altitude, Engebi, Target Area 3

Fig. 27   16 April 51, Oblique, Spot Shot, 12-in. Cone, 500-ft Altitude, Engebi, Target Area 3

Fig. 28 16 April 51, Oblique, Spot Shot, 12-in. Cone, 500-ft Altitude, Engebi, Target Area 3

Fig. 29   16 April 51, Oblique, Spot Shot, 12-in. Cone, 500-ft Altitude, Engebi, Target Area 3

Fig. 30 16 April 51, Oblique, Spot Shot, 12-in. Cone, 500-ft Altitude, Engebi, Target Area 3

Fig. 31 16 April 51, Oblique, Spot Shot, 12-in. Cone, 500-ft Altitude, Engebi, Target Area 4

Fig. 31A   22 April 51, Oblique, Spot Shot, 12-in. Cone, 500-ft Altitude, Engebi, Target Area 4
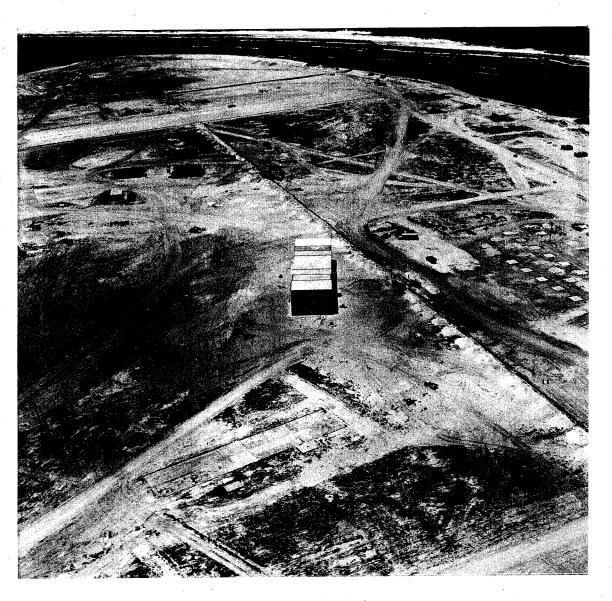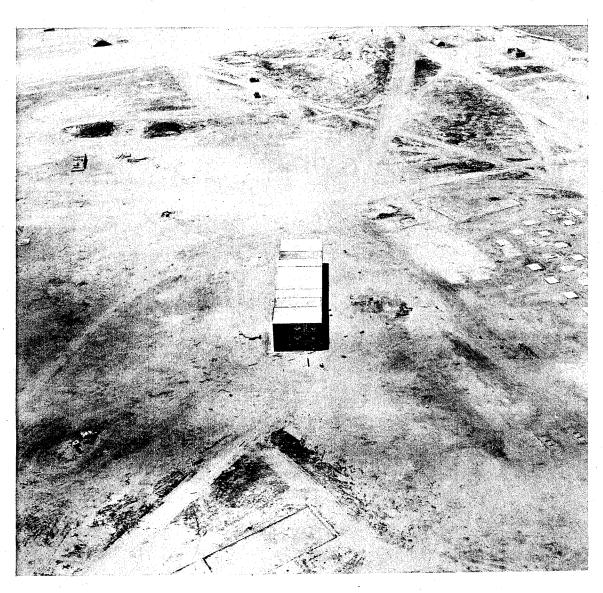
Fig. 32   16 April 51,   Oblique,   Spot Shot,   12-in. Cone,   500-ft Altitude,   Engebi,   Target Area 4

Fig. 32A 22 April 51, Oblique, Spot Shot, 12-in. Cone, 500-ft Altitude, Engebi, Target Area 4

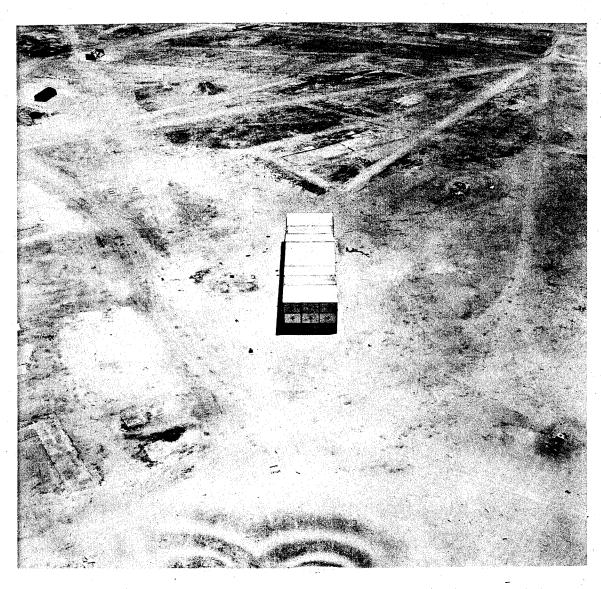Fig. 33   16 April 51, Oblique, Spot Shot, 12-in. Cone, 500-ft Altitude, Engebi, Target Area 4

Fig. 33A   22 April 51, Oblique, Spot Shot, 12-in. Cone, 500-ft Altitude, Engebi, Target Area 4

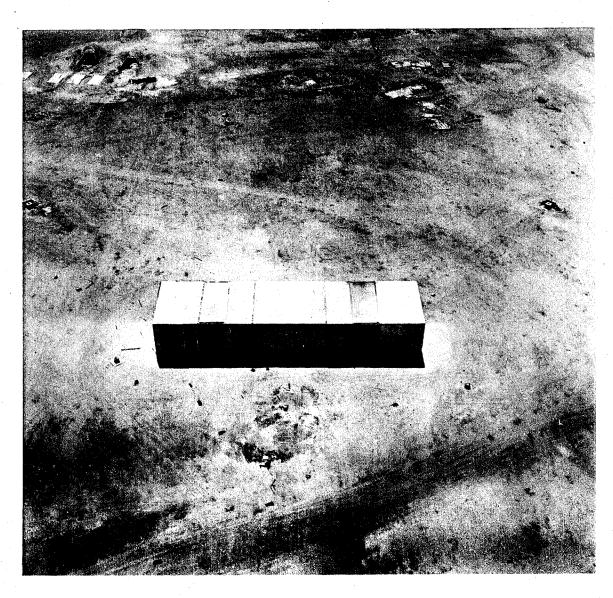Fig. 34   16 April 51, Oblique, Spot Shot, 12-in. Cone, 500-ft Altitude, Engebi, Target Area 4

Fig. 34A   22 April 51, Oblique, Spot Shot, 12-in. Cone, 500-ft Altitude, Engebi, Target Area 4

Fig. 35   16 April 51, Oblique, Spot Shot, 12-in. Cone, 500-ft Altitude, Engebi, Target Area 4
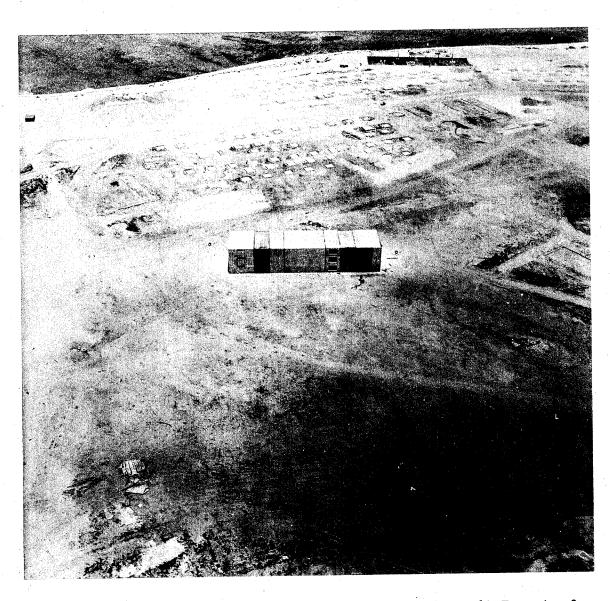
Fig. 35A   22 April 51, Oblique, Spot Shot, 12-in. Cone, 500-ft Altitude, Engebi, Target Area 4

Fig. 36   16 April 51, Oblique, Spot Shot, 12-in. Cone, 500-ft Altitude, Engebi, Target Area 5

Fig. 36A   22 April 51, Oblique, Spot Shot, 12-in. Cone, 500-ft Altitude, Engebi, Target Area 5

Fig. 37   16 April 51, Oblique, Spot Shot, 12-in. Cone, 500-ft Altitude, Engebi, Target Area 5

Fig. 37A 22 April 51, Oblique, Spot Shot, 12-in. Cone, 500-ft Altitude, Engebi, Target Area 5
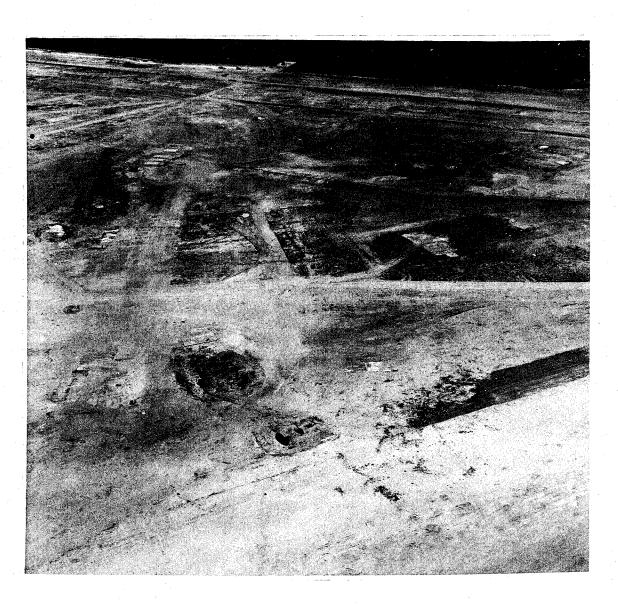
Fig. 38   16 April 51, Oblique, Spot Shot, 12-in. Cone, 500-ft Altitude, Engebi, Target Area 5

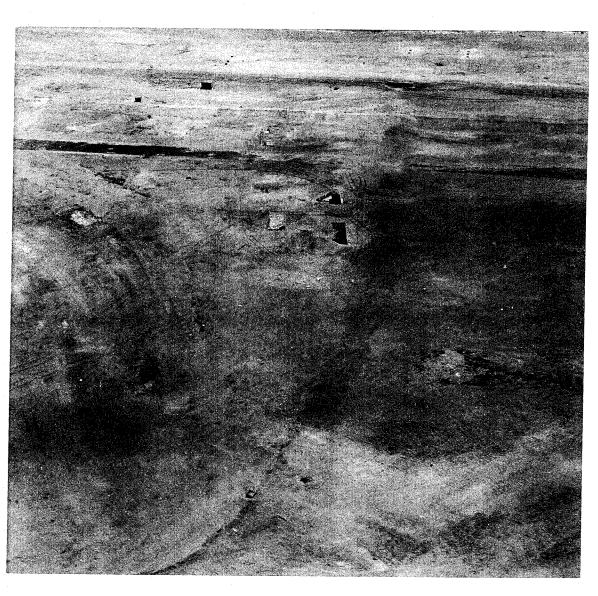Fig. 38A 22 April 51, Oblique, Spot Shot, 12-in. Cone, 500-ft Altitude, Engebi, Target Area 5

Fig. 39   16 April 51, Oblique, Spot Shot, 12-in. Cone, 500-ft Altitude, Engebi, Target Area 5

Fig. 39A   22 April 51, Oblique, Spot Shot, 12-in. Cone, 500-ft Altitude, Engebi, Target Area 5
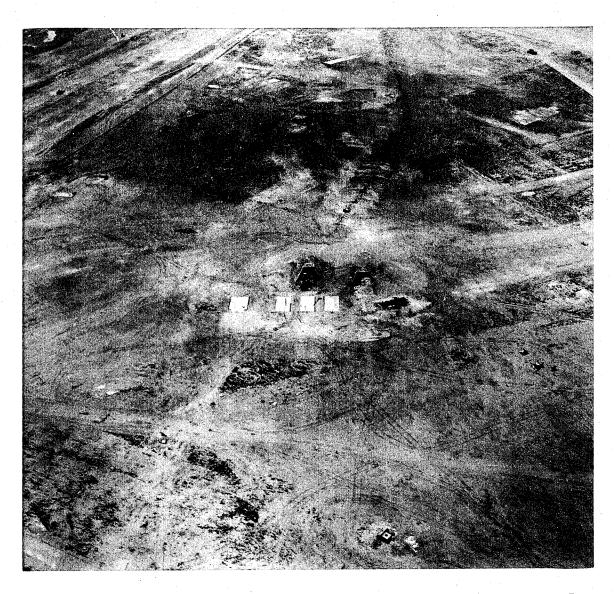
Fig. 40   22 April 51, Oblique, Spot Shot, 12-in. Cone, 500-ft Altitude, Engebi, Target Area 5

Fig. 41   22 April 51, Oblique, Spot Shot, 12-in. Cone, 500-ft Altitude, Engebi, Target Area 5

Fig. 42   16 April 51, Oblique, Spot Shot, 12-in. Cone, 500-ft Altitude, Engebi, Target Area 6

Fig. 42A   22 April 51, Oblique, Spot Shot, 12-in. Cone, 500-ft Altitude, Engebi, Target Area 6
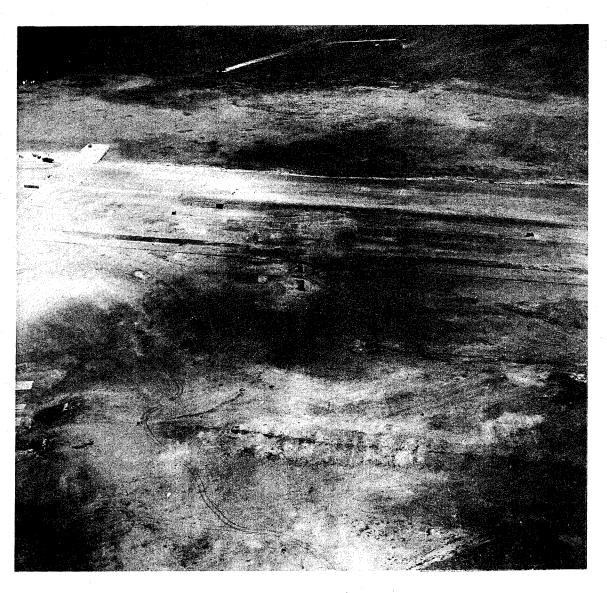
Fig. 43   16 April 51, Oblique, Spot Shot, 12-in. Cone, 500-ft Altitude, Engebi, Target Area 6

Fig. 43A   22 April 51, Oblique, Spot Shot, 12-in. Cone, 500-ft Altitude, Engebi, Target Area 6
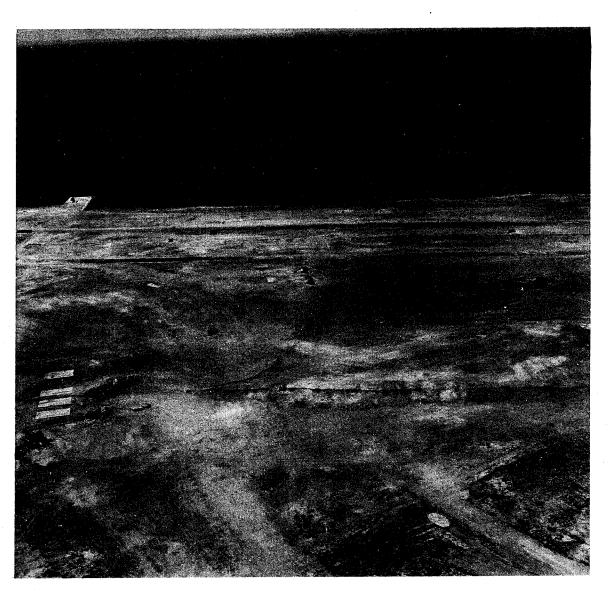
Fig. 44   16 April 51,   Oblique,   Spot Shot,   12-in. Cone,   500-ft Altitude,   Engebi,   Target Area 6

Fig. 44A 22 April 51, Oblique, Spot Shot, 12-in. Cone, 500-ft Altitude, Engebi, Target Area 6

Fig. 45   16 April 51,   Oblique,   Spot Shot,   12-in. Cone,   500-ft Altitude,   Engebi,   Target Area 6

Fig. 45A 22 April 51, Oblique, Spot Shot, 12-in. Cone, 500-ft Altitude, Engebi, Target Area 6

Fig. 46 16 April 51, Oblique, Spot Shot, 12-in. Cone, 500-ft Altitude, Engebi, Target Area 7

Fig. 46A   22 April 51, Oblique, Spot Shot, 12-in. Cone, 500-ft Altitude, Engebi, Target Area 7

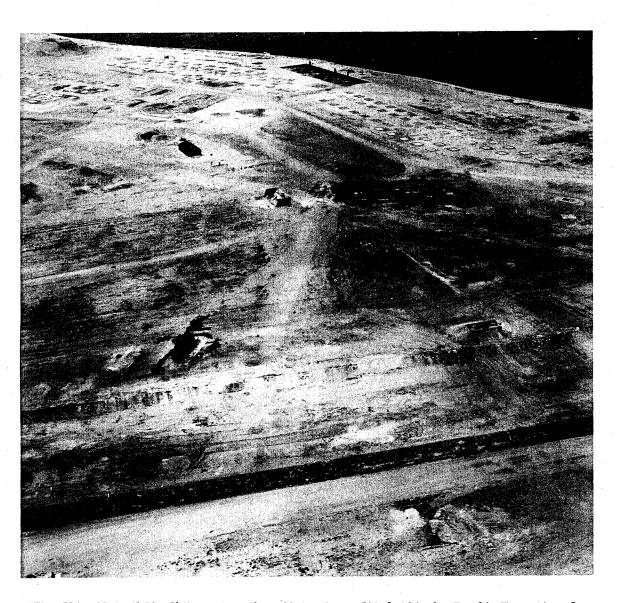Fig. 47   22 April 51, Oblique, Spot Shot, 12-in. Cone, 500-ft Altitude, Engebi, Target Area 7

Fig. 48   22 April 51, Oblique, Spot Shot, 12-in. Cone, 500-ft Altitude, Engebi, Target Area 7

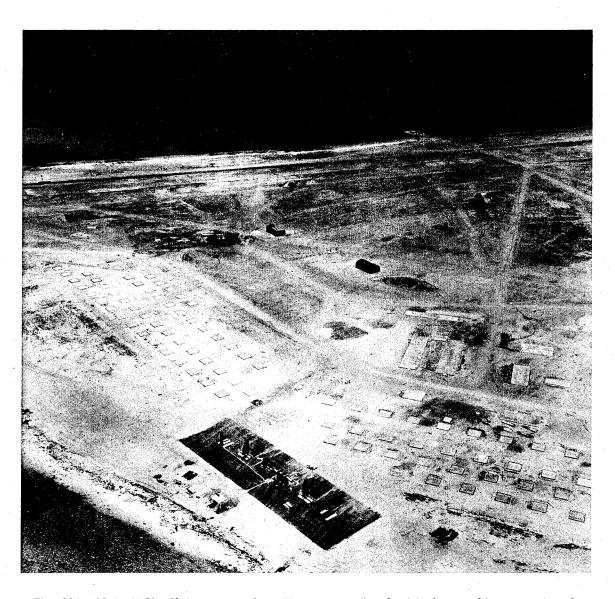Fig. 49   22 April 51, Oblique, Spot Shot, 12-in. Cone, 500-ft Altitude, Engebi, Target Area 7

Fig. 50   22 April 51, Oblique, Spot Shot, 12-in. Cone, 500-ft Altitude, Engebi, Target Area 7

Fig. 51   22 April 51, Oblique, Spot Shot, 12-in. Cone, 500-ft Altitude, Engebi, Target Area 7

Fig. 52   22 April 51, Oblique, Spot Shot, 12-in. Cone, 500-ft Altitude, Engebi, Target Area 7

Fig. 53   22 April 51, Oblique, Spot Shot, 12-in. Cone, 500-ft Altitude, Engebi, Target Area 7

Fig. 54 22 April 51, Oblique, Spot Shot, 12-in. Cone, 500-ft Altitude, Engebi, Target Area 7

Fig. 55   22 April 51, Oblique, Spot Shot, 12-in. Cone, 500-ft Altitude, Engebi, Target Area 7

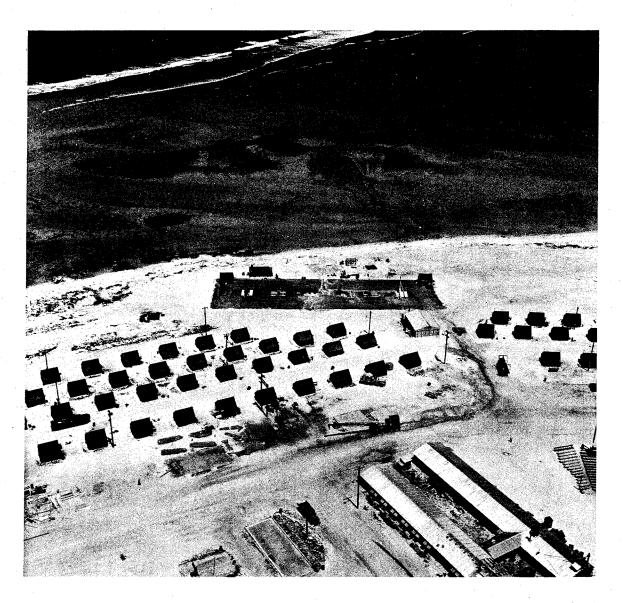Fig. 56 22 April 51, Oblique, Spot Shot, 12-in. Cone, 500-ft Altitude, Engebi, Target Area 7

Fig. 57   16 April 51, Oblique, Spot Shot, 12-in. Cone, 500-ft Altitude, Engebi, Target Area 8
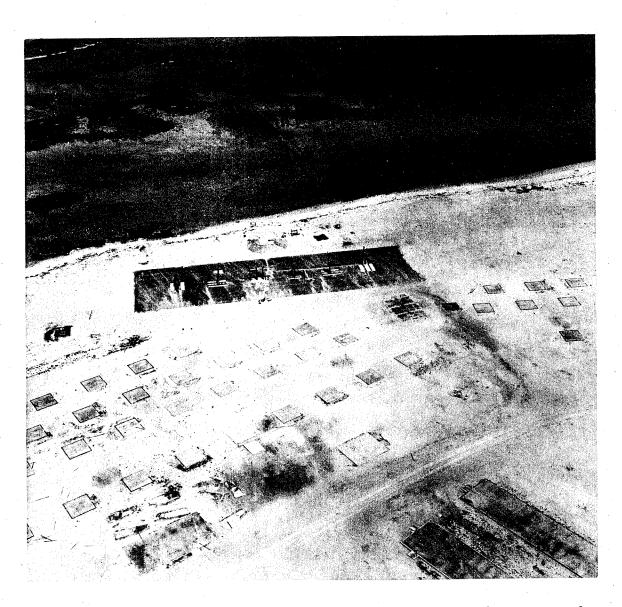
Fig. 57A   22 April 51, Oblique, Spot Shot, 12-in. Cone, 500-ft Altitude, Engebi, Target Area 8

Fig. 58 16 April 51, Oblique, Spot Shot, 12-in. Cone, 500-ft Altitude, Engebi, Target Area 8
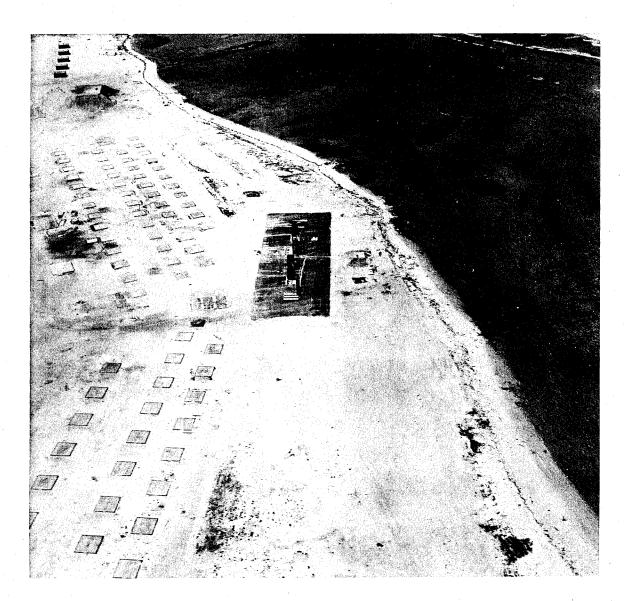
Fig. 58A   22 April 51, Oblique, Spot Shot, 12-in. Cone, 500-ft Altitude, Engebi, Target Area 8
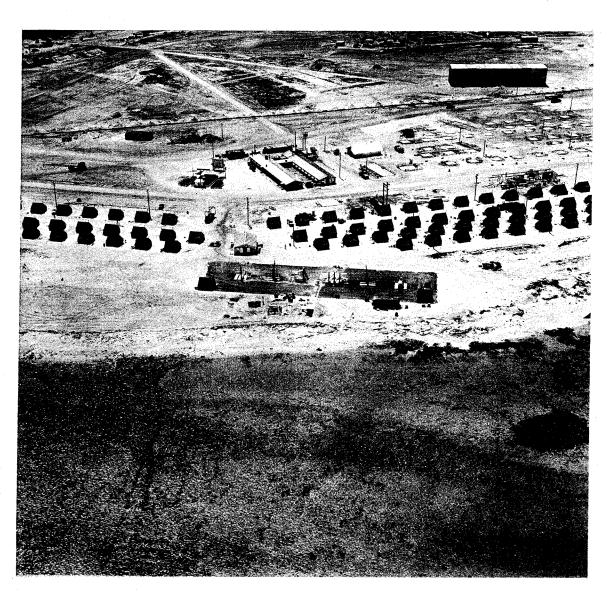
Fig. 59   16 April 51, Oblique, Spot Shot, 12-in. Cone, 500-ft Altitude, Engebi, Target Area 8

Fig. 59A   22 April 51, Oblique, Spot Shot, 12-in. Cone, 500-ft Altitude, Engebi, Target Area 8

Fig. 60   16 April 51, Oblique, Spot Shot, 12-in. Cone, 500-ft Altitude, Engebi, Target Area 8

Fig. 60A   22 April 51, Oblique, Spot Shot, 12-in. Cone, 500-ft Altitude, Engebi, Target Area 8

269

Fig. 61 16 April 51, Oblique, Spot Shot, 12-in. Cone, 500-ft Altitude, Engebi, Target Area 9

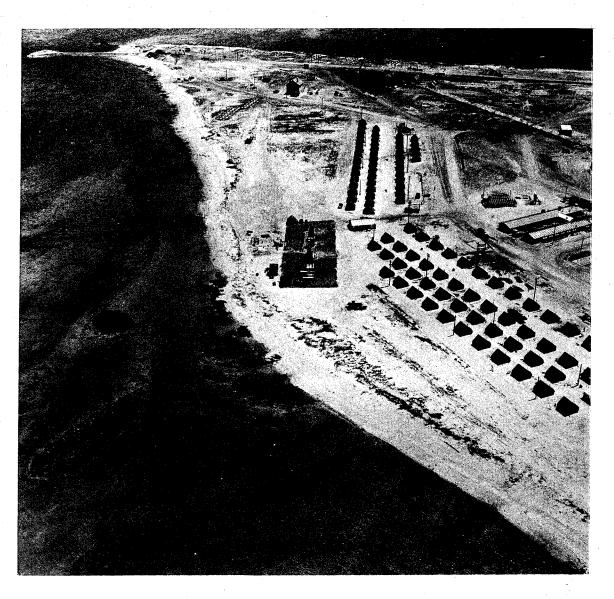Fig. 61A 22 April 51, Oblique, Spot Shot, 12-in. Cone, 500-ft Altitude, Engebi, Target Area 9
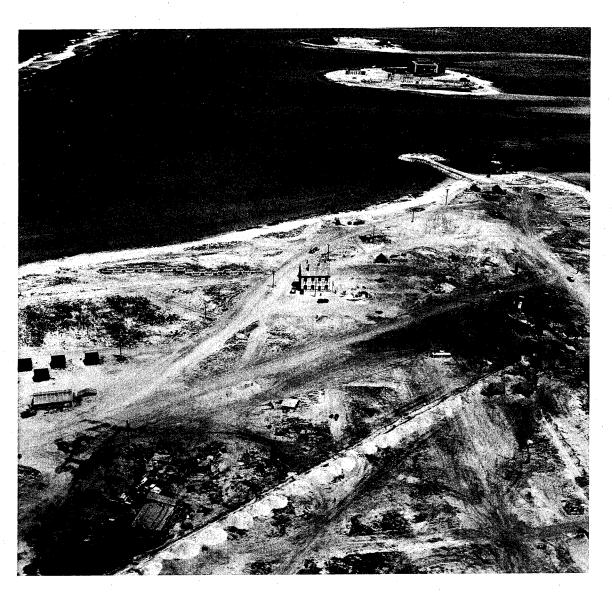
Fig. 62 16 April 51, Oblique, Spot Shot, 12-in. Cone, 500-ft Altitude, Engebi, Target Area 9

Fig. 62A 22 April 51, Oblique, Spot Shot, 12-in. Cone, 500-ft Altitude, Engebi, Target Area 9

Fig. 63   16 April 51, Oblique, Spot Shot, 12-in. Cone, 500-ft Altitude, Engebi, Target Area 9

Fig. 63A   22 April 51, Oblique, Spot Shot, 12-in. Cone, 500-ft Altitude, Engebi, Target Area 9
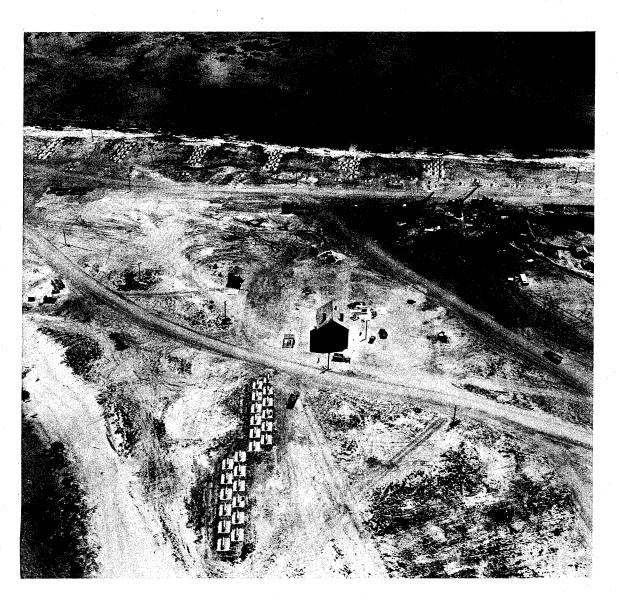
Fig. 64   16 April 51, Oblique, Spot Shot, 12-in. Cone, 500-ft Altitude, Engebi, Target Area 9

Fig. 64A   22 April 51, Oblique, Spot Shot, 12-in. Cone, 500-ft Altitude, Engebi, Target Area 9

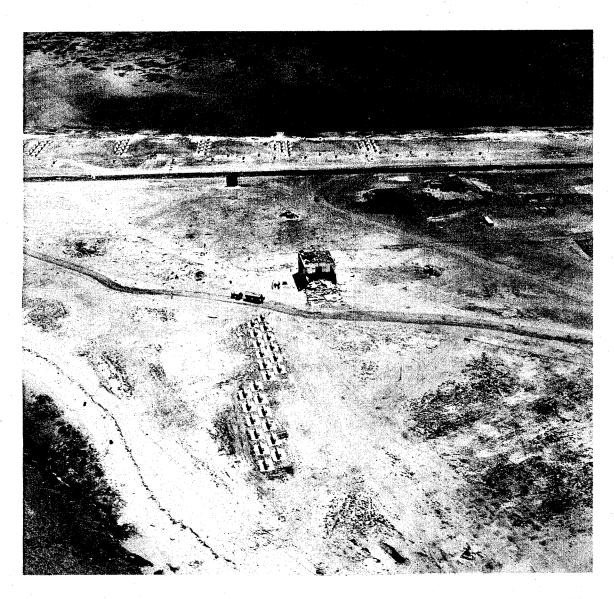Fig. 65   16 April 51, Oblique, Spot Shot, 12-in. Cone, 500-ft Altitude, Engebi, Target Area 10

Fig. 65A   22 April 51, Oblique, Spot Shot, 12-in. Cone, 500-ft Altitude, Engebi, Target Area 10

Fig. 66   16 April 51, Oblique, Spot Shot, 12-in. Cone, 500-ft Altitude, Engebi, Target Area 10

Fig. 66A   22 April 51, Oblique, Spot Shot, 12-in. Cone, 500-ft Altitude, Engebi, Target Area 10

Fig. 67   16 April 51, Oblique, Spot Shot, 12-in. Cone, 500-ft Altitude, Engebi, Target Area 10
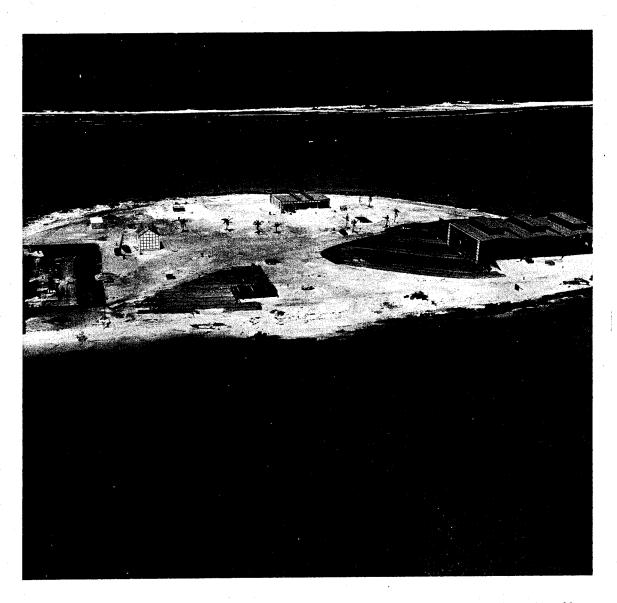
Fig. 67A   22 April 51, Oblique, Spot Shot, 12-in. Cone, 500-ft Altitude, Engebi, Target Area 10

Fig. 68   16 April 51, Oblique, Spot Shot, 12-in. Cone, 500-ft Altitude, Engebi, Target Area 10

Fig. 68A   22 April 51, Oblique, Spot Shot, 12-in. Cone, 500-ft Altitude, Engebi, Target Area 10

Fig. 69 16 April 51, Oblique, Spot Shot, 12-in. Cone, 500-ft Altitude, Engebi, Target Area 10

Fig. 70   16 April 51, Oblique, Spot Shot, 12-in. Cone, 500-ft Altitude, Muzin, Target Area 11

Fig. 70A   22 April 51, Oblique, Spot Shot, 12-in. Cone, 500-ft Altitude, Muzin, Target Area 11

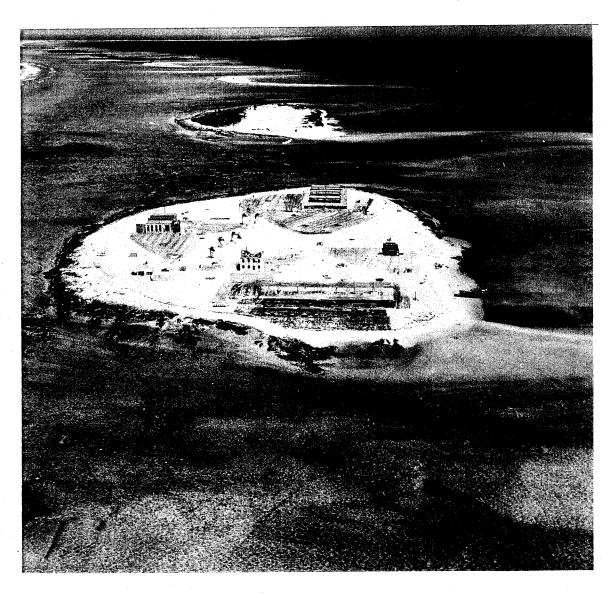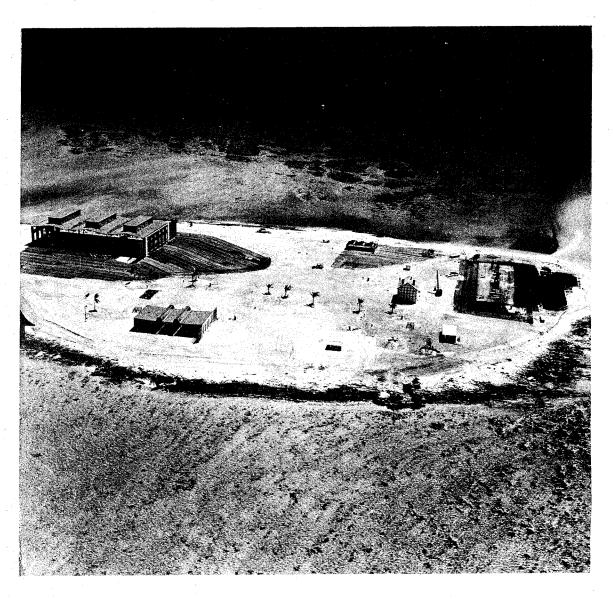Fig. 71 16 April 51, Oblique, Spot Shot, 12-in. Cone, 500-ft Altitude, Muzin, Target Area 11

Fig. 71A   22 April 51, Oblique, Spot Shot, 12-in. Cone, 500-ft Altitude, Muzin, Target Area 11

Fig. 72   16 April 51, Oblique, Spot Shot, 12-in. Cone, 500-ft Altitude, Muzin, Target Area 11

Fig. 72A   22 April 51, Oblique, Spot Shot, 12-in. Cone, 500-ft Altitude, Muzin, Target Area 11

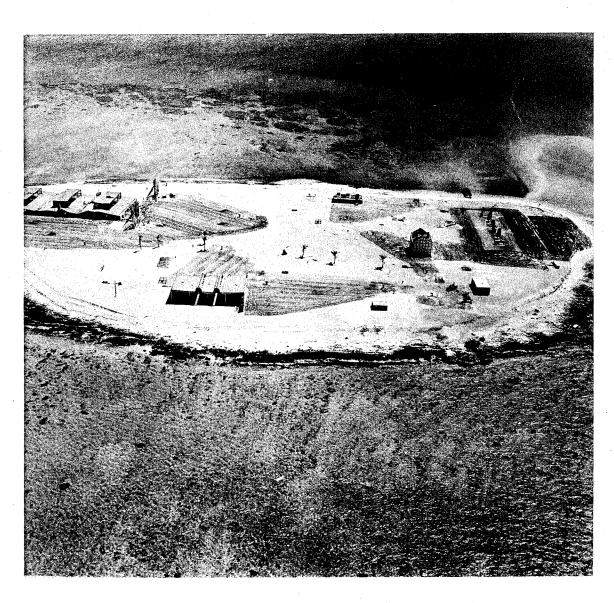Fig. 73   16 April 51, Oblique, Spot Shot, 12-in. Cone, 500-ft Altitude, Muzin, Target Area 11

Fig. 73A   22 April 51, Oblique, Spot Shot, 12-in. Cone, 500-ft Altitude, Muzin, Target Area 11

Fig. 74   22 April 51, Oblique, Spot Shot, 12-in. Cone, 500-ft Altitude, Muzin, Target Area 11

Fig. 75 21 April 51, Vertical, Spot Shot, 12-in. Cone, 25,000-ft Altitude, Engebi, Easy Shot
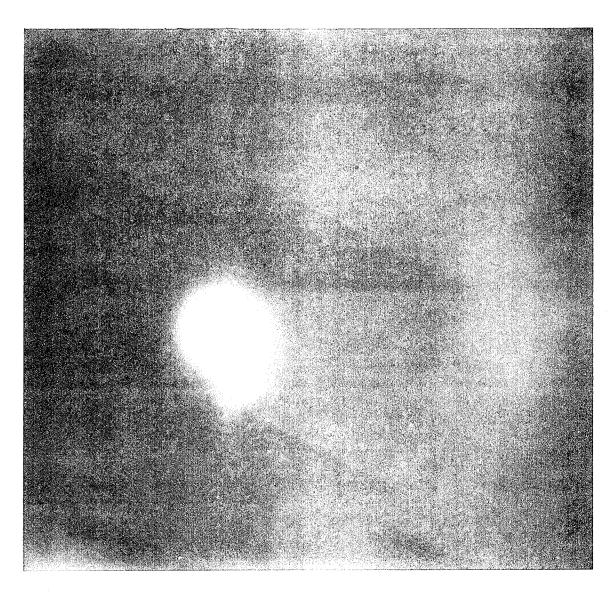
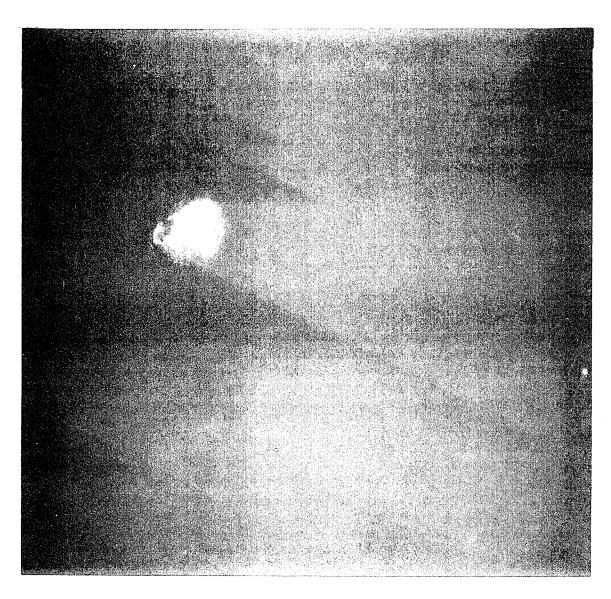Fig. 76   21 April 51, Vertical, Spot Shot, 12-in. Cone, 25.000-ft Altitude, Engebi, Easy Shot

Fig. 77   21 April 51, Vertical, Spot Shot, 12-in. Cone, 25,000-ft Altitude, Engebi, Easy Shot
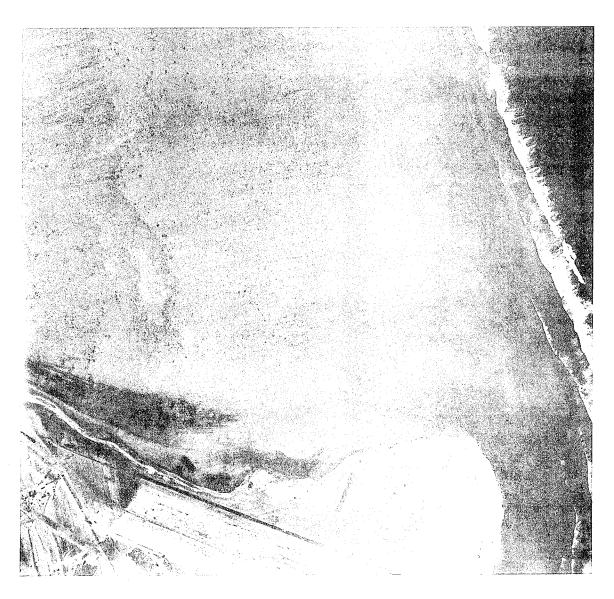
299

Fig. 78   16 April 51, Vertical, Map Shot, 12-in. Cone, 6,000-ft Altitude, Engebi, Flight Line 1

Fig. 79   16 April 51, Vertical, Map Shot, 12-in. Cone, 6,000-ft Altitude, Engebi, Flight Line 1

Fig. 80 16 April 51, Vertical, Map Shot, 12-in. Cone, 6,000-ft Altitude, Engebi, Flight Line 1
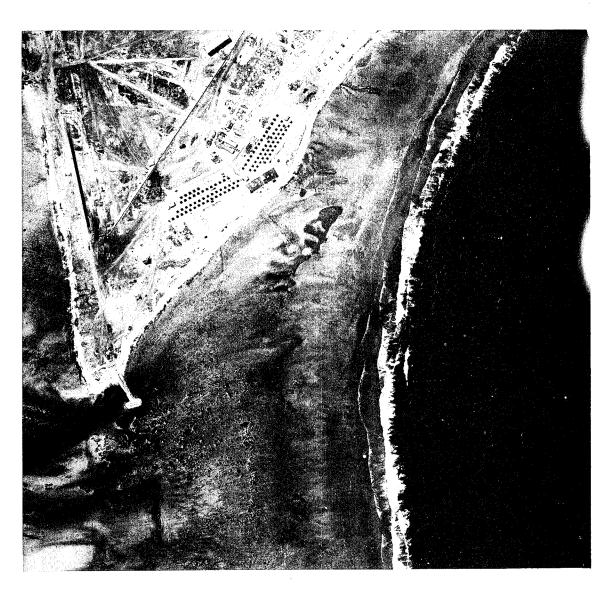
Fig. 81   16 April 51, Vertical, Map Shot, 12-in. Cone, 6,000-ft Altitude, Engebi, Flight Line 1

Fig. 82   16 April 51, Vertical, Map Shot, 12-in. Cone, 6,000-ft Altitude, Engebi, Flight Line 1

Fig. 83   16 April 51, Vertical, Map Shot, 12-in. Cone, 6,000-ft Altitude, Engebi, Flight Line 1
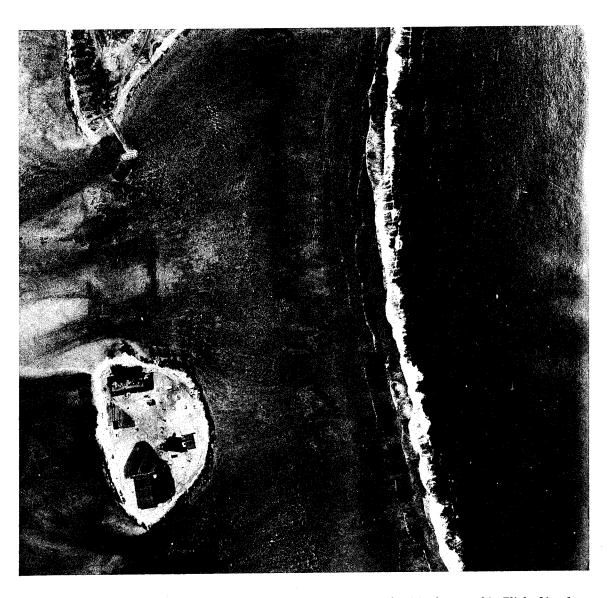
Fig. 84   16 April 51, Vertical, Map Shot, 12-in. Cone, 6,000-ft Altitude, Engebi, Flight Line 3

Fig. 84A   22 April 51,   Vertical,   Map Shot,   12-in.   Cone,   6,000-ft Altitude,   Engebi,   Flight Line 3
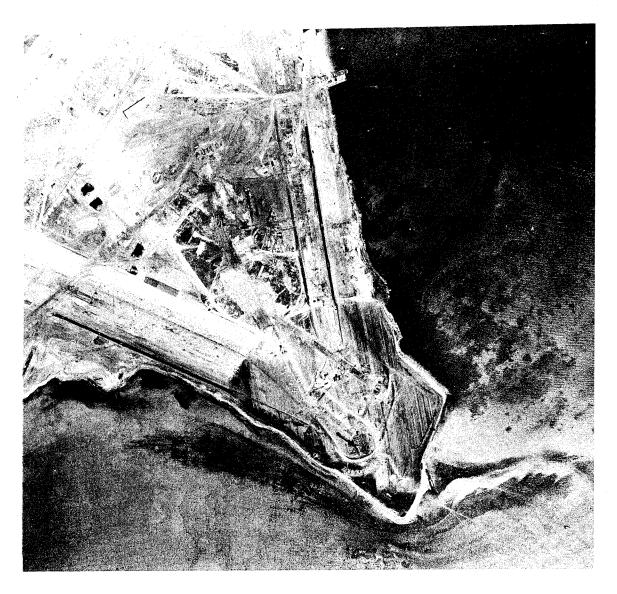
Fig. 85   16 April 51, Vertical, Map Shot, 12-in. Cone, 6,000-ft Altitude, Engebi, Flight Line 3

Fig. 85A   22 April 51, Vertical, Map Shot, 12-in. Cone, 6,000-ft Altitude, Engebi, Flight Line 3

Fig. 86   16 April 51, Vertical, Map Shot, 12-in. Cone, 6,000-ft Altitude, Engebi, Flight Line 3

Fig. 86A   22 April 51, Vertical, Map Shot, 12-in. Cone, 6,000-ft Altitude, Engebi, Flight Line 3
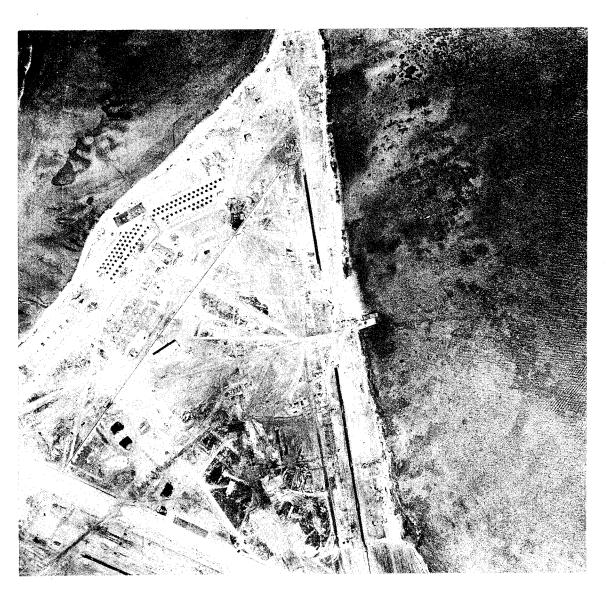
Fig. 87   16 April 51, Vertical, Map Shot, 12-in. Cone, 6,000-ft Altitude, Engebi, Flight Line 3

Fig. 87A   22 April 51,   Vertical,   Map Shot,   12-in. Cone,   6,000-ft Altitude,   Engebi,   Flight Line 3

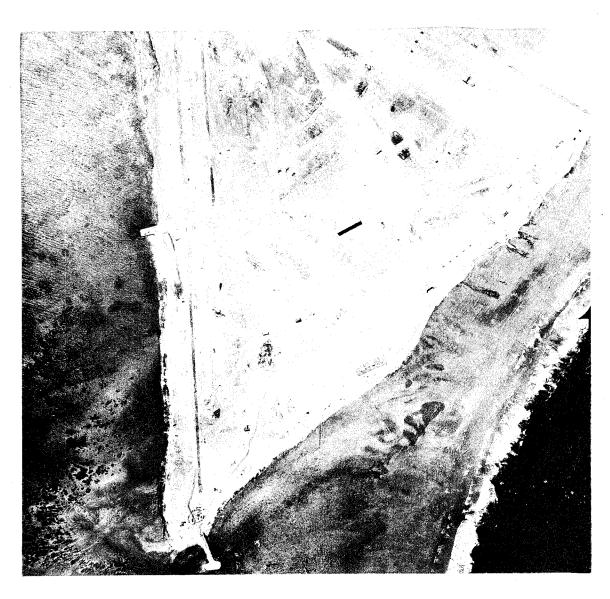Fig. 88   16 April 51, Vertical, Map Shot, 12-in. Cone, 6,000-ft Altitude, Engebi, Flight Line 3

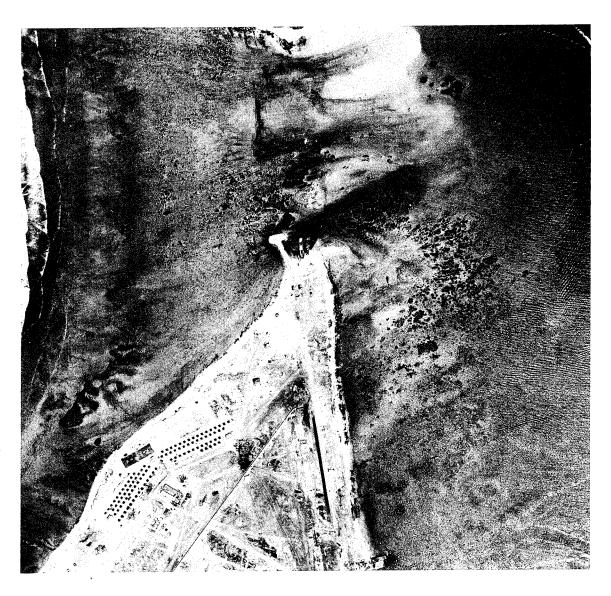Fig. 89   16 April 51, Vertical, Map Shot, 12-in. Cone, 6,000-ft Altitude, Engebi, Flight Line 3

Fig. 90   16 April 51, Vertical, Map Shot, 12-in. Cone, 6,000-ft Altitude, Engebi, Flight Line 3

Fig. 91   16 April 51, Vertical, Map Shot, 12-in. Cone, 6,000-ft Altitude, Engebi, Flight Line 3

Fig. 92   16 April 51, Vertical, Map Shot, 12-in. Cone, 6,000-ft Altitude, Engebi, Flight Line 3

Fig. 93   16 April 51, Vertical, Map Shot, 12-in. Cone, 12,000-ft Altitude, Engebi, Flight Line 1
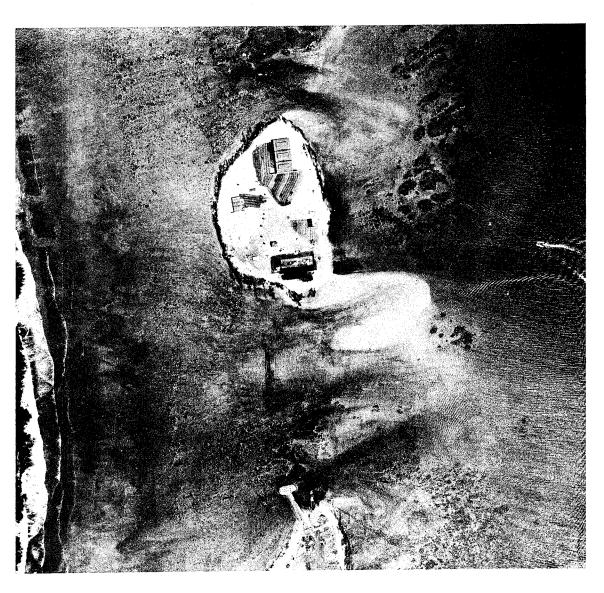
Fig. 94   16 April 51, Vertical, Map Shot, 12-in. Cone, 12,000-ft Altitude, Engebi, Flight Line 1
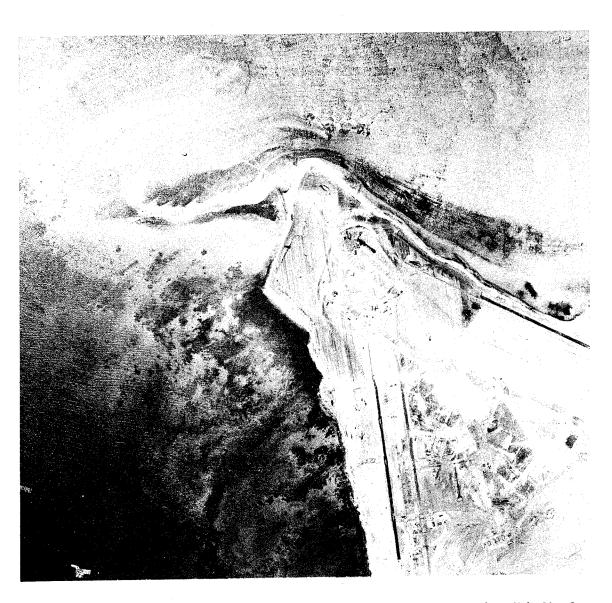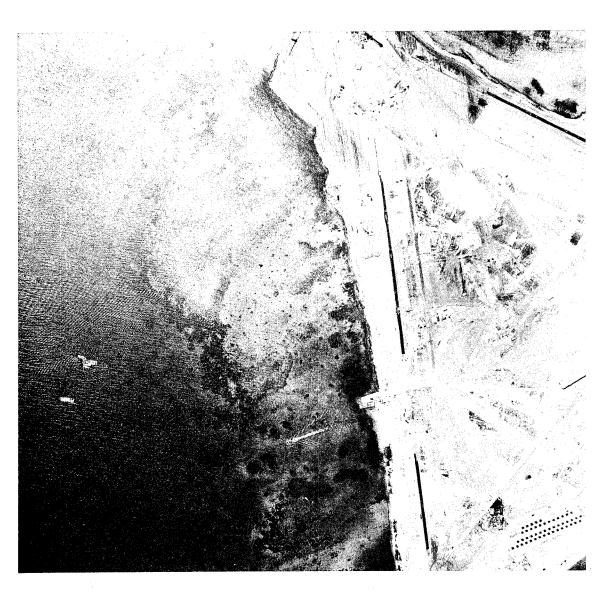
Fig. 95   16 April 51, Vertical, Map Shot, 12-in. Cone, 12,000-ft Altitude, Engebi, Flight Line 1

Fig. 96   16 April 51, Vertical, Map Shot, 6-in. Cone, 12,000-ft Altitude, Engebi, Flight Line 2

Fig. 96A   22 April 51, Vertical, Map Shot, 6-in. Cone, 12,000-ft Altitude, Engebi, Flight Line 2
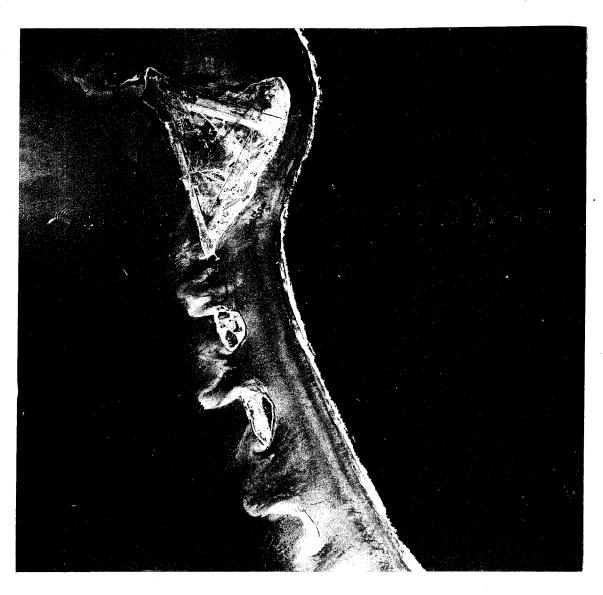
Fig. 97 16 April 51, Vertical, Map Shot, 6-in. Cone, 12,000-ft Altitude, Engebi, Flight Line 2

Fig. 97A   22 April 51, Vertical, Map Shot, 6-in. Cone, 12,000-ft Altitude, Engebi, Flight Line 2
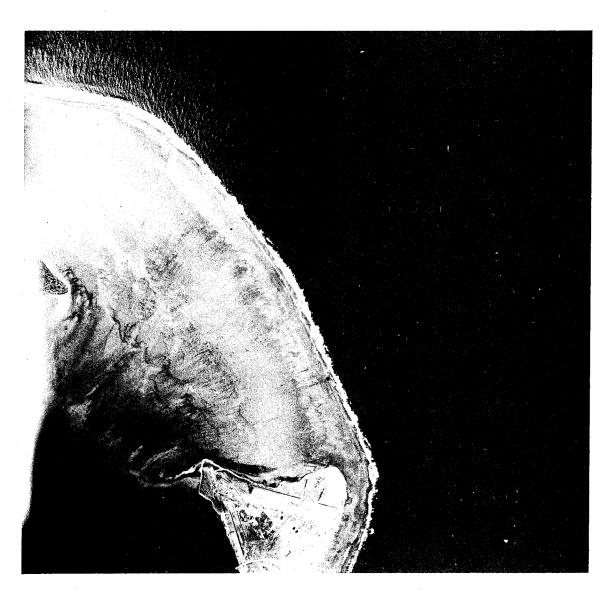
Fig. 98   16 April 51, Vertical, Map Shot, 6-in. Cone, 12,000-ft Altitude, Engebi, Flight Line 2
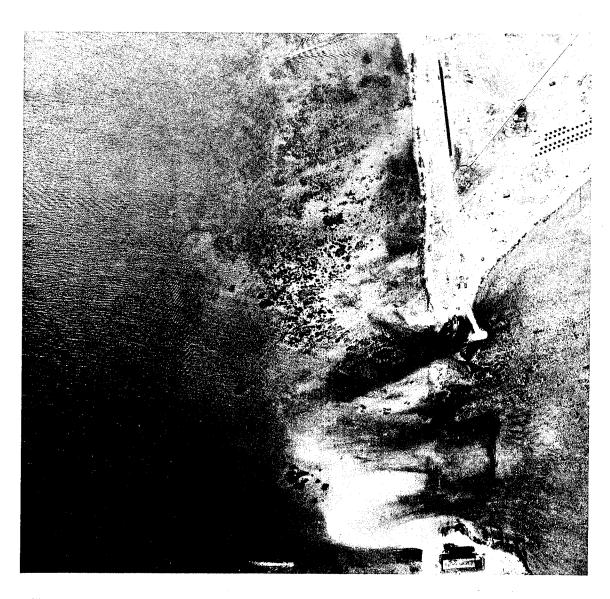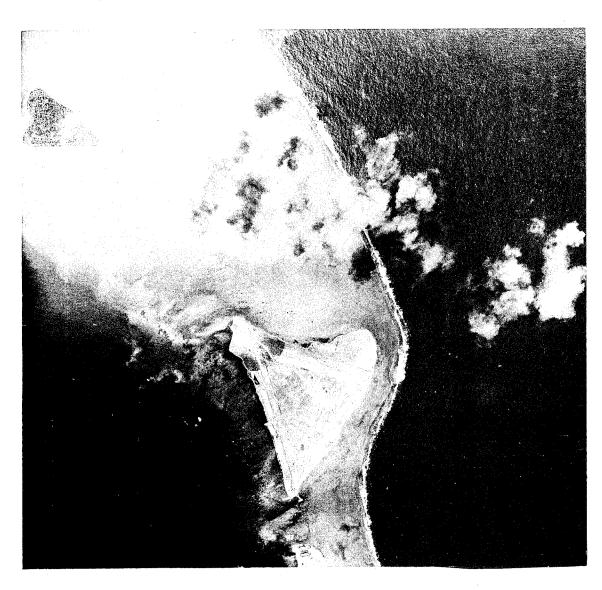
Fig. 98A   22 April 51, Vertical, Map Shot, 6-in. Cone, 12,000-ft Altitude, Engebi, Flight Line 2
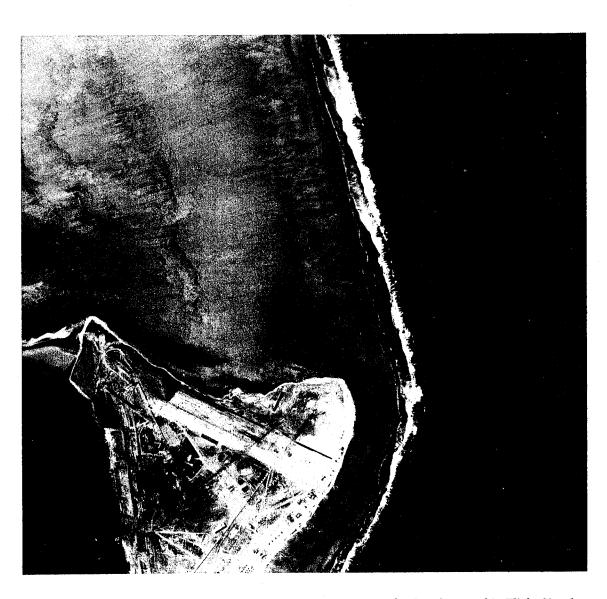
Fig. 99   16 April 51,   Vertical,   Map Shot,   6-in.   Cone,   12,000-ft Altitude,   Engebi,   Flight Line 2
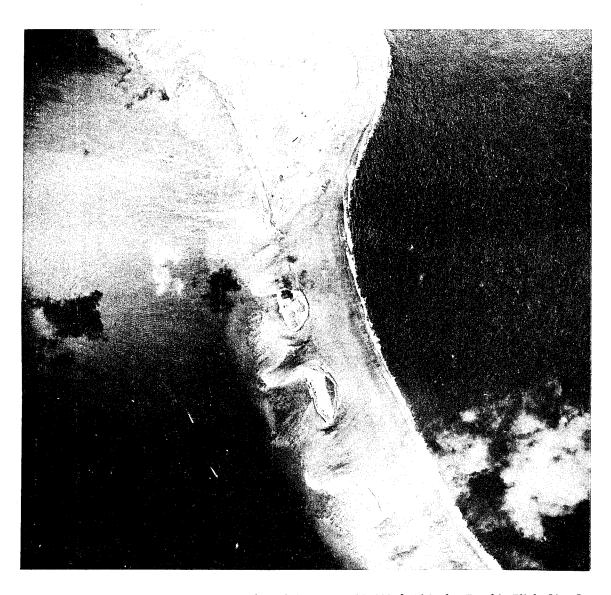
Fig. 99A 22 April 51, Vertical, Map Shot, 6-in. Cone, 12,000-ft Altitude, Engebi, Flight Line 2

Fig. 100   22 April 51, Vertical, Map Shot, 6-in. Cone, 12,000-ft Altitude, Engebi, Flight Line 2

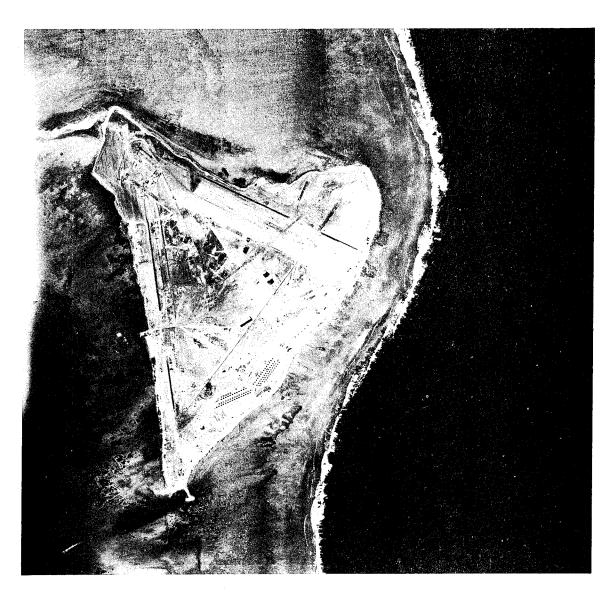Fig. 101 16 April 51, Vertical, Map Shot, 6-in. Cone, 12,000-ft Altitude, Engebi, Flight Line 2
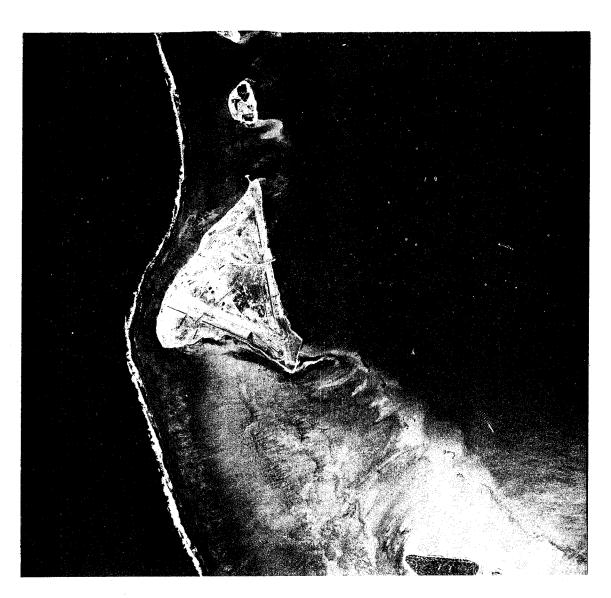
Fig. 102   16 April 51, Vertical, Map Shot, 6-in. Cone, 12,000-ft Altitude, Engebi, Flight Line 2

Fig. 103   16 April 51,   Vertical,   Map Shot,   6-in. Cone,   12,000-ft Altitude,   Engebi,   Flight Line 2
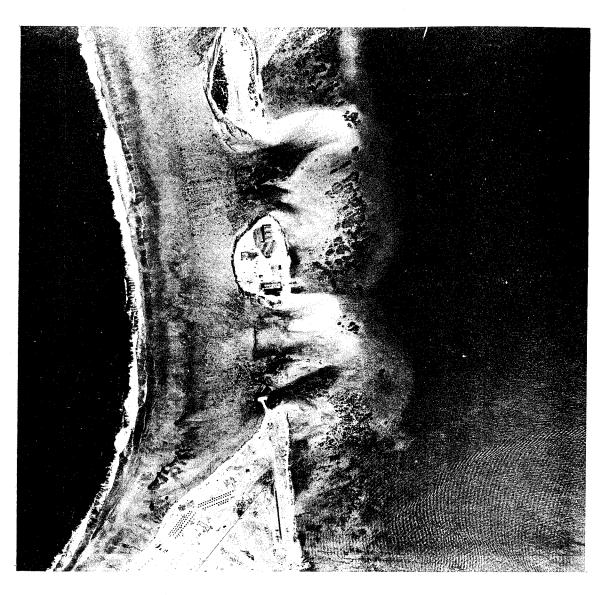
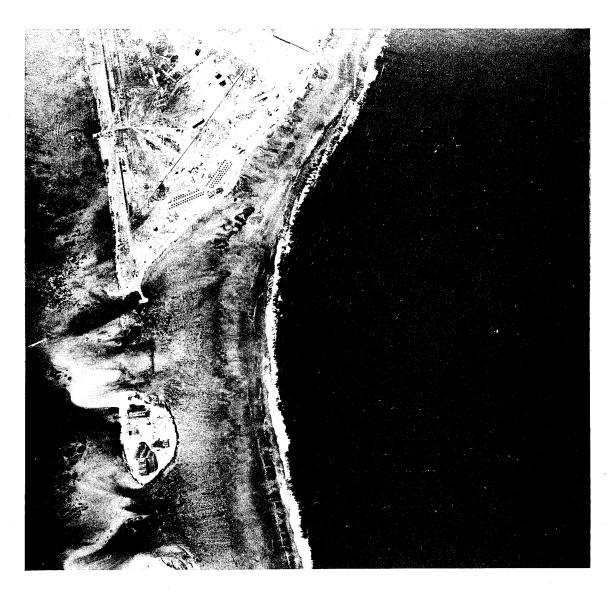Fig. 104   16 April 51, Vertical, Map Shot, 12-in. Cone, 12,000-ft Altitude, Engebi, Flight Line 3

Fig. 104A   22 April 51, Vertical, Map Shot, 12-in. Cone, 12,000-ft Altitude, Engebi, Flight Line 3
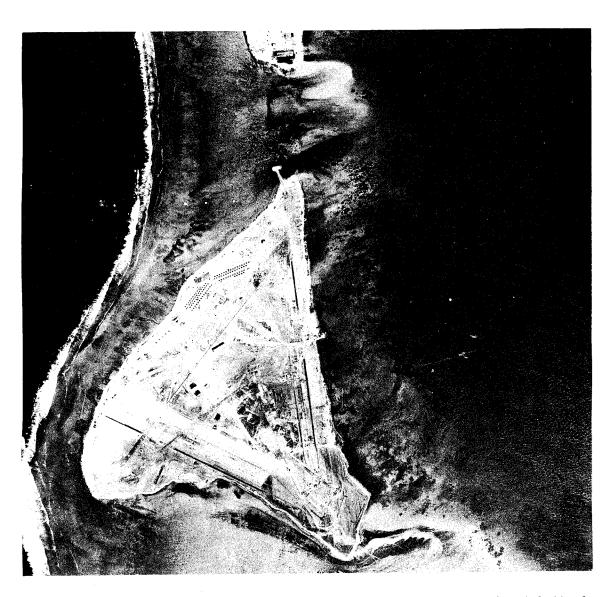
Fig. 105   16 April 51, Vertical, Map Shot, 12-in. Cone, 12,000-ft Altitude, Engebi, Flight Line 3
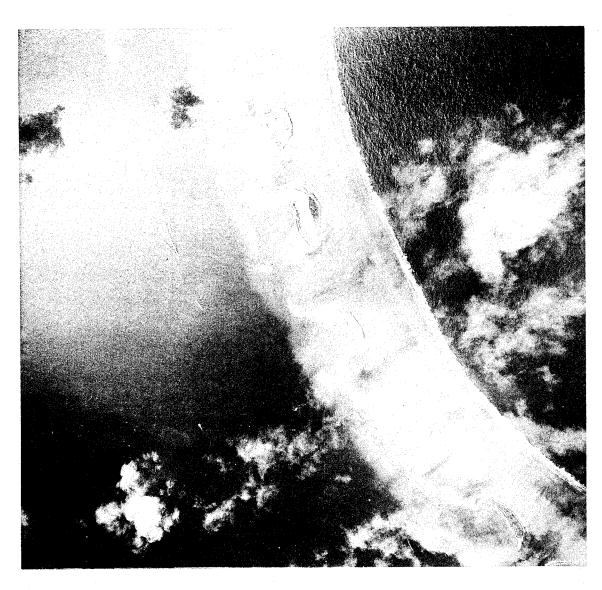
Fig. 105A   22 April 51, Vertical, Map Shot, 12-in. Cone, 12,000-ft Altitude, Engebi, Flight Line 3

Fig. 106 16 April 51, Vertical, Map Shot, 12-in. Cone, 12,000-ft Altitude, Engebi, Flight Line 3

Fig. 106A   22 April 51, Vertical, Map Shot, 12-in. Cone, 12,000-ft Altitude, Engebi, Flight Line 3
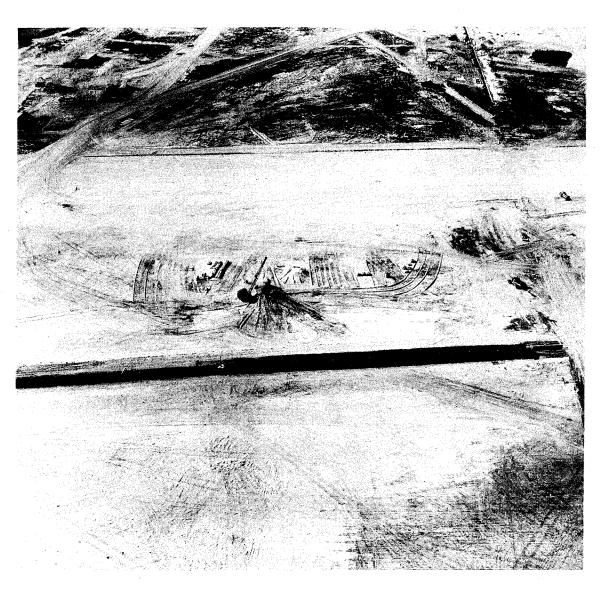
Fig. 107   16 April 51, Oblique, Spot Shot, 12-in. Cone, 500-ft Altitude, Engebi, Looking East

Fig. 108   22 April 51, Oblique, Spot Shot, 12-in. Cone, 500-ft Altitude, Engebi, Looking North

Fig. 109   22 April 51, Oblique, Spot Shot, 12-in. Cone, 500-ft Altitude, Engebi, Looking East

Fig. 110   22 April 51, Oblique, Spot Shot, 12-in. Cone, 500-ft Altitude, Engebi, Looking West

Fig. 111   16 April 51, Oblique, Spot Shot, 12-in. Cone, 500-ft Altitude, Engebi, Tower

Fig. 112   22 April 51, Oblique, Spot Shot, 12-in. Cone, 500-ft Altitude, Engebi, Looking Toward
Crater Area

Fig. 113   16 April 51, Oblique, Spot Shot, 12-in. Cone, 500-ft Altitude, Engebi, Tower Area

Fig. 114 16 April 51, Oblique, Spot Shot, 12-in. Cone, 500-ft Altitude, Engebi, Tower Area

Fig. 115 16 April 51, Oblique, Spot Shot, 12-in. Cone, 500-ft Altitude, Engebi, Tower Area

Fig. 116   16 April 51, Oblique, Spot Shot, 12-in. Cone, 500-ft Altitude, Engebi, Tower Area

Fig. 117   16 April 51, Oblique, Spot Shot, 12-in. Cone, 500-ft Altitude, Engebi, Tower

Fig. 118 22 April 51, Oblique, Spot Shot, 12-in. Cone, 500-ft Altitude, Engebi, Looking North
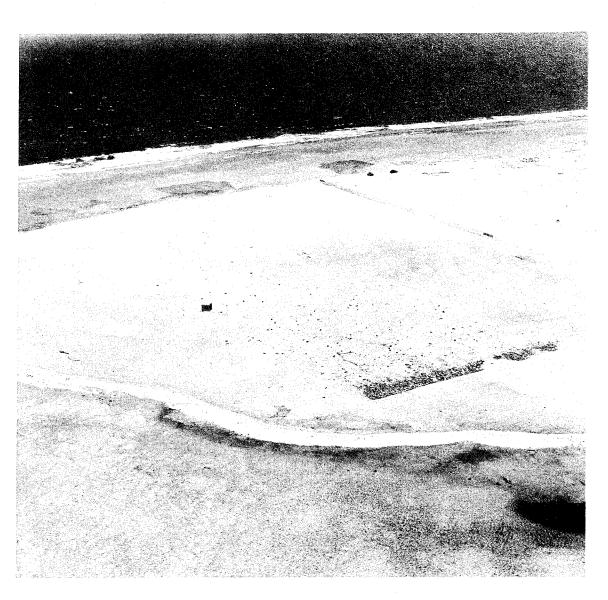
Fig. 119   22 April 51, Oblique, Spot Shot, 12-in. Cone, 500-ft Altitude, Engebi, Looking East

Fig. 120   22 April 51, Oblique, Spot Shot, 12-in. Cone, 500-ft Altitude, Engebi, Crater Area

Fig. 121   22 April 51, Oblique, Spot Shot, 12-in. Cone, 500-ft Altitude, Engebi, Crater Area

Fig. 122   22 April 51, Oblique, Spot Shot, 12-in. Cone, 500-ft Altitude, Engebi, Looking East

Fig. 123   16 April 51, Oblique, Spot Shot, 12-in. Cone, 500-ft Altitude, Engebi, Looking Toward
Tower

Fig. 124   16 April 51, Oblique, Spot Shot, 12-in. Cone, 500-ft Altitude, Engebi, Vicinity of
Target 1

Fig. 125   22 April 51, Oblique, Spot Shot, 12-in. Cone, 500-ft Altitude, Engebi, Vicinity of
Target 1

Fig. 126   22 April 51, Oblique, Spot Shot, 12-in. Cone, 500-ft Altitude, Engebi, Vicinity of
Target 4
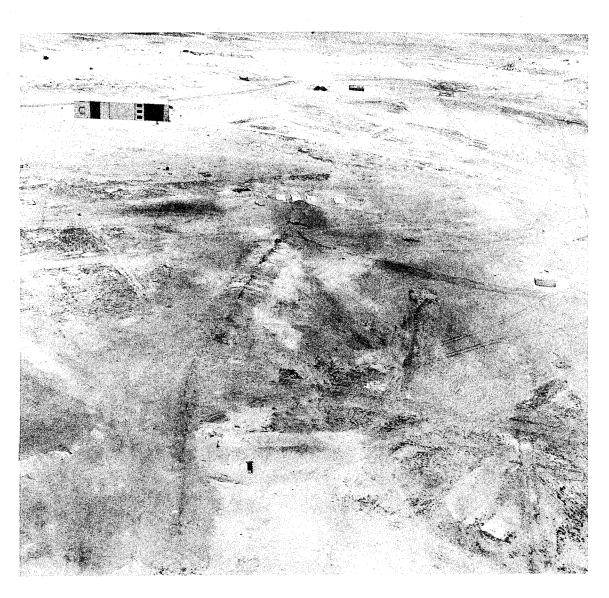
Fig. 127   22 April 51, Oblique, Spot Shot, 12-in. Cone, 500-ft Altitude, Engebi, Vicinity of Target 6
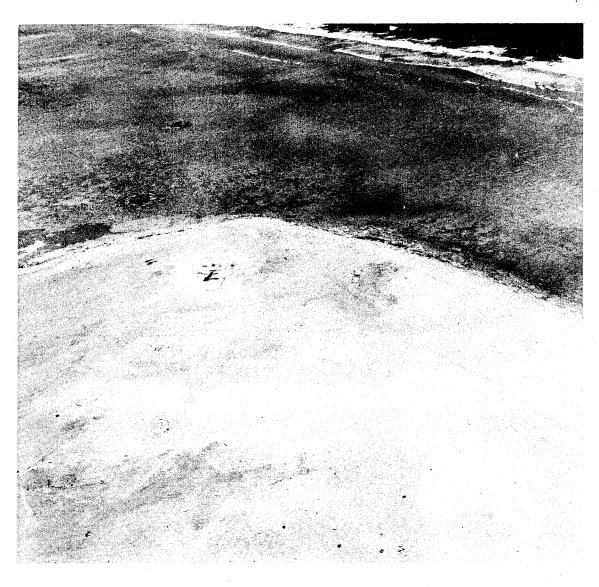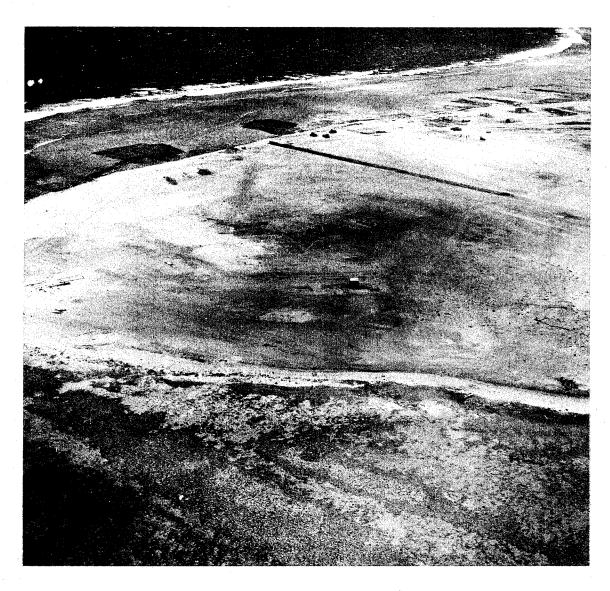
Fig. 128   22 April 51, Oblique, Spot Shot, 12-in. Cone, 500-ft Altitude, Engebi, Looking Toward
Target 2

Fig. 129   22 April 51, Oblique, Spot Shot, 12-in. Cone, 500-ft Altitude, Engebi, Looking Toward
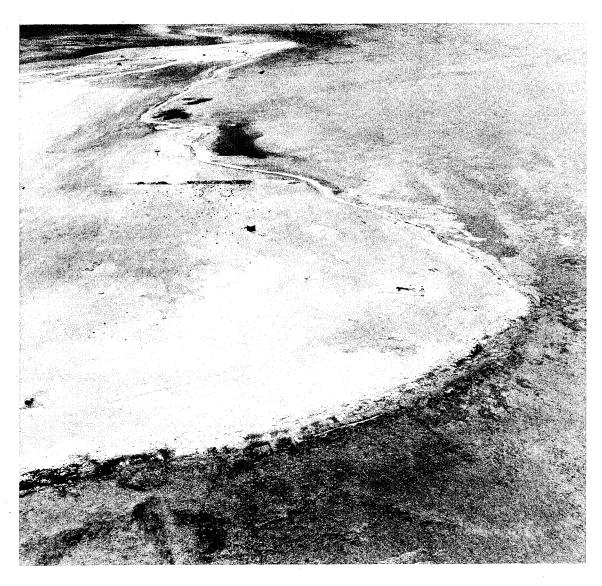Targets 1, 4, 5, and 7

Fig. 130   22 April 51, Oblique, Spot Shot, 12-in. Cone, 500-ft Altitude, Engebi, Crater Area
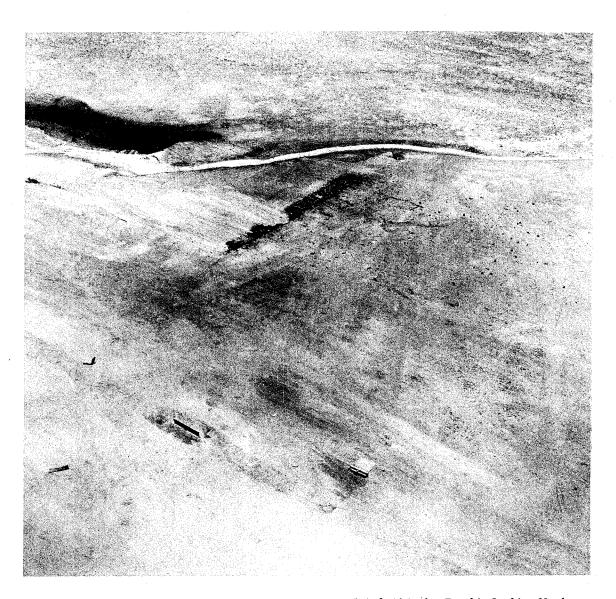
Fig. 131   22 April 51, Oblique, Spot Shot, 12-in. Cone, 500-ft Altitude, Engebi, Looking Northeast

Part IV
FILM FOGGING STUDIES

by

ROBERT E. KEEGAN
Major, USAF

Preface

This report, although based on limited sampling, gives quite conclusive results on three particular types of aerial reconnaissance film. Owing to the very limited time available and the late arrival of equipment at Eniwetok, it was not possible to make more extensive and comprehensive tests during Operation Greenhouse.

Acknowledgments

Chapter 1

Introduction

1.1 PURPOSE

This Project was established 6 May 1951 to determine the effects of atomic bomb radiation on photographic film carried in reconnaissance and drone aircraft participating in George Shot, 9 May 1951.

1.2 JUSTIFICATION

The Strategic Air Command (SAC) of the United States Air Force (USAF) has the problem of planning reconnaissance missions where avenues of penetration and withdrawal border target areas. Important to this problem is the knowledge of the response in density of aerial film as a function of an integrated dosage from an atomic bomb explosion. Determination of radiation levels in the clouds and cloud trajectories is also pertinent to the SAC problem. Data on these subjects are available in separate project reports for correlation with the dosage-vs-fogging data given in this report.

Although irradiation of film is properly a laboratory test, some effects of a nuclear bomb explosion on aerial film carried in operational reconnaissance aircraft can be determined only during an atomic testing program. It is for this reason primarily that this study was undertaken.

1.3 SCOPE

A rather complete coverage of different altitudes and dosage ranges on George Shot was made possible by the placement of loaded film magazines in the six drone sampling aircraft as well as in the SAC RB-29 and in the two AFOAT-1 WB-29's.

The placement of film strips in the drone sampling aircraft on Easy Shot made possible the extension of dosage ranges and the addition of more data on other types of film.

Chapter 2

Experimental Procedure

2.1 FILM AND EQUIPMENT FOR GEORGE SHOT

On George Shot two types of standard aerial reconnaissance film (L- and N-types) were exposed. These films were loaded in A-5A aerial-camera magazines and placed in six AEC B-17 sampling drone aircraft and three B-29 manned aircraft, as well as at five ground stations preselected to give a particular dosage range. The altitude and compartment location for each airborne magazine and the distances from George zero for each magazine on the ground are tabulated in Tables 3.1 and 3.2.

The number of passes made by each aircraft is not included in this report since this information is included in other reports and is of no value to this project, which is concerned only with the total integrated dosage to which each film was exposed.

With each magazine was placed either a National Bureau of Standards (NBS) film packet and/or a radiological-safety badge to furnish an extra dosage value for correlation with the 10 additional film packets and badges on each drone aircraft and to furnish an average dosage value for the manned aircraft and the ground stations.

2.2 FILM AND EQUIPMENT FOR EASY SHOT

Seven strips of film 5 in. long were placed in each of six film cans. Each can was placed on an AEC B-17 drone sampling aircraft and contained samples of the following:

1. One strip of unexposed film, L-type, undeveloped
2. One strip of gray-scale exposed film, L-type, undeveloped
3. One strip of unexposed film, N-type, undeveloped
4. One strip of gray-scale exposed film, N-type, undeveloped
5. One strip of unexposed film, N-type, undeveloped (This negative was later exposed before development.)
6. One strip of unexposed film, A-type, undeveloped
7. One strip of gray-scale exposed film, A-type, undeveloped

The aerial film cans and reels were washed, and the seven strips of film were taped to the reels. Each reel upon which these strips were affixed with tape was placed in its film can, which was then sealed with waterproof tape and with black photographic tape. In addition, one strip of L-type film was kept in the Photographic Laboratory on Parry Island for development with the film after exposure. This strip later served to give a background density.

The altitude and compartment location for each can are tabulated in Table 3.3, as well as the NBS average dosage value for each aircraft, which is an average of the readings of 10 film packets. The drone aircraft were flown, for the most part, through the stem of the atomic cloud from H+3 to H+30 min.

Chapter 3

Test Results

3.1 RECOVERY

The film cans in the Easy Shot drone aircraft were removed shortly after the aircraft were on the ground and clearance was given by the radiological-safety officer in charge.

After George Shot the loaded film magazines were similarly removed from the drones. The B-29's were flown through portions of the atomic cloud during the period G+45 min to G+3 hr and then landed on Eniwetok Island. The magazines from these aircraft were removed within 2 hr after landing.

The magazines at the ground stations were not recovered until G+1 day because residual radiation levels on the island location were too high for prolonged human exposure. The placement of these magazines was made according to a predicted dosage range of 10 to 50 r. The higher range of 32 to 64 r was occasioned by the delay in recovery, as well as by a probable underestimation in the prediction.

3.2 DEVELOPMENT OF FILM

The Easy Shot film strips were returned to the Parry Island Photographic Laboratory and were processed during the following week. The contents of each sample can were individually processed in Developer D-19 at 68°F for 9 min. The developer was mixed with distilled (not re-processed) water.

The George Shot film rolls were removed from the magazines in total darkness, placed in individual film cans, sealed with waterproof tape and black photographic tape, appropriately numbered, and securely packed in wooden boxes for subsequent air shipment to Los Alamos Scientific Laboratory. The films, as well as the nonirradiated films for blank densities, were processed during July 1951. Development was in D-19 with a pH of 10.05 at 72°F for 5 min.

3.2.1 Density Measurements

The density readings were made in an Eastman Visual Densitometer, Model B. Each density value included in the tables of this chapter represents the average of at least 10 readings. The human error inherent in the densitometer reading was reduced and kept constant by having the same experienced operator make the readings for all the film associated with each test.

The George Shot data are tabulated in Tables 3.1 and 3.2 and the Easy Shot data are in Table 3.3. In Table 3.4 is summarized all pertinent dosage-vs-density information from both tests. This table serves as a basis for the individual curves of the three film types shown in Fig. 3.1.

3.3 EXPOSURE OF REPRESENTATIVE SAMPLES

Although scene photography on irradiated film was not a specified requirement of this Project, it should have been included. However, security restrictions, as well as time limitations, precluded any picture exposure of the aerial films before, during, and after George Shot.

It has been demonstrated on EK Super XX 35-mm film that films fogged by as much as 100 r of gamma radiation have been found capable of producing pictures of satisfactory contrast, provided subsequent exposures of the scene are increased by a large factor over

TABLE 3.1 L-TYPE FILM DATA, GEORGE SHOT

Altitude (ft)	Dosage (r)	Density	Emulsion No.	Compartment
B-29 Aircraft				
21,000*	0.625	0.31	55-33-42	Bomb bay
	0.760	0.30	55-33-42	Rear pressure
	1.410	0.43	55-15-1	Rear pressure
23,000†	1.680	0.57	55-33-42	Rear pressure
	2.500	0.96	55-33-42	Bomb bay
23,000‡	2.800	0.81	55-33-42	Rear pressure
AEC Drones				
18,000	11.4	1.56	55-33-44	Radio
20,000	16.4	1.74	55-33-44	Radio
24,000	23.5	1.99	55-33-44	Radio
26,000	29.1	1.93	55-33-44	Radio
22,000	22.0	2.11	55-33-44	Radio
28,000	28.6	2.05	55-33-44	Radio

Distance from George Zero (ft)	Dosage (r)	Density	Emulsion No.	Compartment
Ground Locations				
8,900	32.4	2.21	55-33-42	
8,775	37.4	2.17	55-33-42	
8,650	34.4	2.32	55-33-44	
8,350	51.4	2.42	55-33-44	
7,950	64.4	2.41	55-33-44	

Emulsion Speed	Dosage (r)	Density	Emulsion No.	Compartment
Blank Densities				
100		0.12	55-33-42	
		0.12	55-12-1	
		0.12	55-33-44	

*Serial number 7,335.
†Serial number 1,762.
‡Serial number 2,202.

TABLE 3.2   N-TYPE FILM DATA, GEORGE SHOT

Altitude (ft)	Dosage (r)	Density	Emulsion No.	Compartment
B-29 Aircraft			
21,000*	0.55	0.55	57-207-16	Bomb bay
	0.76	0.57	57-207-16	Rear pressure
23,000†	1.08	0.74	57-207-16	Bomb bay
	1.71	0.93	57-208-12	Bomb bay
23,000‡	2.67	1.34	57-207-16	Bomb bay
	2.75	1.15	57-207-16	Rear pressure
AEC Drones			
18,000	11.4	1.66	57-208-12	Radio
22,000	22.0	1.84	57-208-12	Radio
20,000	16.4	1.53	57-208-12	Radio
24,000	23.5	1.80	57-208-12	Radio
28,000	28.6	1.64	57-208-12	Radio
26,000	29.1	1.70	57-208-12	Radio

Distance from George Zero (ft)	Dosage (r)	Density	Emulsion No.	Compartment
Ground Locations			
8,900	32.4	1.84	57-207-16	
8,775	37.4	1.84	57-207-16	
8,650	34.4	1.92	57-208-12	
8,350	51.4	1.85	57-208-12	
7,950	64.4	1.97	57-208-12	

Emulsion Speed	Dosage (r)	Density	Emulsion No.	Compartment
Blank Densities			
200		0.12	57-207-16	
		0.12	57-208-12	

*Serial number 7,335.
†Serial number 1,762.
‡Serial number 2,202.

normal.[1] Therefore scene or gray-scale exposures were made on six portions of each of the four representative films, i.e., two of L-type and two of N-type, representing four points of the dosage range. Exposure time, development time, and use of anti-foggant were varied to determine conditions for optimum results.

The pictures were all taken on 26 July 1951. The light-meter reading was 400. Normal exposure settings for L-type film was f/22, 1/100 sec, and for N-type film was f/22, 1/200 sec.

3.3.1 Use of Anti-foggant in Development

At the suggestion of Loris Gardner, CTU 3.1.6, Eastman Kodak Anti-foggant No. 2 (6-nitrobenzimidazole) was used in varied amounts in the developer. The normal amount of anti-foggant consists of 10 cc of 0.1 per cent

TABLE 3.3 FILM DATA,* EASY SHOT

Altitude (ft)	Dosage (r)	Density A	L	N
20,000	140	3.51	3.16	3.09
22,000	190	3.87	3.38	3.16
24,000	190	3.86	3.33	3.11
26,000	120	3.95	3.40	3.29
28,000	82	3.44	3.03	2.93
30,000	120	3.38	3.02	2.95

*Data collected from waist compartment of AEC drones.

EK No. 2 per 8 oz of D-19. The factors over this normal amount that were tested are given in the legends under Figs. 3.2 to 3.25. Overdevelopment and underdevelopment are indicated by percentages over and under normal, which reflect the addition of D-19 to, and the dilution of, the normal solution, respectively.

3.3.2 Density Measurements

The average density reading for each negative is included in the legend under each figure. This value is listed for comparison with the base density for each sample. The base densities for the samples are as follows:

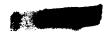| Figure Nos.	Film	Density
3.2–3.7	N-type	0.55
3.8–3.13	L-type	1.74
3.14–3.19	N-type	1.64
3.20–3.25	L-type	0.81

3.3.3 Comparison of Prints

This discussion reflects not only the impressions of visual analysis but also full consider-

TABLE 3.4 DOSAGE VS DENSITY FOR THREE FILM TYPES

Dosage (r)	Density A	L	N
0.55			0.55
0.625		0.31	
0.76		0.30	0.57
1.08			0.74
1.41		0.43	
1.68		0.57	
1.71			0.93
2.50		0.96	
2.67			1.34
2.75			1.15
2.80		0.81	
11.4		1.56	1.66
16.4		1.74	1.53
22.0		2.11	1.84
23.5		1.99	1.80
28.6		2.05	1.64
29.1		1.93	1.70
32.4		2.21	1.84
34.4		2.32	1.92
37.4		2.17	1.84
51.4		2.42	1.85
64.4		2.41	1.97
82	3.44	3.04	2.93
120	3.45	3.00	2.95
140	3.51	3.16	3.09
190	3.87	3.36	3.14

ation of the negative density as compared with the base density for each representative sample. Since the processing of the positive prints was exactly regulated so as to be the same for all 24 prints, the relative merits of varying exposures and development techniques are shown,

although at the expense of not producing good clear pictures in all cases. With precautions and individual printing, good pictures could be produced from all negatives, although that would not serve the purpose of this report, which is concerned with development techniques applicable to operational film irradiated by atomic bomb radiation.

Figure 3.2 shows slightly better contrast than Fig. 3.3 because of increased exposure time. Figures 3.4 and 3.5 are about the same, although anti-foggant was used on Fig. 3.5. Figure 3.6 is clearer than Fig. 3.2 because exposure time was doubled.

Twice normal exposure and slight overdevelopment with four times normal anti-foggant produced the negative for Fig. 3.7 with higher density than the negative for Fig. 3.5, although prints from both are good. Figures 3.8 and 3.9 are evidence that dense negatives from normal exposure and normal development can make fine prints. The processing for these prints was apparently about optimum. The clarity of Fig. 3.10 compared with Fig. 3.11 is evidence of the advantage of anti-foggant. Figure 3.12, although overdeveloped and with four times normal anti-foggant, is practically the same as Fig. 3.11, which had normal development only. Figure 3.13 shows the low density possible, even below the base density for the film, with underdevelopment and use of anti-foggant. An excellent print can be made from the negative of this film.

A comparison of Fig. 3.14 with Fig. 3.15 again points up the advantage of overexposure.

Figure 3.16 is a poor print because of the low density of the negative. However, it shows that gross overexposure and underdevelopment produce low-density negatives and excellent prints with careful processing. Figures 3.14 and 3.17 involve the same technique and are essentially the same by comparison. A comparison of the densities of Figs. 3.17 and 3.18 points up the advantage of anti-foggant in the developer. Figure 3.19 demonstrates how overdevelopment adversely affects the density even though the film was overexposed and four times anti-foggant was used in the developer.

Figures 3.20 and 3.21 prove that density is a simple function of exposure when development is normal. Figure 3.22 has a lower density than Fig. 3.20 even though these were similarly exposed and developed. This is hardly explainable except for the difference in the scenes photographed which makes densitometer readings more difficult. A comparison of Fig. 3.23 with Fig. 3.24, in which overdevelopment was exactly the same, shows that, with reasonable overexposure and with a normal amount of anti-foggant, lower film densities are possible. Figure 3.25 shows the advantage of anti-foggant when compared with Fig. 3.21. Figure 3.24 indicates again that excessive overdevelopment, despite overexposure and use of normal anti-foggant, offers little or no advantage.

REFERENCE

1. F. W. Brown III, NRDL Memorandum AD-190(0), Jan. 11, 1950.

Chapter 4

Conclusions

From the data it is quite obvious that film density (fogging) increases with radiation dosage. It appears from Fig. 3.1 that this fogging increases rapidly in the lower radiation levels, 1 to 40 r, which are realistic dosages to be expected by operational aircraft. It then assumes a small slope in the higher radiation levels, which are intolerable for manned aircraft. Although some of this information has been known from previous tests, it has not been documented.

A correlation of the Easy Shot data with the George Shot data produced Table 3.4 and enough information to conclude that fogging of A-, L-, and N-types of aerial film varies inversely to the film sensitivities. Hence A-type film has a more dense over-all response than L-type film, and L-type film more than N-type film for an equal dosage. This fact offers an immediate advantage to operational planning since faster film is more desirable as aircraft speeds increase and radiation exposure is inversely proportional to speed.

On all three types of film there is a mottled effect in the upper dosage ranges, i.e., above 20 r, although the mottling is more pronounced in N-type film than in L-type. It is more evident in L-type film than in A-type.

The readability of the film exposed in the B-29's with dosages under 3 r was very good. Prints made from these films were excellent when picture exposure time was doubled and normal development with normal amount of anti-foggant was used.

There appeared to be more random spot fogging on film carried in bomb bays and unpressurized and unsealed compartments, probably due to particulate contamination. The over-all densities for films in sealed compartments were slightly lower than for films in open compartments even though the indicated integrated dosages were greater.

Radiation levels in the atomic cloud during the first hour, as experienced by the AEC drones, are in the range of 30 to about 200 r, and the film from this early exposure has a high density and great amount of mottling. Fairly good readable prints were made from this film by long overexposures, e.g., eight times over normal exposure, with normal development and use of a normal amount of anti-foggant.

Penetration of the outer fringes of the atomic cloud after the first hour will not seriously affect reconnaissance film. A complete record of integrated dosage should be kept to serve as a guide to later development. Since it is recognized that current radiological-safety tolerances are not based on combat conditions, the upper limit of exposure to be tolerated by combat crews might be much higher. However, the lower dosages experienced by the B-17 drones, although high for personnel, would not be an upper limit for fast aerial film. The limit is on the crew, not on the film.

A comparison of film exposed on the ground with film exposed in the aircraft shows higher densities for the ground film for equal dosage indications. This is due to thermal-radiation fogging immediately at explosion time and subsequent heat fogging during G-day and G+1 day before these magazines could be recovered.

In overexposing irradiated film the density difference between the peak density reading and the shadow density reading is increased, which provides more actual contrast. However, overexposure gives this advantage only up to a certain point, after which the density differ-

ential will decrease. Figure 4.1 demonstrates what seems to be an optimum overexposure for N-type film irradiated with 90 r. A rigorous study of all radiation exposures and varied scene overexposures should be undertaken.

It is recommended that all air reconnaissance organizations be informed of these results for planning purposes and for establishing operational procedures involved in proper treatment of film to obtain maximum clarity and readability. A continuing requirement should be established for a similar project to be accomplished on any future atomic testing program, with proper planning so that before-, during-, and after-shot photography can be done within the prevailing security limitations by the actual operational personnel.
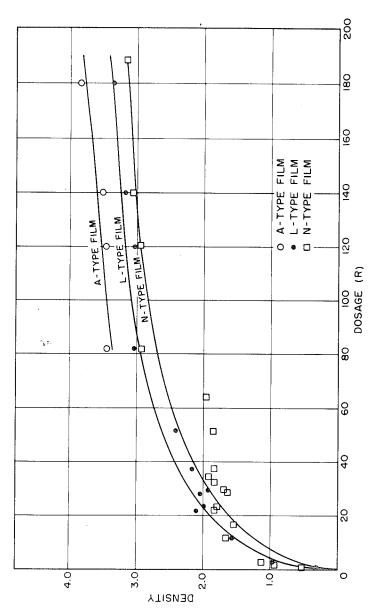
Fig. 3.1   Dosage vs Density Curves for A-, L-, and N-type Film
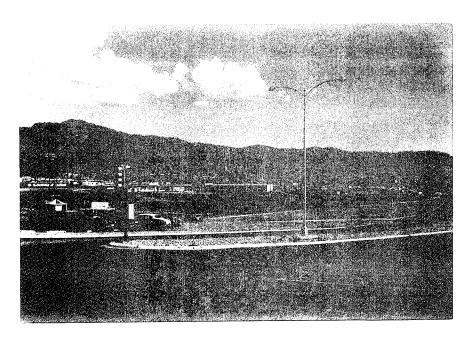
Fig. 3.2   Dosage 0.55 r, 2× Normal Exposure, Normal Development, Film Density 1.85
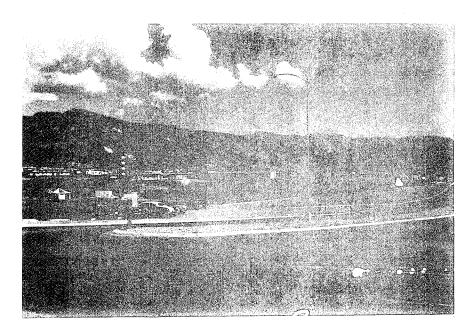
Fig. 3.3   Dosage 0.55 r, Normal Exposure, Normal Development, Film Density 1.77
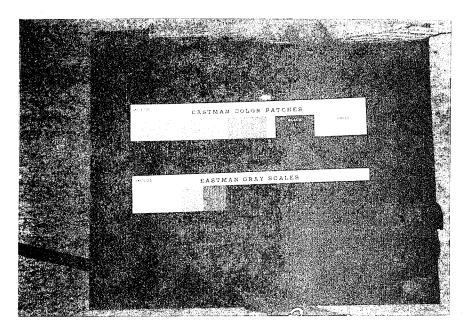
Fig. 3.4   Dosage 0.55 r, 2 × Normal Exposure, Normal Development, Film Density 1.29
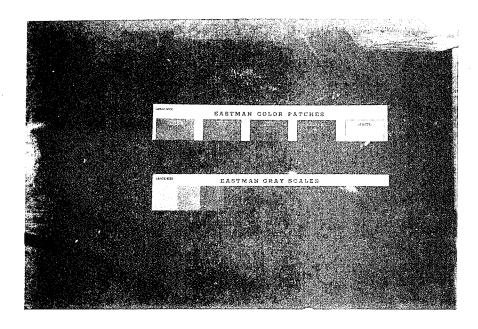
Fig. 3.5   Dosage 0.55 r, 2× Normal Exposure, Normal Development, Normal Anti-foggant,
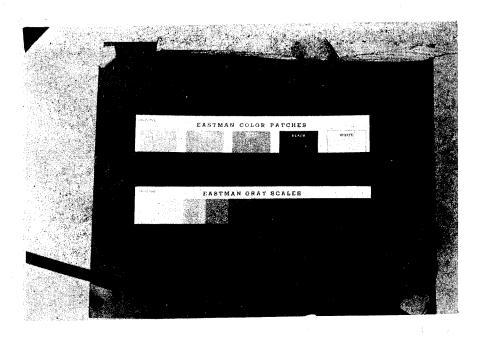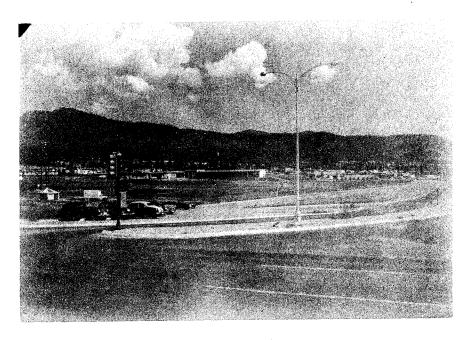Film Density 1.28
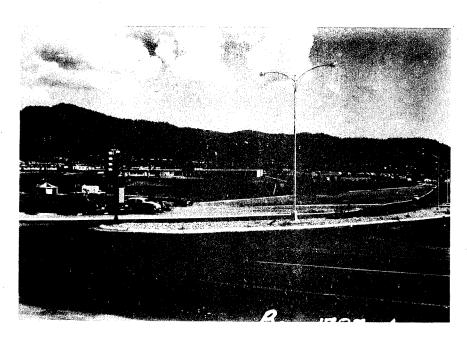
Fig. 3.6 Dosage 0.55 r, 4 × Normal Exposure, Normal Development, Film Density 2.15
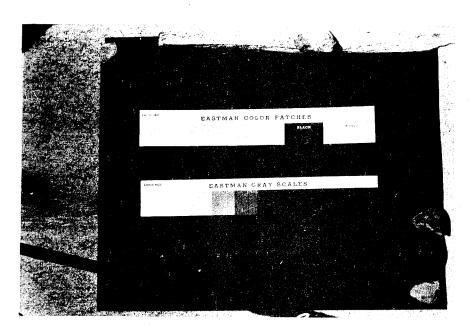
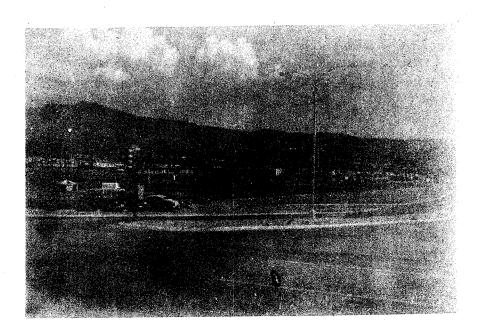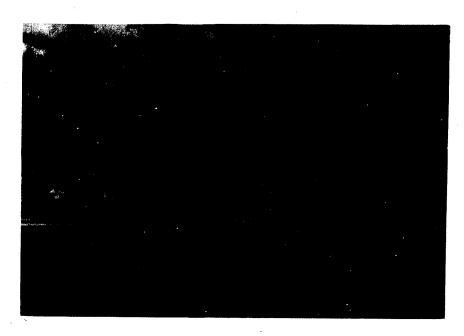**Fig. 3.7** Dosage 0.55 r, 2× Normal Exposure, 50 Per Cent Over Normal Development, 4× Normal Anti-foggant, Film Density 1.57
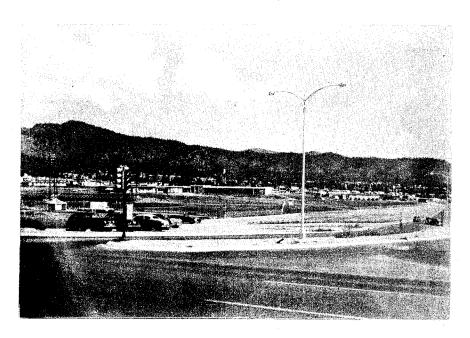
Fig. 3.8   Dosage 16.4 r, 1/2 Normal Exposure, Normal Development, Film Density 2.35
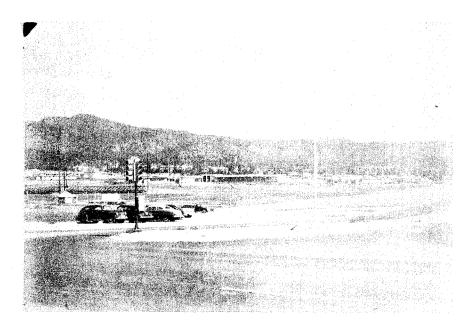
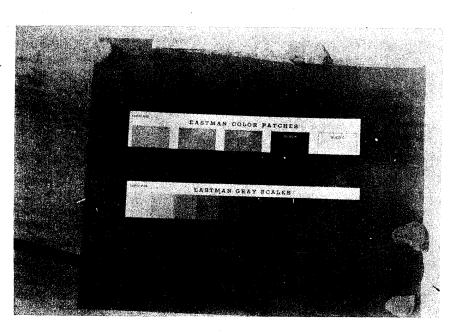Fig. 3.9   Dosage 16.4 r, Normal Exposure, Normal Development, Film Density 2.50
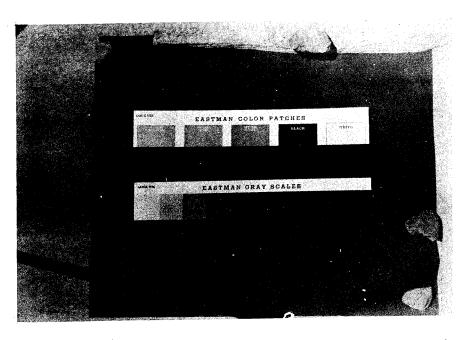
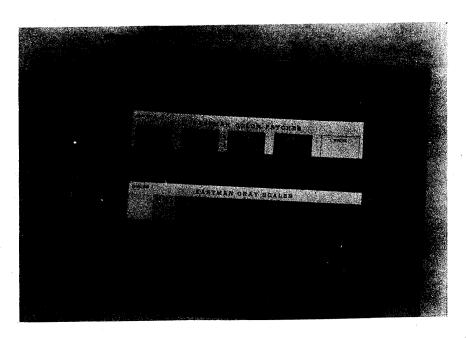**Fig. 3.10**   Dosage 16.4 r, 1/2 Normal Exposure, Normal Development, Normal Anti-foggant,
Film Density 2.00
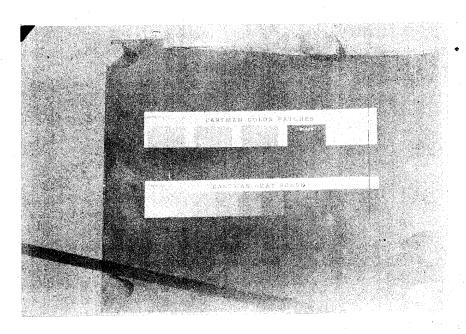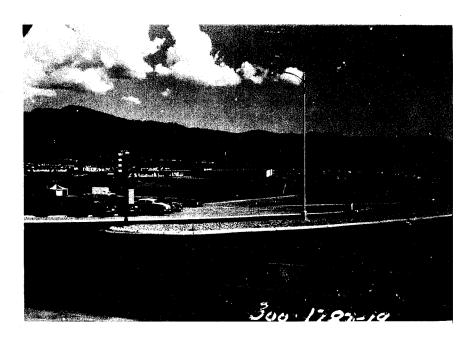

Fig. 3.11   Dosage 16.4 r, 1/2 Normal Exposure, Normal Development, Film Density 2.09

386
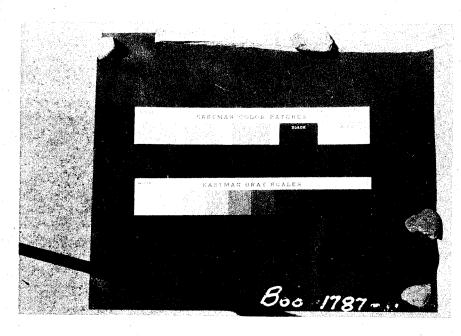
Fig. 3.12 Dosage 16.4 r, 1/2 Normal Exposure, 50 Per Cent Over Normal Development, 4× Normal Anti-foggant, Film Density 2.12

Fig. 3.13 Dosage 16.4 r, 1/2 Normal Exposure, 20 Per Cent Under Normal Development, 10× Normal Anti-foggant, Film Density 1.41

Fig. 3.14 Dosage 28.6 r, 8× Normal Exposure, Normal Development, Film Density 2.23


Fig. 3.15 Dosage 28.6 r, 2× Normal Exposure, Normal Development, Film Density 2.32

Fig. 3.16 Dosage 28.6 r, 32× Normal Exposure, 3-min Development, Film Density 1.69

Fig. 3.17 Dosage 28.6 r, 8× Normal Exposure, Normal Development, Film Density 2.22

Fig. 3.18 Dosage 28.6 r, 8 × Normal Exposure, Normal Development, Normal Anti-foggant, Film Density 1.93

Fig. 3.19 Dosage 28.6 r, 8 × Normal Exposure, 50 Per Cent Over Normal Development, 4 × Normal Anti-foggant, Film Density 2.39

Fig. 3.20   Dosage 2.8 r, 1/2 Normal Exposure, Normal Development, Film Density 1.85
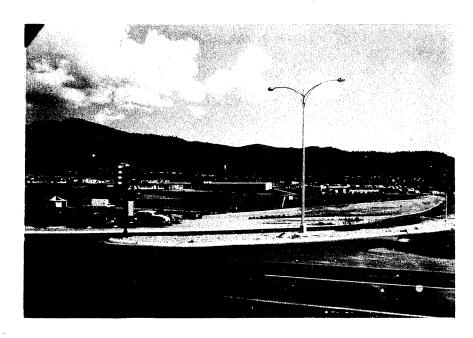
Fig. 3.21   Dosage 2.8 r, Normal Exposure, Normal Development, Film Density 2.13
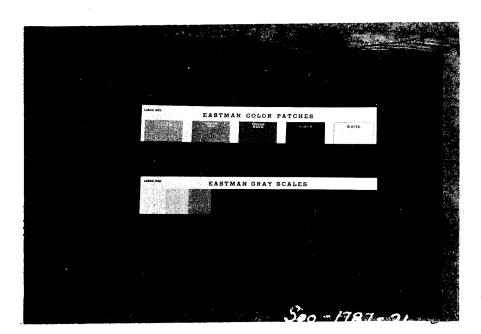
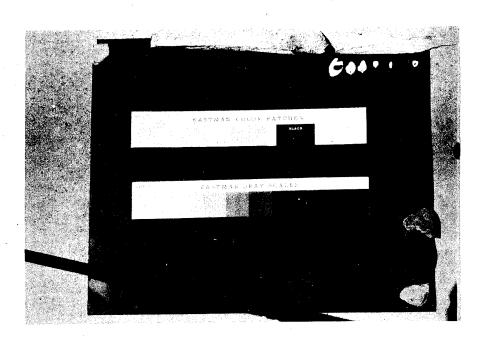**Fig. 3.22** Dosage 2.8 r, 1/2 Normal Exposure, Normal Development, Film Density 1.47

Fig. 3.23 Dosage 2.8 r, Normal Exposure, 50 Per Cent Over Normal Development, Film Density 1.85
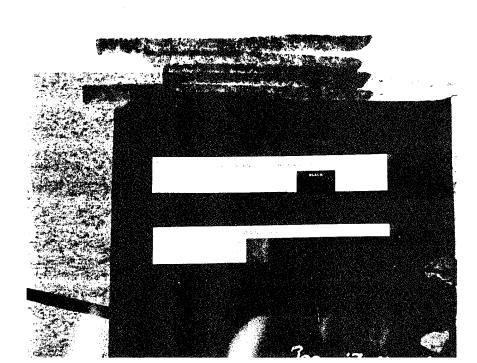
Fig. 3.24 Dosa   .8 r, 2× Normal Exposu   Per Cent Over Normal Development, **Normal Anti-**
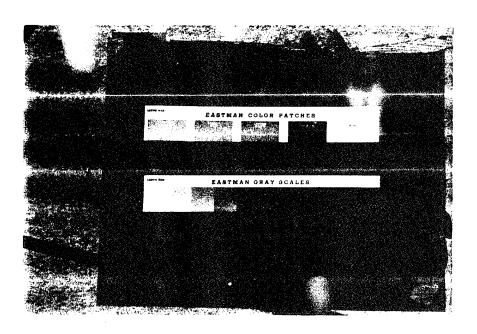foggan: Density 1.62

Fig. 3.25   Dosage 2.8 r, Normal Exposure, Normal Development, Normal Anti-foggant,
Film Density 1.57

Fig. 4.1   N-type Film, Dosage 90.0 r, 8× Normal Exposure, Normal Development, Normal Anti-
foggant, Film Density 2.64